

Advances in shape memory polymers: Remote actuation, multi-stimuli control, 4D printing and prospective applications

Xiaofei Wang^a, Yang He^a, Yanju Liu^b, Jinsong Leng^{a,*}

^a Center for Composite Materials and Structures, Harbin Institute of Technology, Harbin, 150080, P. R. China

^b Department of Astronautic Science and Mechanics, Harbin Institute of Technology, Harbin, 150001, P. R. China

ARTICLE INFO

Keywords:

Shape memory polymer
Remote actuation
Multi-stimuli-control
4D printing
Application

ABSTRACT

Shape memory polymer (SMP) is an excellent smart material, which can sense and perform active shape change as preprogrammed. So far, there are a wide variety of stimulus-responsive SMPs being developed, including thermal-, electro-, magnetic-, photo-, microwave-, ultrasound-responsive SMPs and so on. Heating and electricity are traditional stimuli for contact actuating SMPs. In recent decades, the remote actuation of SMPs through light irradiation, magnetic field, microwave field and ultrasound field have received tremendous attentions, especially applied in biological environment, aqueous environment as well as aerospace environment. Besides, the multi-stimuli control and multi-stage deformation of SMP intelligent systems can be flexibly realized by combining various actuation methods. For rapid fabrication of personalized smart structures and architectures, 4D printing using SMPs have been proposed and underwent increasing growth to meet the practical demands. This review summarizes the progress in SMP research, with the focus on remote-actuation strategies, multi-stimuli-controlled structures, and the 4D printing of intelligent integrated systems. Besides, the comprehensive exploitation of their shape memory functions in biomedical engineering, soft robots, actuators, aerospace engineering and information storage are addressed effectively. At last, the application prospects, current problems and future challenges facing research are elaborated, so as to provide appropriate guidance for interdisciplinary study and further development.

1. Introduction

Commonly seen in nature, active shape-changing behavior is crucial for the survival of plants and animals in response to the ever-changing environment. Since the 20th century, researchers have paid widespread attention to the intelligent materials and structures with active shape morphing properties and functions, such as shape memory polymer [1], artificial muscle material [2–4], and dielectric polymer [5,6]. As a promising smart material with intrinsic characteristics including large deformation capability, excellent flexibility, light weight, and high processability, shape memory polymer (SMP) plays an increasingly vital role in intelligent structures and systems [7,8]. The polymers with shape memory effect can hold "programmed" temporary shape and return to the original shape with the assist of the action of heat field [9,10], light irradiation [11,12], electric field [13,14], magnetic field [15], chemical solvent [16,17] or other external stimuli [18–21]. By contrast, the twisted fiber artificial muscles have outstanding output, high actuation stroke, and high temperature sensitivity, but the shape is not

programmable. And dielectric polymer actuators have fast response and large deformation, but the preparation process is complicated and the actuation voltage is high.

Over the past decades, various SMPs have been successfully developed, including polyurethane [22], polyimide [23], polylactic acid [24], poly(ϵ -caprolactone) [25], styrene-butadiene copolymer [26], epoxy resin [27] and so on. These SMP materials have presented a broad prospect of applications in biological devices, medical materials, drug release, aerospace engineering and automatic control systems [28–34]. Furthermore, various shape memory constitutive models have been built by researchers, e.g. viscoelastic theory model, phase transition theory model and some other novel constitutive model. These models are effectively used in simulating the thermodynamic behavior of SMPs, thus providing theoretical references for the engineering applications of SMPs. This content will be discussed in Section 2.

In early stages SMP is typically referred to a kind of thermal-responsive materials. As a stimulation approach, thermal field exhibits the advantages of wide source, simple operation and easy

* Corresponding author.

E-mail address: lengjs@hit.edu.cn (J. Leng).

<https://doi.org/10.1016/j.mser.2022.100702>

Received 28 September 2021; Received in revised form 19 May 2022; Accepted 20 October 2022

Available online 4 November 2022

0927-796X/© 2022 Elsevier B.V. All rights reserved.

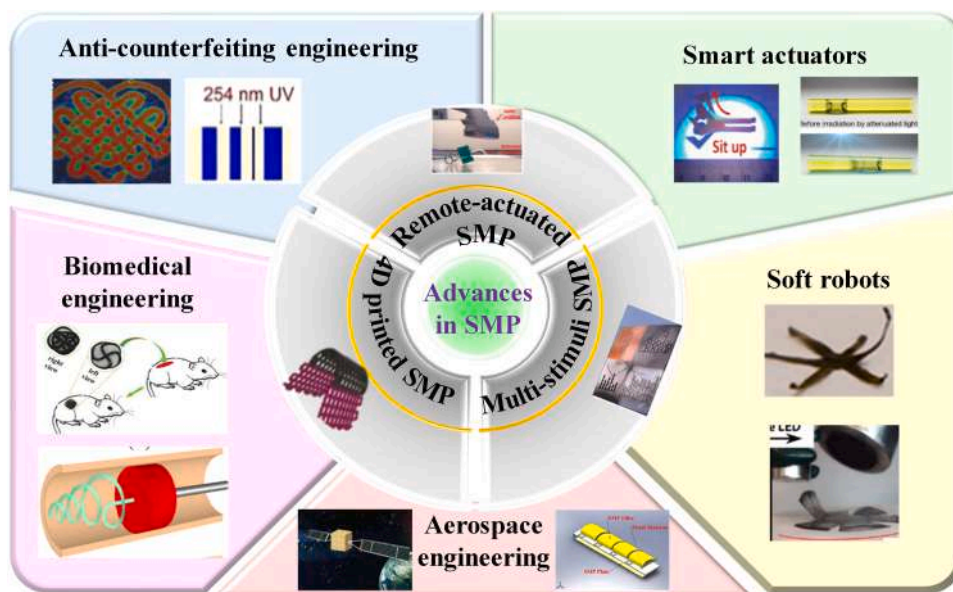


Fig. 1. The scheme of remote-actuated SMPs, multi-stimuli-controlled SMPs, 4D printing of integrated SMPs, and applications.

implementation [35]. However, thermal-actuated SMPs cannot be remotely controlled, which limits their further applications in wireless-controlled intelligent systems [36]. Remote-actuated SMPs have fast, accurate, wireless-controlled shape morphing properties [37], and have become a current hot topic due to their great prospects in many fields. More specifically, there are several major types of remote-actuated SMPs, including magnetic-actuated SMPs, microwave-actuated SMPs, ultrasound-actuated SMPs and photo-actuated SMPs, which will be discussed in Section 3. With the development of intelligent system, the requirements on the controllability and programmability of smart materials are gradually rising up,

the multi-stage programming and multi-stimuli control of SMPs have also been investigated and developed extensively. These SMP-based structures and systems have multiple shape deformation capability, multi-stage programmable performance, and selective actuation behavior. Accordingly, the scopes of their applications are expanded to the industries of smart actuators, bionic robots, and advanced security, etc. These will be discussed in Section 4.

4D printing technology is developed by adding the time dimension to the conventional 3D printing technology, indicating that the printed structures have shape morphing behavior over time, thus opening up new horizons in the smart structures and intelligent systems [38]. The

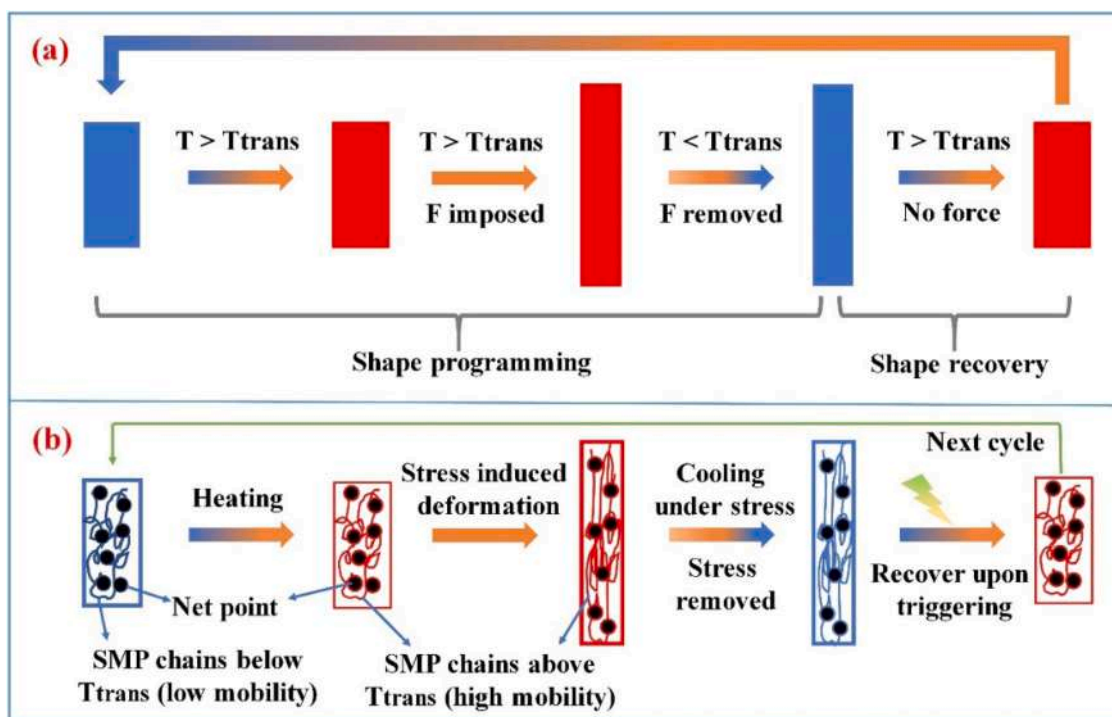


Fig. 2. The schematic diagram of one-way shape memory process for the thermal-actuated SMP and microscopic mechanism: (a) one-way shape memory process; (b) the microscopic molecular mechanism of the shape memory effect.

[49]. Copyright 2015 Elsevier Ltd.

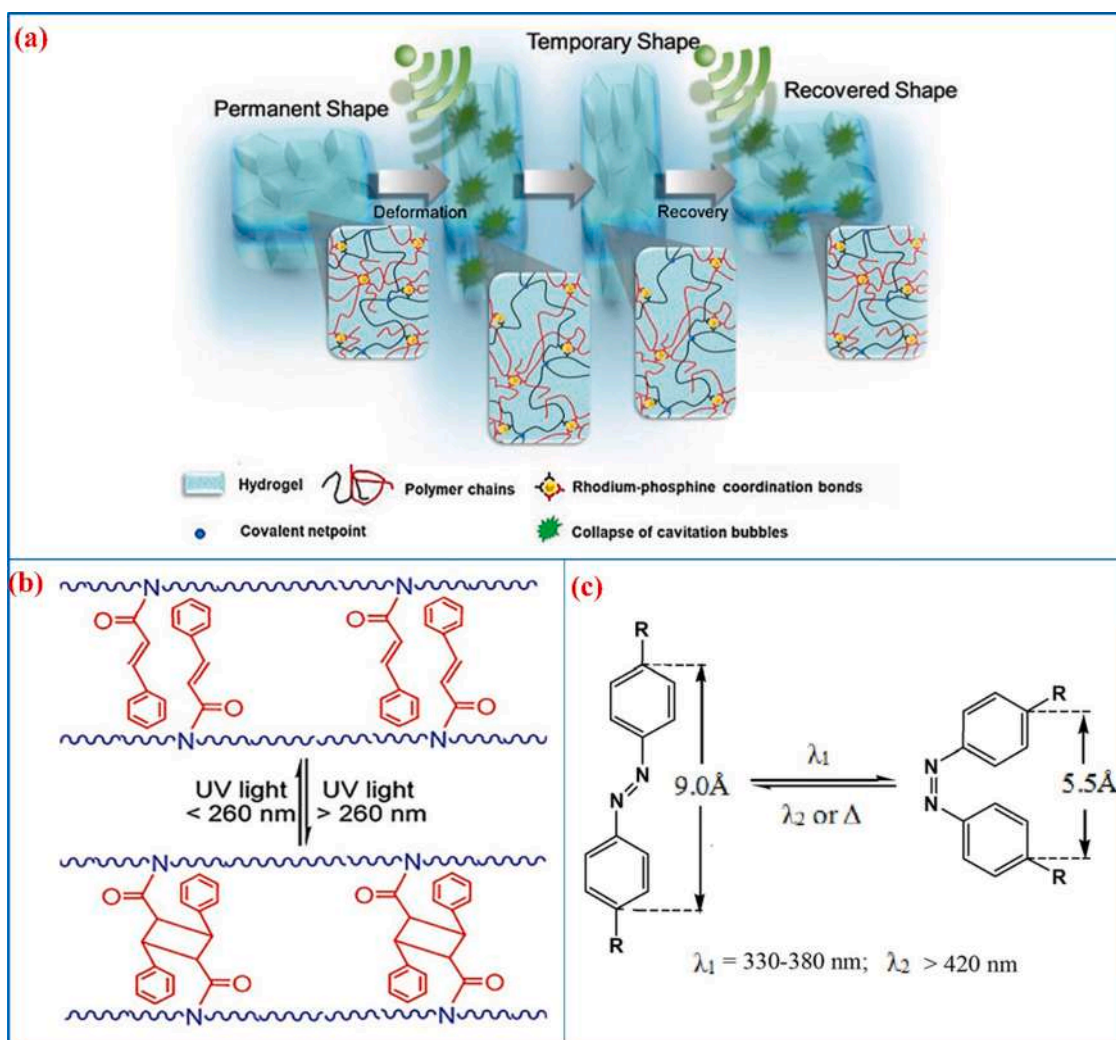


Fig. 3. (a) The shape memory mechanism of the ultrasound-actuated shape memory hydrogels (b) The shape memory mechanism of the photocycloaddition-based SMP (c) The photo-actuated morphing mechanism of the azobenzene group.

(a) [50]. Copyright 2020 Wiley-VCH. (b) [51]. Copyright 2005 Nature Publishing Group. (c) [52]. Copyright 2010 Royal Society of Chemistry.

4D printing technology can be realized by combining 4D printable SMPs (e.g. thermal-, photo-, magnetic-, or electric-actuated SMPs) and printing approaches (e.g. stereolithography, digital light processing, fused deposition modeling, and direct ink writing, etc.). The 4D printing is regarded to be a cutting-edge additive manufacturing technology for constructing personalized smart and interactive objects, which possesses applications in intelligent robots, biomedical engineering (artificial organs, artificial muscles, tracheal stents, and drug delivery, etc.), and the aerospace industry (self-deployable hinge, self-deployable truss, self-deployable lenticular tube, and release devices, etc.). These will be discussed in Section 5.

Up to now, the existing reviews of SMPs are mainly focused on the types, synthesis and applications of thermal-, light-, electro-, magnetic-, pH-actuated SMPs and so on. Nevertheless, the academic information is still limited for the specific progresses made in remote-actuation methods, multi-stimuli selective control, and 4D printing technologies for SMPs. This review aims to provide an overview of SMP research from these perspectives, as shown in Fig. 1. Within this review, a system summary is made of the progresses in shape memory polymers and structures, including molecular design strategies, various remote-actuation, multi-stimuli control, 4D printing technology, integrated intelligent structure, mechanical behavior and potential applications. To better take advantage of the intelligent material in the near future, the current tough challenges and prospects facing SMP research are

proposed and discussed.

2. General aspects of SMPs

2.1. Mechanisms

SMP is generally comprised of a reversible phase for fixing the temporary shape and a stationary phase for holding the permanent shape [39]. It is worth noting that SMP is also denoted as phase change material. The reversible phase consists of crystalline regions with a relatively lower melting point or molecular chains with a relatively lower glass transition temperature, and thereby the reversible change to the molecular structure will induce crystallization / melting phase transformation [40,41] or glass / rubber transition [42–44]. The stationary phase consists of physically crosslinked (thermoplastic) or chemically crosslinked (thermosetting) polymers with a higher melting point or higher glass transition temperature. During the shape memory cycle, the stationary phase prevents the molecular chain from slipping, so that the SMP with temporary shape can return to the original state upon external stimuli [45,46]. SMPs can be divided into one-way SMPs [47] and two-way SMPs [48] based on whether the shape memory process is reversible. According to such classifications, we introduce one-way shape memory effect and two-way shape memory effect in the following parts, respectively.

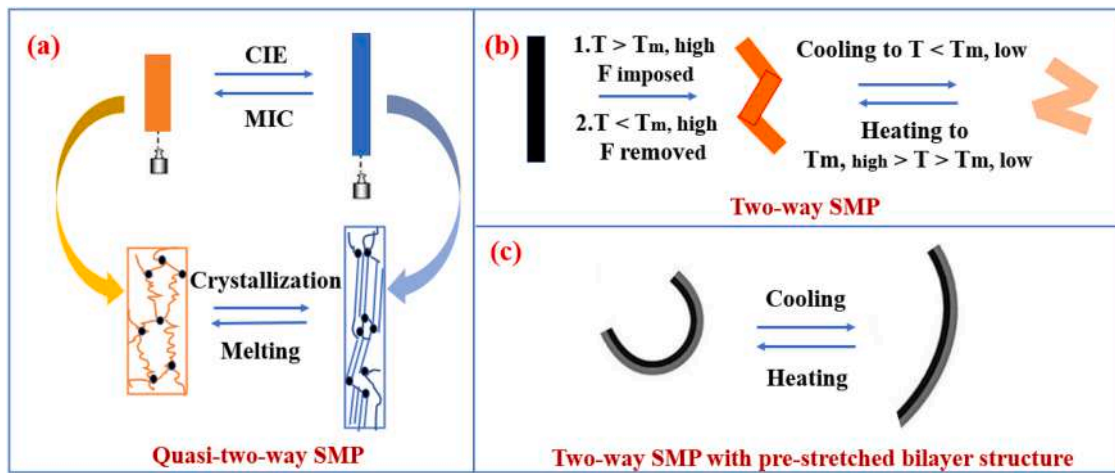


Fig. 4. Schematic diagram of diverse two-way shape memory behaviors: (a) quasi-two-way SMP under a constant stress; (b) two-way SMP with programmable two-way shape memory effect; (c) two-way SMP with pre-stretched bilayer structure and the reversible bending process over zero external force. [49]. Copyright 2015 Elsevier Ltd.

2.1.1. One-way shape memory effect

A typical one-way shape memory process for thermal-actuated SMPs is shown in Fig. 2a [49]. Firstly, the SMP is subjected to heat treatment over the shape memory transition temperature (T_{trans}) and is manually programmed into the pre-designed shape upon external force. After then, the SMP material is cooled to below the T_{trans} , so that the SMP can remain the temporary shape without any external force. Finally, the SMP is reheated over T_{trans} , and the temporary shape can be recovered to the original shape. As for microscopic molecular mechanism, the shape memory effect is attributed to the "activation" and "freezing" of molecular chains caused by external stimuli. As illustrated in Fig. 2b, on microscopic scale, all the molecular chains of the reversible phase of SMPs can be shifted from the frozen status (blue) to the active status (red) by heating over T_{trans} . The "black dot" indicates the crosslinked netpoints in the molecular chains of the stationary phases for maintaining the permanent shape. When a temporary shape is programmed at active status, the temperature of the SMP is reduced below the T_{trans} so that the reversible phase is recovered to the "frozen" state, leading to the fixation of the temporary shape. Subsequently, through reheating SMP over T_{trans} , the "frozen" molecular chains are transformed into active molecular chains. As a consequence, the internal stress in "frozen" molecular chains is released to actuate the shape recovery of SMP.

The shape fixation and shape recovery properties of SMPs are mainly evaluated by the following parameters: (a) shape transition temperature (T_{trans}), which directly affects the operating temperature range of SMP, (b) shape fixation ratio (R_f), which represents the ability of SMP to fix the temporary shape, and (c) shape recovery ratio (R_r), which describes the property of SMP to recover the original shape. The equations are expressed as follows.

$$R_f = \frac{\epsilon}{\epsilon_{load}} \times 100\%$$

$$R_r = \frac{(\epsilon - \epsilon_{rec})}{\epsilon} \times 100\% \quad (1)$$

Where ϵ_{load} , ϵ , ϵ_{rec} represent the deformation strain after loading, fixed deformation strain and the deformation strain after recovery to the SMP at the deformation temperature T_d , fixed temperature T_f and recovery temperature T_r , respectively.

As for the shape memory mechanism of ultrasound-actuated SMPs, ultrasound has cavitation functions, which enables the interaction with polymer molecular chains to cause the molecular chain relaxation and the change from temporary shape to original shape (Fig. 3a). Specifically, during the process of sonication, the ultrasound waves are capable to locally compress and expand the liquids. When the bubble exceeds a critical size, the bubble occurs collapse. This collapse of

bubbles can result in shock waves with a velocity around 1000 m/s in liquid media or generate microjets (velocity: several 100 m/s) directed toward the solid surface [50]. Then, the cavitation-based mechanical force (CMF) is converted into motion energy in a polymeric material, resulting in the SMP recovering the original shape, such as melamine, rhodium-phosphine (Rh-P) coordination polymer network, and semi-IPN Rh-P polymer network [50].

Photochemical-actuated SMP mainly contains photochemical reactive groups or molecules as "molecular switches" in the polymer networks. The "molecular switches" include cinnamic acid (CA) molecule [51], azobenzene molecule [52] and spiropyran. For the cinnamic acid (CA) molecule, when irradiated with a wavelength greater than 260 nm, two CA molecules in the polymer chains experience poly-cyclization reaction to form cyclobutene, while the temporary shape is fixed. When the wavelength is below 260 nm, the cyclobutene experiences photolysis reaction, accompanied with the polymer returning to the original status (Fig. 3b). As for the azobenzene molecule, when irradiated with a 366 nm UV light irradiation, azobenzene groups are transformed into cis-structures, thus causing the shift of polymer chain from nematic structure to isotropic structure. Macroscopically, the polymer thin film exhibits shape bending behavior. When irradiated under a visible light with a wavelength greater than 540 nm, the polymer thin film is transformed from isotropic phase to nematic phase, and the sample shows shape recovery behaviors macroscopically (Fig. 3c). Another light-actuated shape memory mechanism can be described that when spiropyrans are excited by UV light, the C-O bonds of the molecular structure are cleaved, thus forming ring-opened structures. The interaction force of the polymer molecular chains weakened by these ring-open structures is conducive to the deformation of the amorphous region and the soft segment crystallization region for the shape restoration of the polymer.

2.1.2. Two-way shape memory effect

The SMPs with two-way shape memory effect exhibit reversible transformation between temporary shape and initial shape in response to external stimulus, and they are usually divided into quasi-two-way SMP and two-way SMP on the basis of the operating conditions [53]. Quasi-two-way SMP is defined as the polymer with a two-way shape memory effect (2 W-SME) under constant external force (i.e. $F \neq 0$), which is related to the characteristics of melting induced contraction (MIC) and crystallization induced elongation (CIE) as shown in Fig. 4a. Such quasi-two-way SMPs include PCL, EVA, PE, polyester polyurethane (PEU) and so on. By contrast, two-way SMPs have reversible shape memory effect in the absence of external force. Typically, the core-shell

structure of polycyclooctene-acrylate elastomer [53], the crosslinked double networking polymer PCL-PTMEG [54], the two components of crystal polymer SBS-PU [55], and the chemically crosslinked and physically crosslinked crystalline polymer EVA with a wide range of melting transition temperature [56], are found to possess thermal-actuated two-way shape memory effects (Fig. 3b). In addition, as temperature changes, the two-way SMP composites that combining pre-stretched elastomer and SMP display two-way shape memory effect [57], as shown in Fig. 4c.

Mather and his colleagues [58] are the first to report quasi-two-way SMPs consisting of crosslinked semi-crystalline poly(cyclooctene) [PCO]. The molecular mechanism of shape memory effect is illustrated in Fig. 4a. In general, polymeric molecular chains are randomly arranged in the molten status. After cooling, the reversible phases are frozen in a random arrangement status, while the macroscopic shape of the SMP remains unchanged. However, the molecular chains of the reversible phases will be reoriented at the molten status under the action of a constant external force. When reducing the temperature under a constant force, the sample will be crystallized to maintain the orientation of molecule chains and the macroscopic shape of the sample gets elongated due to CIE effect. After reheating, the molecular chain orientation is eliminated by the re-melting of the crystalline regions, and thereby the macroscopic shape is contracted and the temporary shape is regained (corresponding to the MIC effect).

Additionally, the first pure two-way SMP is shape memory polyester urethane which is polymerized by poly(ω -pentalactone) (PPDL) and PCL [59]. In the PEU, the two polyester segments provide two different melting points temperature, with one of $\sim 64^\circ\text{C}$ ($T_{m, \text{high}}$) and the other of $\sim 34^\circ\text{C}$ ($T_{m, \text{low}}$). Fig. 4b shows the shape programming and reversible shape memory behavior. When the temperature is cycled between 0°C and 50°C , the sample undergoes reversible shape transition. The molecular mechanism of shape memory cycle can be described that the deformed PPDL region produces a crystalline geometric framework. During the processes of crystallization and melting, the PCL segments undergo a significant change to cause reversible geometric shape. When heating to the temperature of 50°C , only the molecular chains of the PCL segment lose orientation, while the molecular chains fixed by the PPDL remain unchanged. Accordingly, the shape transformation behavior of PCL segment can be observed without applying external force, which is considered to be a typical two-way memory effect.

Except for the pure two-way SMP, the special bilayers structure can also be regarded as an ideal construction, which performs two-way shape memory effect. For instance, the bilayers structure by bonding a pre-stretched shape memory polyurethane (SMPU) with a non-stretched polyurethane elastomer is a kind of two-way SMP [57]. Fig. 4c shows the two-way shape memory process repeated many times for the double-layers of SMP. The occurrence of compression can be found in the pre-stretched SMPU at an elevated temperature while the polyurethane elastomer film provides the resistance force required to prevent the self-contracting process. In the first cycle, as the temperature increasing from 25°C to 60°C , the double-layer sample is bent to the SMPU direction, and the bending angle is progressively increased over time. When cooled down, the SMP bilayers start to recover the original shape.

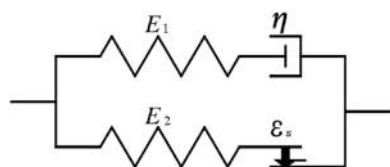


Fig. 5. SMP four-element model. [61]. Copyright 1997 Taylor & Francis.

2.2. Fabrication strategies

After cross-linked shape memory polyethylene was discovered for the first time, SMP and its composite have received extensive attention from researchers because of their unique shape memory effects. Conventionally, the construction strategies of SMP mainly include cross-linking, copolymerization, and molecular self-assembly [60].

In particular, with regard to the cross-linking method, the molecules generate corresponding free radicals upon external energy such as temperature or light, and then the free radicals undergo a coupling reaction to make the polymer crosslink. During the chemical cross-linking process, the linear molecules inside the polymer are connected by chemical bonds to form cross-linked networks, e.g. cross-linked polyethylene (PE), thermosetting epoxy resin (EP), polystyrene (PS), polylactic acid (PLA), polycaprolactone (PCL), polyvinyl alcohol (PVA), polynorbornene, polyisoprene and so on. For the copolymerization method, monomers are mixed at different conversion temperatures, and then the polymerization reaction is used to construct block polymers. By mixing different types and ratios of monomers, a series of SMPs with different phase transformation temperatures and memory behaviors can be prepared, e.g. polyethylene-vinyl acetate copolymer (EVA), polyurethane (PU), and polyester copolymer, etc. The molecular self-assembly method is associated with the internal energy between molecules for spontaneous aggregation to form supramolecular structures, e.g. melamine enhanced PVA physical hydrogel based on hydrogen bond self-assembly property.

Nowadays, the synthetic methods of SMPs are relatively mature and could produce excellent shape memory behavior, shape diversity and complexity, but there are still some drawbacks in mechanical properties that are further improved, such as lower toughness, ductility, and heat stability. Additionally, multi-functionality is also a requirement for intelligent materials systems in the near future, e.g. thermomechanical, optical, magnetic, electrical, and biological properties. It is well known that chemical modification or physical modification is an effective strategy to obtain the SMP materials with outstanding comprehensive properties.

Chemical modification is to use blocked or grafted methods to meliorate the mechanical properties of memory polymers. It also can provide a technical foundation for the development and application of multifunctional SMPs. For example, the LCE-blocked-azobenzene has optical actuation characteristics. In contrast, physical modification is to mix functionalized nanoparticles or fibers to fabricate SMP composites (SMPCs) with high mechanical properties, e.g. the wear resistance of the SMPs enhanced by carbon black, and the stiffness and strength of the SMPs improved by carbon fiber. Simultaneously, physical modification is also a significant approach to construct multi-actuated SMPs. For instance, carbon nanotubes are mixed to the SMP matrix to prepare photo-actuated SMPCs, and SiC nanoparticles are mixed to prepare microwave-actuated SMPCs, while Fe_3O_4 nanoparticles are mixed to prepare magnetic-actuated SMPCs, etc.

2.3. Classic constitutive models

In order to provide theoretical guidance for complex engineering applications, it is imperative to construct constitutive models for SMPs. At present, a series of SMP constitutive models have been built and demonstrated to be effective in predicting the mechanical behavior of SMP under different conditions, for example, the stress and strain of SMP at constant or varied temperatures, as well as the shape memory and recovery behaviors under free space or constrained conditions. The constitutive theories of SMPs are mainly divided into two categories. One is based on the classical viscoelastic theory, with the focus placed on the macroscopic phenomenological theory model for characterizing the mechanical behavior of SMP at different temperatures and stages. The other is based on the phase transition theory, with the focus placed on the meso-mechanical model for describing the internal "crystallization"

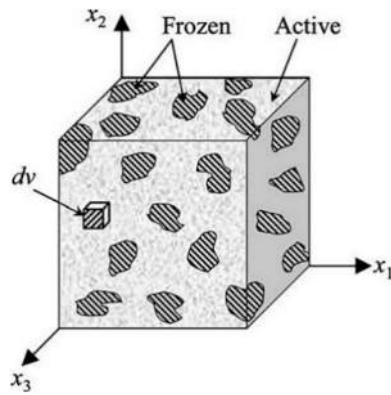


Fig. 6. Schematic diagram of the solid phase transition theory of the SMP constitutive model.

[66]. Copyright 2006 Elsevier Ltd.

and "melting" behaviors of SMP. This section reviews the researches on the typical constitutive models for the SMPs developed in recent years.

2.3.1. Viscoelastic theory modeling

The viscous rheological continuity model for simulating the thermodynamic cycle process of SMP was shown in Fig. 5 [61]. The model was designed by modifying the single linear viscoelastic model, and an internal friction slip element was introduced to describe the unrecoverable strain in the creep process. Up to now, the majority of the thermodynamic and viscoelastic constitutive equations for SMP have been established on the basis of this model. The model was inferred by assuming that the thermal expansion was irrelevant to the mechanical behavior. Besides, it is mainly purposed for predicting the thermodynamic behavior of SMP under the context of minor deformation.

It is a very meaningful to establish viscoelastic theoretical models to predict the thermodynamic behavior of SMP during the shape memory cycle. Therefore, great efforts have been made to explore the related mechanics theory. Nguyen's group [62] incorporated the modified Eyring viscous flow model and nonlinear Adam-Gibbs structural relaxation model into the continuum finite deformation thermoelastic model so as to establish a thermodynamic viscoelastic constitutive model for amorphous SMP. Zhou et al. [63] extended the thermodynamic constitutive equation established by Tobushi [61], which made it suitable for a wide range of three-dimensional SMP samples and effective in describing the relationship between the parameters and temperature of the styrene-based SMP in the glass transition process. Besides, a thermodynamic viscoelastic constitutive model was designed by Guo et al. for simulating the typical thermomechanical cycle behavior of thermal-actuated SMP [64]. This model can be applied to accurately calculate the thermodynamic and irreversible mechanical change occurring to SMP during the cooling / heating process. Leng's group [65] developed a constitutive model of thermodynamic viscoelastic finite deformation for the SMP composites reinforced by short fibers. Based on a generalized three-element theory model, the constitutive model consisting of a viscoelastic branch and a hyperelastic branch was established, in which the tensile yielding stress and the volume fraction of SMPs were described using a modified Eyring model. The simulation results were well consistent with the experimental data, indicating that the constitutive model provided an effective solution to predicting the thermomechanical behaviors of the thermal-activated SMP composites.

As mentioned above, the SMP constitutive model based on the viscoelastic theory is intuitive, comprehensive and clear in describing the aging characteristics such as creep and relaxation. Nevertheless, the shortcoming is that it cannot reasonably explain the strain storage and release mechanisms, which limits the predictive function performed by this type of constitutive model.

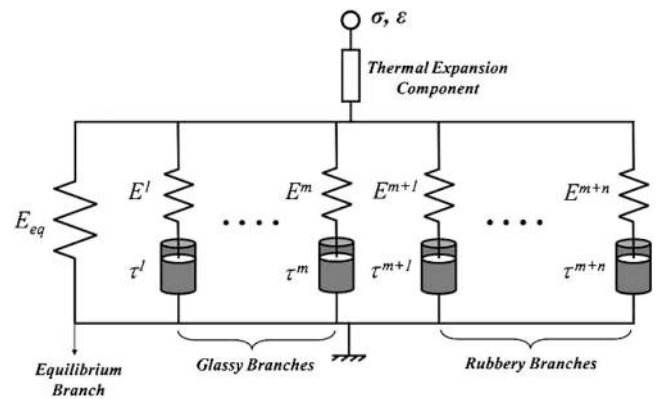


Fig. 7. The 1D rheological representation of the parallel dashpot model. [71]. Copyright 2014 Springer.

2.3.2. Phase transition theory modeling

The micromechanics modeling based on solid phase transition theory is widely practiced for the SMPs consisting of a frozen phase and an active phase. Both strain storage and release behaviors are derived from the reversible transformation between the frozen phase and the active phase. As shown in Fig. 6, Liu and colleagues [66] proposed a thermodynamic constitutive model for the three-dimensional active small deformation to SMP based on the phase transformation theory of microscopic molecular chains. This model simplified the classic viscoelastic issue by assuming that the volume fractions of the frozen phase and the active phase in SMP were represented as a function of temperature. At the shape fixation stage, the internal molecular chains of the SMP material were transformed from the active phase to the frozen phase, thus causing the storage of strain. During the reheating process in the shape recovery stage, the polymer changed from the frozen phase to the active phase, as a result of which the stored strain was released and the fixed shape changed to the original shape.

Afterward, new concepts or parameters are introduced to establish a complete constitutive model of SMP, and it is expected that the as-obtained theoretical results are consistent with actual experimental data. For example, a thermodynamic constitutive model for SMP was established by the frozen fraction concept with the polymer crystallization theory [67]. This model can be used to explore the viscoelastic properties and shape memory mechanism of SMP at the transition temperature, with the predicted value basically consistent with the results of experimental test. Additionally, a new phase-changing constitutive theory model based on the energy method can describe the shape memory effect [68]. In this model, SMP was divided into strain-induced crystallization phase and amorphous rubber phase. Through introducing the relationship between the elongation of each phase and the applied external stress, a new model can be proposed to describe both single and multiple shapes memory behaviors. Gilormini et al. [69] developed the inclusion theory by considering SMP as a composite consisting of a glass phase and a rubber phase, and then established the law of stiffness tensor and the storage strain with temperature changes. Additionally, by introducing the "phase transition" concept, Leng et al. [70] assumed that SMP was consisted of glass phase and rubber phase, and that the volume fractions of each phase were varied with temperature. According to the different thermal-mechanical behaviors of the glass phase and rubber phase, two different constitutive models were developed to estimate the thermal-mechanical property of SMP during the shape memory process.

The phase transition theory model can reasonably explain the strain storage and release mechanism of SMP. In spite of this, it cannot verify the timeliness and viscoelasticity well because of the limitation imposed by the framework of the thermoelastic theory. To address this issue, it is necessary to construct the new constitutive theory models combining the advantages of the two models as mentioned above.

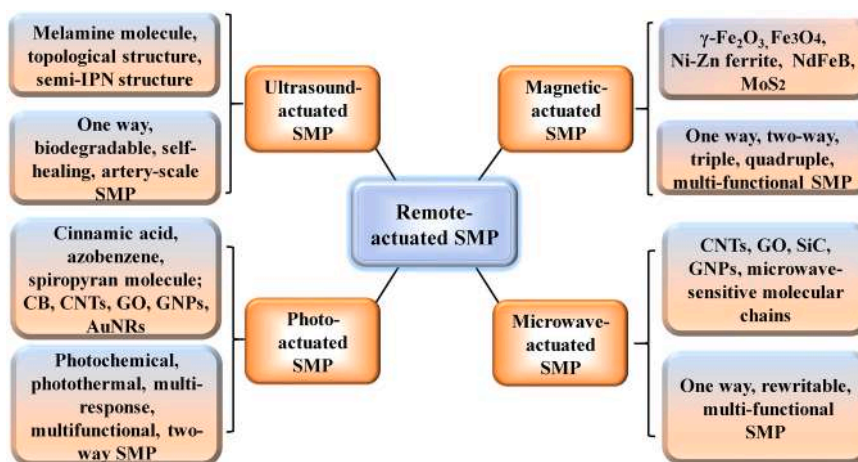


Fig. 8. A brief summary of remote actuation methods for SMPs.

2.3.3. New constitutive modeling

New SMP constitutive models are established by considering both the phase transition theory model and the viscoelastic theory model, which improves the complementarity of the aforementioned two types of modeling theory. Yu et al. [71] established a parallel dashpot model involving three states: equilibrium state, glass state and rubber state. Upon a study of the viscoelastic properties possessed by the dashpot in each state, the new model can be accurate in predicting the thermal-mechanical and shape recovery properties of SMP under different loading parameters. Fig. 7 shows the 1D rheological representation of the applied multi-branch models. The equilibrium branch is a hyperelastic spring used to represent the equilibrium behavior of SMPs. The non-equilibrium branch is a nonlinear Maxwell element consisting of an elastic spring and a dashpot placed in series. In the nonequilibrium branches, m branches represent the relaxation behavior in the glassy state, and n nonequilibrium branches represent the relaxation processes in the rubber state. In the i^{th} nonequilibrium branch ($1 \leq i \leq m+n$), the initial elastic modulus of the spring is denoted as E_i , and the relaxation time of the dashpot is indicated by τ_i (when $1 \leq i \leq m$, it represents the branch of the glass state, and when $m+1 \leq i \leq m+n$, it represents the branch of the rubber state).

Subsequently, new constitutive models are innovated to make precise predictions for the thermodynamic behavior of the SMP. For instance, Zhang and colleagues [72] designed a 3D constitutive model according to the assumption that SMP is isotropic materials and volume deformation is its elastic property, and that its rheological properties satisfy the one-dimensional constitutive model established by Tobushi [73]. Considering that SMP contains a viscoelastic hard segment phase and two super-elastic soft segment phases, Kim's group [74] conducted a 3D phenomenological constitutive model for shape memory polyurethane, among them, the two soft segment phases were identified to be the frozen phase and the active phase, respectively. Besides, based on the classical viscoelastic theory and the two-phase deformation theory, Leng et al. [75] designed a hybrid SMP constitutive equation to evaluate the thermo-mechanical behavior of SMP during the heating or cooling process.

3. Remote actuation methods for SMPs

The SMPs actuated by remote or non-contact stimulus are testified to be of particular importance in the application scenarios, in which direct thermal actuation cannot be carried out. Despite the intensive fabrication of intrinsic light responsive SMPs using photosensitive functional groups, remote-actuated SMPs can also be easily prepared by incorporating stimulus sensitive particles (e.g. photothermal-, magnetothermal-, microwave-, ultrasound-actuated, etc.) into the thermal-responsive

SMP matrix, for example, photothermal particles (CNTs, GO, AuNPs, AgNWs, etc.), magnetic sensitive particles (Fe_2O_3 , Fe_3O_4 , Ni-Zn ferrite, etc.), microwave sensitive particles (silicon carbide, four-pin zinc oxide, Fe_3O_4 , MWCNTs) and ultrasound sensitive particles (furan-maleimide adducts, melamine, rhodium coordination and so on). In Section 3, the preparation strategies, shape memory mechanisms and utilization of remote-actuated SMPs will be analyzed and discussed in detail. A brief summary of remote actuation methods for SMPs is shown in Fig. 8.

3.1. Magnetic-actuated SMPs

As reported in literature, non-contact magnetic-actuated SMPs are mainly prepared by doping magnetic nanoparticles (MNPs) into thermal-actuated SMP matrix [76–78]. When SMP is exposed to an alternating magnetic field (AMF), due to hysteresis loss and eddy current loss, inductive heat is generated to cause the temperature of SMP matrix increase to above T_{trans} . As a result, the magnetic-actuated SMP exhibits shape recovery behavior from temporary shape to the original shape [79]. Among various magnetic Fe-based nanoparticles including $\gamma\text{-Fe}_2\text{O}_3$ [80], Fe_3O_4 [81], neodymium iron boron (NdFeB) [82], nickel zinc ferrite [83] and so on., Fe_3O_4 nanoparticles demonstrate high magnetization ability, low cytotoxicity, and high biocompatibility, which allows the magnetic-actuated SMP with Fe_3O_4 nanoparticles to be extensively used in medicine and bioengineering fields [84–88].

Fig. 9a shows the preparation strategy of the first magnetic-actuated SMP composites. Obviously, it consisted of polyetherurethane (TFX) and a biodegradable copolymer (PDC) with PCL as soft segment and poly(*p*-diox-anone) as hard segment [89,90]. Iron (III) oxide cores were processed with silica before doping into the polymer matrix. Notably, the treatment of particles with silica can improve the compatibility between the TFX and PDC, as a result of which the nanoparticles have a mean aggregate size of 90 nm (photon correlation spectroscopy of water dispersion) and an average domain size of 23 nm (X-ray diffraction) in composites. Under 22 s alternating magnetic field, the wave structure (temporary shape) is changed to the straight structure (permanent shape) (Fig. 9b). The smart composites are considered to have broad prospects in the area of smart implants or instruments.

Electrospinning technology can be utilized to prepare nano-scale intelligent polymer, such as nanofibers, which has many advantages of simple preparation, uniform density and high precise structure [91–97]. Zhou et al. [98] adopted the electrospinning technology to fabricate biodegradable magnetic-actuated SMP composite nanofibers consisting of chemical-linked PCL and multi-walled carbon nanotubes (MWCNTs) as modified by Fe_3O_4 nanoparticles. According to the magnetization hysteresis curve (Fig. 9c), the saturation magnetization (M_s) reached 71.549 emu/g, indicating the superparamagnetism of the sample. Under

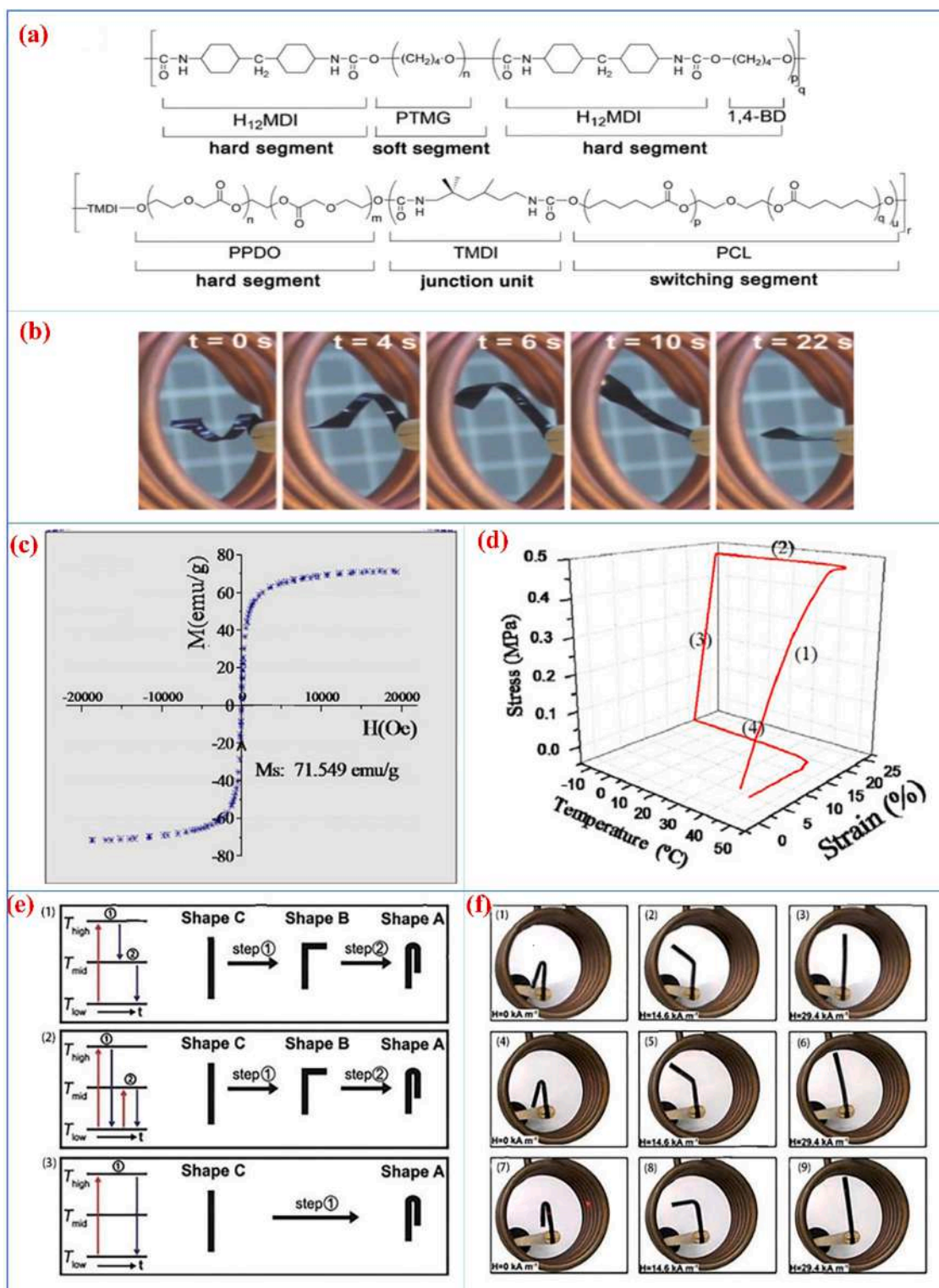


Fig. 9. (a) Molecular structures of the shape memory polymer matrix (TFX and PDC); (b) photos of the shape recovery performances of the composite with 10% wt magnetic-particle actuated by AMF. (c) The magnetization hysteresis curve of Fe₃O₄ @CD-M nanoparticles; (d) the thermomechanical cyclic tensile curves of PCL/Fe₃O₄ @CD-M composite nanofibers. (e) The different triple shapes programs; (f) the photos of shape recovery process in different magnetic field strengths. (a,b) [89]. Copyright 2006 National Academy of Sciences of the United States of America. (c,d) [98]. Copyright 2012 Elsevier Ltd. (e,f) [101]. Copyright 2010 Royal Society of Chemistry.

the action of AMF, the nanoparticles exhibited hysteresis loss, and thermal energy was generated to heat the sample. When the temperature reached above T_g, the molecular chains became flexible and the fibers returned to their initial shape (Fig. 9d). As revealed by the cytotoxicity

test, the composites possessed the high biocompatibility and satisfied for tissue scaffolds engineering.

The universal preparation strategy for the magnetic-actuated intelligent materials is to dope magnetic particles into the SMP matrix.

Table 1
The research progress of non-contact magnetic-actuated SMPs.

Materials	Alternating magnetic field	Type	Application area
Polyetherurethane and a biodegradable copolymer / iron(III)oxide[89]	258 kHz and 30 kA/m	One-way SMP	Smart implants and controlled medical instruments
PCL nanofibers / Fe ₃ O ₄ -loaded MWCNTs[98]	16 Hz and 1 kA/m	One-way SMP	Tissue scaffolds
Oligo(ϵ -caprolactone) dimethacrylate / butyl acrylate thermosets / Fe ₃ O ₄ nanoparticles[99]	300 kHz and 5.0 W	One-way SMP	Medical applications, sensor- and actuator systems
LDPE / NdFeB ferromagnetic microparticles[100]	8 kHz and 15 kW	One-way SMP	Actuator
SMPU / Fe ₃ O ₄ nanoparticle [87]	260 kHz and 48 kA/m	One-way SMP	Medical engineering and actuator
Carboxylic styrene butadiene rubber / Fe ₃ O ₄ / zinc dimethacrylate[86]	Alternating magnetic field	One-way SMP	Intelligent biomedical devices
PCL and poly-(cyclohexylmethacrylate) / iron (III) oxide core in a silica matrix[101]	14.6 kA/m, 29.4 kA/m, respectively	Triple-SMP	Biomedical engineering and programmable smart actuators
Nonwoven fiber composite Nafion / Fe ₃ O ₄ nanoparticle [102]	50–200 kHz and 2 kW	Triple or quadruple SMP	Implants and elsewhere in biomedical science
Oligo(ω -pentadecalactone) / FeCl ₃ ·6 H ₂ O and FeCl ₂ ·4 H ₂ O[103]	258 kHz and 18.2 kA/m	Two-way SMP	Magnetic-controlled actuators

Because of simple process, environmental friendliness, and wide applications, the magnetic-actuated SMPs have been rapidly developed in recent years. For example, the oligo(ϵ -caprolactone) dimethacrylate / butyl acrylate thermosets containing 0.5 wt% Fe₃O₄ nanoparticles as magnetic heating source showed rapid temperature rise to 43 °C and shape recovery from temporary shape as a result of 300 kHz alternating magnetic field actuation [99]. Nanocomposites by doping NdFeB ferromagnetic microparticles into the low crosslinked density polyethylene (LDPE) with 2 wt% organoclay was developed by Golbang group [100]. Besides, the SMPs consisting of carboxylic styrene butadiene rubber (XSBR), Fe₃O₄ nanoparticles and zinc dimethacrylate (ZDMA) were found to have a shape fixation ratio of almost 100%, and a shape recovery ratio of nearly 100% in magnetic field [86]. In fact, the physical doping strategy also has intrinsic limitations, such as uneven dispersion, easy precipitation, and low mechanical strength caused by stress concentration sites. Thus, it is necessary to modify magnetic nanoparticles to obtain better compatibility with the matrix. The optimized preparation strategy is to construct intrinsic magnetic-actuated SMPs, which avoids the drawbacks of physically blended SMPs, and it is also the future development direction of the intelligent materials.

Except for the one-way shape morphing property, multi-functional magnetic-actuated SMPs have manifested multiple responsiveness, biodegradability, self-healing, hydrophobicity, and reversibility to meet the requirements of wider practical applications. The multiphase polymer networks were selected as matrix to produce the magnetically switchable triple-shape composites [101]. More specifically, the preparation strategy of the triple-shape memory composites was that PCL segments and poly-(cyclohexylmethacrylate) (PCHMA) segments was chemically synthesized together, and magnetic nanoparticles (iron (III) oxide core in a silica matrix) as the filler was doped into the copolymer. Fig. 9f shows the triple-shape recovery process of the sample according to the steps as programmed in Fig. 9e. Besides, nonwoven fiber composite Nafion and Fe₃O₄ particles were employed to produce magnetic-actuated SMP composites [102]. As confirmed by DMA tests, the magnetic-actuated SMPs exhibited triple or quadruple shape

memory behaviors. Based on this, the authors designed the smart actuators capable of 2D and 3D shape conversions for potential biomedical applications.

Magnetic-actuated two-way SMP is prepared by doping magnetic nanoparticles (e.g. Fe₃O₄, which directly convert magnetic energy into heat energy) into a thermal-responsive two-way SMP matrix (e.g. EVA, PCL, etc.), which can be utilized to grasp objects in wireless-controlled environment. Lendlein et al. [103] designed the first magnetic-actuated two-way SMP on the basis of magnetic nanoparticles / OPDL composites [103]. The SMP matrix was the oligo (ω -pentadecalactone) (OPDL) with two-way shape memory properties, and the secondary phase particles were magnetic nanoparticles fabricated via co-precipitation of aqueous FeCl₃·6 H₂O and FeCl₂·4 H₂O. When the magnetic field was switched "on" or "off", the position of the sample firstly raised and then declined, due to the melting-induced contraction (MIC) and crystallization-induced elongation (CIE) of the SMP matrix [104]. This SMP composite overcame the inhomogeneities problem caused by the addition of nanoparticles into the SMP matrix and achieved consistent heating performance, so that the magnetic-actuated two-way SMP performed consistently in shape memory function.

To better show the research progress of magnetic-actuated SMP in recent years, we have summarized as shown in Table 1. The dispersion of the nanoparticles and the interface interactions within the SMP matrix are significant to rapid magnetic-responsive shape memory effect [105–109]. For the precise heating of SMP via an alternating magnetic field, it is essential to apply the specific spatial and orientational control to the position of magnetic nanoparticles within the matrix [110,111]. Despite many successful demonstrations of the magnetic heating SMPs, the remote control of magnetic-actuated SMPs in various environments remain challenging [112,113].

3.2. Microwave-actuated SMPs

Microwave (MW) is a variety of electromagnetic spectrum with its wavelength ranging from 1 mm to 1 m and frequency ranging from 300 MHz to 300 GHz [114]. The most commonly used frequency for catering or consumer heating is 2450 MHz [115]. The heat energy is generated by the temporary dipole movement of molecules under the alternating electromagnetic field, and could actuate the shape morphing behavior of SMPs [116,117]. The heating effect of microwave depends on the dielectric properties of the material. Dielectric loss and tangent angle (i.e. the ratio of dielectric loss to dielectric constant) are two typical parameters indicating their capability to convert microwave electromagnetic energy into heat energy [118–120].

Unlike traditional heating methods, microwave radiation could penetrate to show uniform heat distribution throughout the sample [121–125]. Therefore, it can actuate the deformation to SMP remotely, environment friendly and highly efficiently [126–128]. Due to the weak microwave absorption ability of polymers, microwave sensitive particles are conventionally introduced to enhance the microwave absorption performance of microwave-actuated SMPs, e.g. carbon nanotubes (CNTs) [129], graphene oxide (GO) [130] and SiC [131]. The predecessors made lots of efforts on the microwave-actuated SMPs and their applications in such fields as biomedicine, regenerative medicine and tissue engineering.

For example, a microwave-actuated SMP on the basis of chemical crosslinked PVA hydrogel networks (SMP-PVA) exhibited rapid shape recovery rate under 2450 MHz microwave irradiation, whereas the dry sample experienced no shape changes when irradiated [132]. Due to the hydrophilic property of PVA, the hydroxy groups within PVA had a strong combination force with water molecules when the PVA was immersed in water. The polar water molecules in the SMP-PVA hydrogel can absorb microwave energy and move towards the direction of electromagnetic field. The friction motion of water molecules in the matrix led to the transformation of microwave energy into other forms of energy such as heat energy [133]. It should be pointed out that the shape

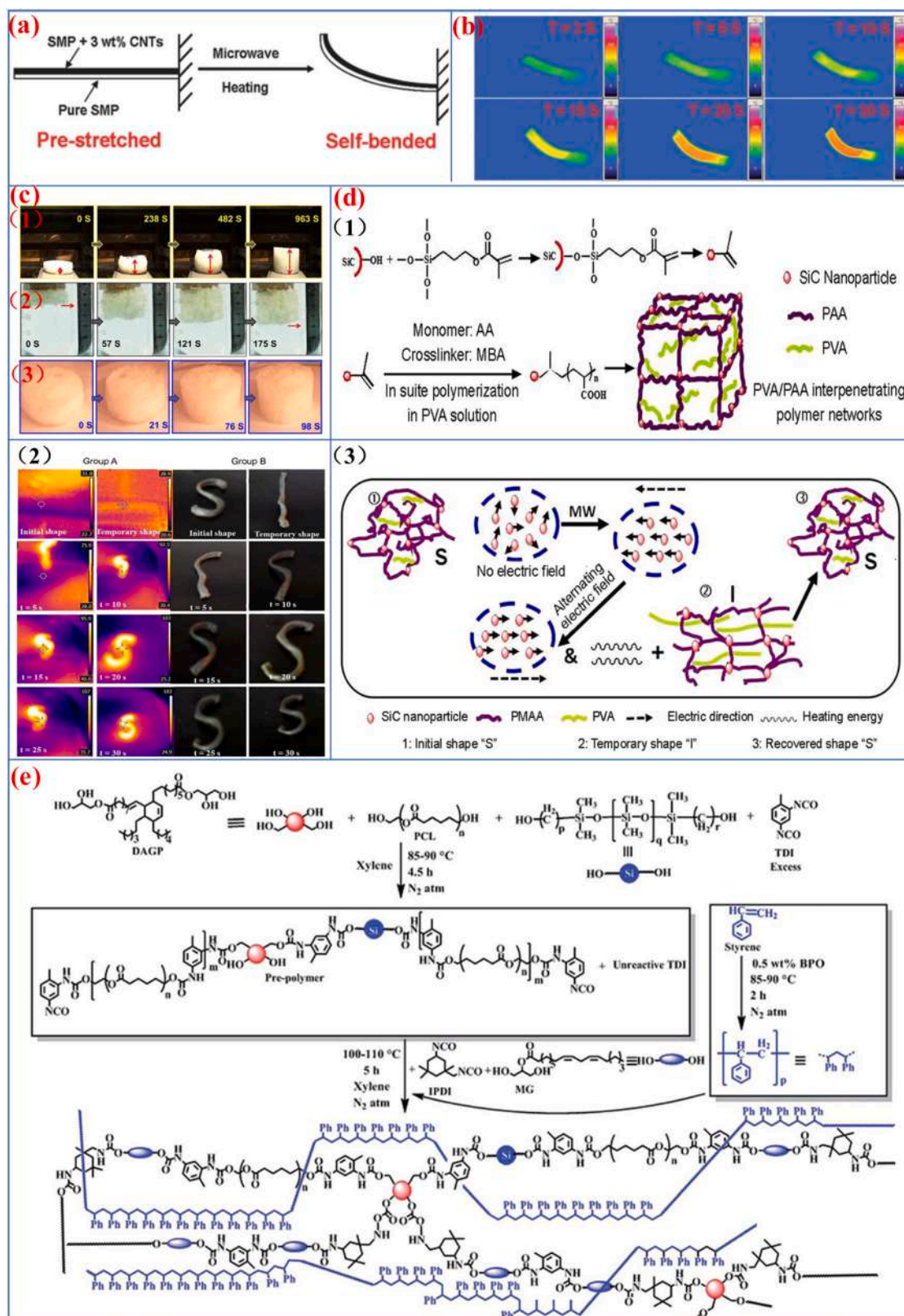


Fig. 10. (a) The schematic of the self-bended SMP composites; (b) thermal infrared images of the shape changing process. (c) The photos of shape recovery performances for c-PCL foam: (1) water bath; (2) electrical field; (3) microwave field. (d) The PVA / PAA-SiC IPN shape memory composites: (1) the synthesis routes; (2) microwave-actuated shape recovery behavior (2.5 wt% SiC); (3) the molecular mechanism of shape memory behavior. (e) The synthetic route of the shape memory polymer IPNs structures.

(a,b) [134]. Copyright 2014 Royal Society of Chemistry. (c) [135]. Copyright 2015 Nature Publishing Group. (d) [137]. Copyright 2018 Springer. (e) [140]. Copyright 2018 Royal Society of Chemistry.

Table 2

The research progress of non-contact microwave-actuated SMPs.

Microwave-actuated SMP	Preparation strategy	Property	Prospect application
PVA hydrogel [132]	Chemical crosslinking	Non-toxic	Sensors, vascular stents, and other medical devices
Pure SMP and pre-stretched CNTs / SMP [134]	Mechanical structure design	Rapid remote and wireless actuation	Wireless remote-controlled sensors
c-PCL foams [135]	Chemical crosslinking	Biocompatible and biodegradable	Foam scaffold
SMPU / GNPs composite [136]	Physical blending	Remote shape control capability	Wireless actuators
SiC-doped PVA / PAA IPNs [137]	Situ polymerization	Environmental friendliness	MW-responsive sensors, implantable devices
SMPU-based macroporous photonic crystals [139]	Templating nanofabrication	Rewritable / reconfigurable, chromogenic	Nano-optical devices, chromogenic multifunctional sensors
PU / PS IPNs [140]	Simultaneous polymerization	Self-healing, self-cleaning, biodegradability	Textile, coating, smart actuators and bio-medical engineering

recovery rate was improved as the water content increasing, and the shape recovery rate of the SMP-PVA was enhanced with the MW irradiation intensity increasing.

For the preparation strategy of microwave-actuated SMP, in addition to chemical synthesis, it can also be constructed through doping microwave sensitive nanoparticles into thermal-actuated SMP matrix. Leng's group [134] is the first to prepare microwave-actuated self-bending composite structure by bonding pure SMP and pre-stretched CNTs / SMP (Fig. 10a). Under microwave field irradiation (40 W, 2.45 GHz), CNTs can absorb the electromagnetic energy to heat the SMP matrix, as a result of which the pre-stretched CNTs / SMP film recovered the original "constrict" shape at a higher temperature than T_{trans} . By contrast, the pure SMP film exhibited neither temperature rise nor shape change. Therefore, only the pre-stretched CNTs / SMP exhibited inhomogeneous strain and upward-bending movement (Fig. 10b). It is thus considered to be an ideal solution to the rapid remote actuation of SMP.

Subsequently, Leng's group fabricated biocompatible and biodegradable shape memory crosslinked-PCL (c-PCL) foams with high shape morphing rates upon microwave field [135]. The shape recovery capability of c-PCL foams upon external stimuli was tested as shown in Fig. 10c. It can be seen that the sample rapidly recovered its shape within 98 s under microwave irradiation, with the shape recovery rate improving by 9.8 times and 1.8 times as compared to thermal and electrical actuation, respectively. In addition, by introducing graphene nanoplatelets (GNPs), researchers produced thermoplastic polyurethane / GNPs composites with microwave-actuated shape morphing capability [136]. When the content of GNPs was 2 wt%, the specimen recovered the original shape within 30 s of microwave irradiation. The maximum strength and the yield strength for this specimen increased by 20% and 35% as compared to neat polyurethane, respectively. Du et al. [137,138] fabricated microwave-actuated shape memory SiC-doped PVA / PAA interpenetrating networks (IPNs). In this case, SiC nanoparticles were modified using a silane couple agent (KH570) to improve their compatibility with the polymer matrix, thus stable properties were significantly improved and the capability of shape recovery was promoted. Under 400 W microwave field irradiation, it reverted from the 'S' shape (i.e. temporary shape) to the "straight rod" shape (i.e. permanent shape) within 20 s (Fig. 10d).

Another strategy for microwave response is to construct specific photonic crystals (e.g. man-made periodic dielectric structures with

photonic band-gap (PBG) characteristics), which can enormously enrich the types of the SMPs and provide a new perspective for intelligent materials. The templating nanofabrication of SMPU-based copolymer was investigated for obtaining either rewritable or reconfigurable macroporous photonic crystals with the capability of microwave-responsive shape deformation [139]. The innovation achieved by the research is reflected in two aspects. One is that the combination of shape memory copolymer and macroporous structure achieved the shape memory cycle processes at room temperature. The other is that the SMP photonic crystals produced microscopic shape memory effects and can be used as optical switch in nano-optical devices.

Besides, multi-functional microwave-actuated SMP has received intensive attention, because of the advantages of intelligence, applicability, and practicality. Ghosh et al. [140] further developed the multi-functional microwave-actuated SMP composites with shape memory effect, self-healing, self-cleaning, biodegradability, excellent mechanical properties, thermostability and chemical resistance. As given in Fig. 10e, the authors fabricated the IPNs structures of bio-degradable SMPU (which was grafted by part of silicone) and polystyrene using simultaneous polymerization technique. The intelligent IPNs resolved such problems as non-intelligence, no bio-degradability, and the brittleness of polymers, which allowed them to have excellent prospects in textile, coating, smart actuators and bio-medical applications. Table 2 shows the current research progress of non-contact microwave-actuated SMP.

As mentioned above, it is apparent that there are two strategies to fabricate microwave-actuated SMPs, i.e. microwave-sensitive molecular chains [132,135] and microwave-thermal nanoparticles [134,136]. The two strategies have their own advantages and disadvantages. The microwave-sensitive molecular chains system is pure and free of impurities, but the preparation process is more complicated, however, the microwave-thermal nanoparticles system is simple to construct, but it is easy to form stress concentration points and reduce the mechanical strength. Therefore, combining the above two systems and developing new SMP system, searching for new microwave sensitive particles, and expanding functionality are the future development direction of microwave-actuated smart materials.

3.3. Ultrasound-actuated SMPs

Ultrasound, especially the high intensity focused ultrasound (HIFU), possesses some unique advantages over other stimuli, for instance, the spatiotemporal controllability by tuning exposure time and position, and the superior capability of penetration into the interior of SMP sample compared to light, as well as magnetic and microwave stimuli [141]. For ultrasound-actuated SMPs, ultrasound has cavitation functions [142,143], which enables the selective interaction with polymer molecular chains to cause the molecular chain relaxation. After the absorption of the concentrated mechanical sound wave energy, the SMPs change from temporary shape to the original shape [144–151]. Researchers have developed a lot of ultrasound-actuated SMPs for diverse applications, such as control drug release, sensors and actuators, etc. [152,153].

In terms of chemical-crosslinked poly(methyl methacrylate-co-butyl acrylate) (named P(MM-BA)) shape memory copolymers, the smart structure of ultrasound-actuated drug release was fabricated for the first time by Guo et al. [141]. The innovation of the self-shaping polymer is that the synchronized shape memory behavior and drug release performance could be adjusted by tuning HIFU intensity and exposure time. When ultrasound field was imposed on the upper areas in two steps, with the shape memory processes from "I" temporary shape to "V" intermediate shape, to "N" intermediate shape and then to "M" permanent shape observed as a result (Fig. 11a and Fig. 11b). The spatial and temporal control on the multi-shape recovery of SMP as well as concomitant drug release was achieved by switching on and off the ultrasound field.

A series of studies have been demonstrated that the intelligent

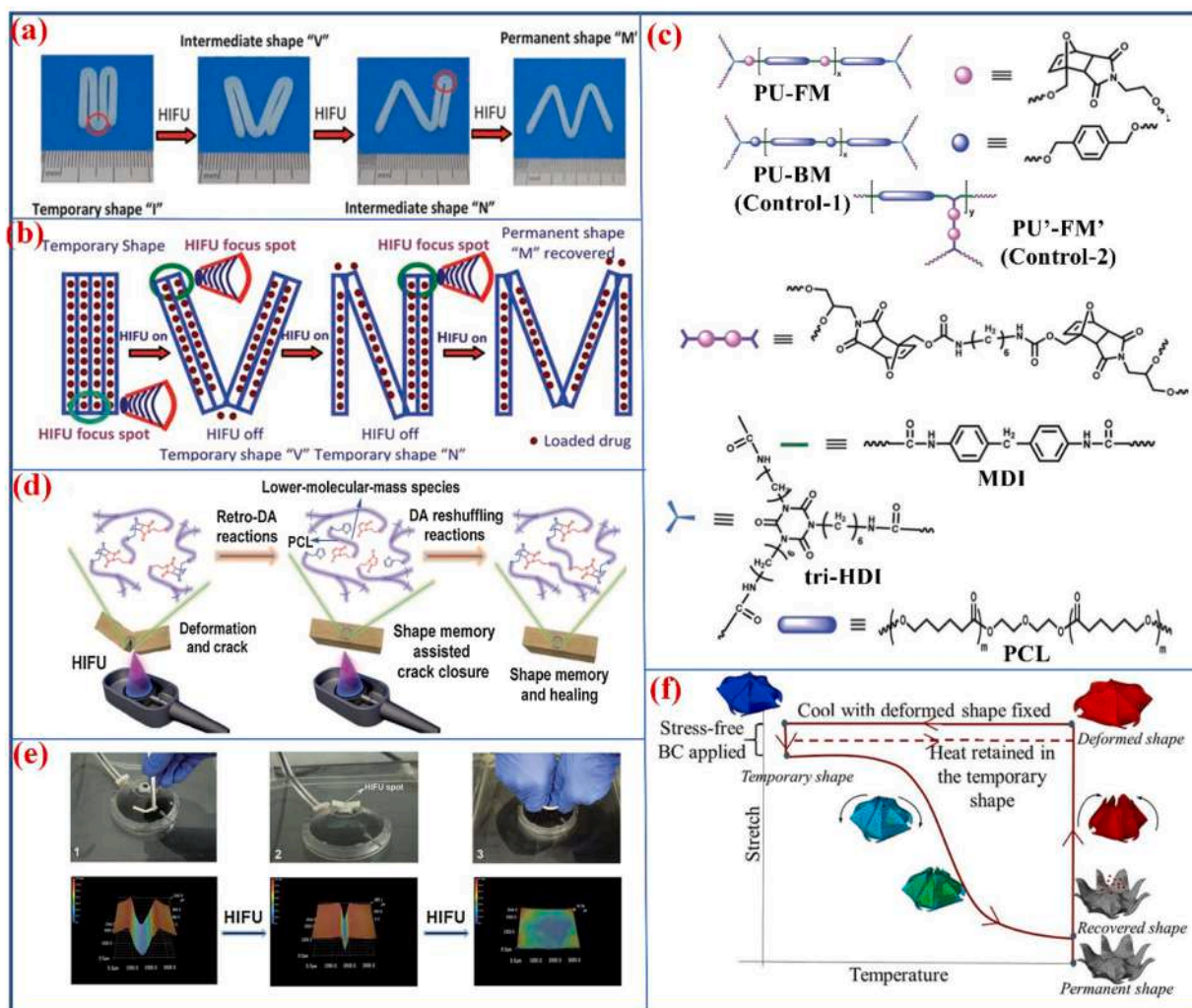


Fig. 11. (a) The photos of shape recovery process of HIFU-actuated SMP; (b) the mechanism followed by the HIFU-actuated shape recovery of the SMP and drug release. (c) The synthesis of PCL-based polyurethane bearing Diels-Alder bonds; (d) the mechanism of shape memory property and self-healing effect by ultrasound actuation; (e) the photos and 3D images of shape recovery of the PCL-based polyurethane and self-healing processes. (f) The shape memory performance of a flower shaped drug delivery container. (a,b) [141]. Copyright 2012 Royal Society of Chemistry. (c-e) [154]. Copyright 2014 Royal Society of Chemistry. (f) [158]. Copyright 2018 SPIE.

polymer with self-healing function can extend the service life, because of the advantages of durability and reliability. For instance, the dynamic reversible covalent bonds (DA bonds) was grafted into PCL-based shape memory polyurethane, which presented shape change and self-healing properties under high-intensity focused ultrasound field [154]. The synthesis strategy of the polymer is shown in Fig. 11c. With the accumulation of ultrasound energy, the temperature of the damaged area was increased rapidly to bring about the relaxation of molecular chains. Meanwhile, the DA bonds underwent a retro-DA reaction to result in the reversible degradation of the polymer networks. Thus, the sample exhibited both shape recovery behavior and self-healing property (Fig. 11d and Fig. 11e). A novel concept for ultrasound-actuated SMP with self-healing property was proposed for the first time, thus presenting a broad prospect for anti-fatigue medical devices.

It is well known that the strength of polymers is usually inferior to that of metals and ceramics, especially hydrogel materials, of which the mechanical strength is generally less than 3 MPa. However, the melamine enhanced PVA physical hydrogel displayed excellent mechanical ability, biocompatibility, self-healing and ultrasound responsive shape memory capability [155]. In the polymer system, the melamine as an effective physical crosslinker reacted with hydrogen bonds of the PVA to generate a stable physical hydrogel and the tensile strength reached

about 4.5 MPa. Through the ultrasound-actuated (3 MHz, 2 W/cm²) shape recovery experiment, the SMP hydrogel had shape changing behavior, which would be utilized to treat blood clots, etc.

Moreover, biodegradable ultrasound-actuated intelligent polymers, which can act as drug delivery container to apply to biomedical engineering, have received intensive attention from researchers. Han and colleagues [156] studied on the properties of ultrasound-actuated shape memory biodegradable polyurethane composites. Min et al. [157] prepared an ultrasound-actuated shape memory biodegradable cylinder structure consisting of chitosan-functionalized PLA microspheres. Bhargava et al. [144] presented an ultrasound-actuated thermal actuation of shape memory polymers, which can be applied as a potential drug delivery system in biomedical engineering. Besides, Bhargava et al. [158] constructed an ultrasound-actuated artery-scale SMP structure as drug delivery container in Fig. 11f which showed the shape memory process and drug release behavior of a flower shaped container upon focused ultrasound stimulus. Accordingly, the ultrasound-actuated SMP has bright prospects for microscale capsules. Using ultrasound-actuated SMP as a drug delivery carrier, it can be applied to medical engineering and has many advantages. For example, it can achieve targeted and controlled drug release behaviors, thereby reducing the systemic harm and side effects to the patient. More importantly, it can enormously

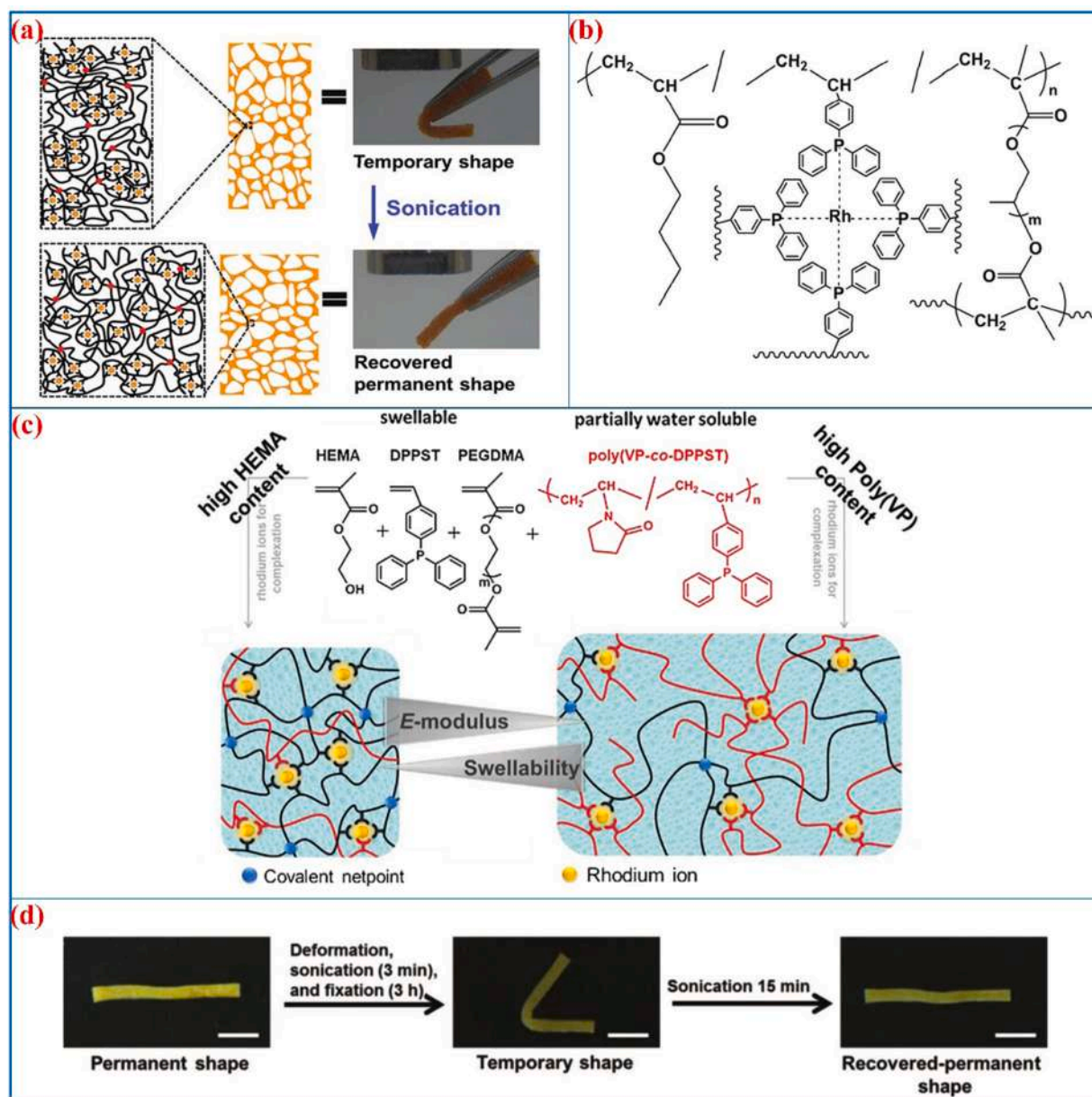


Fig. 12. (a) The shape memory effect of the Rh-P coordination polymer networks; (b) the molecular structure of the polymer networks. (c) The molecular structure of ultrasound-actuated shape memory semi-IPN hydrogels; (d) the photos of shape memory processes of the semi-IPN hydrogels. The scale bars were 10 mm. (a,b) [159]. Copyright 2016 Wiley-VCH. (c,d) [50]. Copyright 2020 Wiley-VCH.

improve the efficacy of medicines to cure disease.

Another approach for responsive intelligent polymer is to construct the topological structure, which can produce shape change upon ultrasound stimulus [159]. The SMP was formed by the macroporous rhodium-phosphine (Rh-P) coordination polymeric networks, and the ultrasonic cavitation based mechanical force dissociated the Rh-P microphases reversibly, thus leading to the topological rearrangement of the SMP molecular switches. The rearrangement of the molecular switches released the internal stress in the polymer networks to result in ultrasound-actuated shape memory behavior (Fig. 12a). The molecular structure of the Rh-P coordination SMP networks was composed of poly(n-butyl acrylate) and poly(propylene glycol) dimethacrylate as the elastic polymer backbone and the covalent netpoints, respectively (Fig. 12b). This structure addressed the key challenge that the ultrasound field acted effectively throughout the entire polymer sample rather than being limited to the surface of the sample. Subsequently, a hydrophilic shape morphing semi-IPN hydrogel based on the Rh-P

coordination bonds was designed, which could be triggered by ultrasound field as well [50]. More specifically, the hydrogel molecular chain structures were composed of diphenylphosphinostyrene (DPPST), poly(ethylene glycol) dimethacrylate (PEGDMA), hydroxyethyl methacrylate (HEMA) and poly(VP-co-DPPST) (Fig. 12c). Both the swelling characteristics and mechanical properties of the smart hydrogel can be dramatically improved by the combination of poly(VP) and poly(HEMA) [160]. Rh-P coordination bonds could be considered as temporary crosslinked points [161] and applied as mechanical sensitive molecular switches in shape memory hydrogel (Fig. 12d).

The present research progress of ultrasound-actuated SMPs is summarized in Table 3. The currently ultrasound-actuated SMPs are all intrinsic responsive materials, which have the following advantages: overall uniformity, no impurities, no stress concentration points, and fatigue failure resistance. However, there are few molecular structures available for ultrasonic cavitation, which hinder the further development of the SMPs. Thus, the exploration of new ultrasound-actuated

Table 3
The research progress of ultrasound-actuated SMPs.

Ultrasound-actuated SMP	Preparation strategy	Property	Prospect application
Poly(MM-co-BA) copolymers [141]	Chemical-crosslinking	Non-toxic, biocompatible	Drug release
PCL-based polyurethane [154]	Chemical-crosslinking	Self-healable	Anti-fatigue medical devices
Melamine enhanced PVA physical hydrogel [155]	Physical-crosslinking, hydrogen bonds	Biocompatibility, self-healable	Hydrogel dressing
SMPU [156]	Chemical-crosslinking	Biodegradable	Minimally invasive interventional therapy devices
PLA microspheres [157]	Water-in-oil-in-water emulsion method	Biodegradable	Minimally invasive implants and scaffolds
Artery-scale SMP [158]	Chemical-crosslinking, acoustic-thermoelastic modeling	Biocompatibility, biodegradable	Drug delivery container
Poly(n-butyl acrylate) and poly(propylene glycol) dimethacrylate hydrogel [159]	Rh-P coordination, topological structure	Porous, CMF	Mechanosensors or ultrasound-controlled switches
DPPST, PEGDMA, HEMA and poly(VP-co-DPPST) hydrogel [50]	Rh-P coordination bonds, semi-IPN structure	Porous, CMF	Witches or mechanosensors

SMPs and the endowment of them with more powerful functions, such as biocompatibility, biodegradability, adaptability, self-cleaning, etc., as well as clinical reliability verification will be the focus of future challenges.

3.4. Photo-actuated SMPs

Photo-actuated SMPs are capable to deform or recover shape under illumination, including visible light, near infrared (NIR) light and ultraviolet (UV) light [162–167]. According to the exact chemical compositions, photo-actuated SMPs are divided into two categories: photochemical-actuated SMP [168,169] and photothermal-actuated SMP [170–173]. Photochemical-actuated SMP is referred to the polymer networks grafted or blocked the photo-chemical reactive groups, and the corresponding macroscopic reshaping properties are determined by light-controlled chemical structure variation. Apart from the intrinsic photo-responsive SMPs, the photo-thermal fillers with high light-to-heat conversion efficiency are also commonly introduced into thermal-actuated SMP matrix for producing photo-actuated shape memory effects. Below is a detailed discussion about photo-actuated shape memory polymers, shape memory mechanism and their prospects.

3.4.1. Photochemical-actuated SMPs

Photochemical-actuated SMPs are prepared by introducing photochemical reactive groups or molecules as "molecular switches" into the polymer networks [174,175]. According to the types of shape memory mechanism, the photochemical-actuated SMPs are divided into photocycloaddition-based SMP, photoisomerization-based SMP and photoplasticization-based SMP. The photocycloaddition-based SMP is identified as the polymer containing cinnamic acid molecules with photo-dimerization characteristics. The two adjacent cinnamic acid molecules undergo poly-cyclization reaction to form cyclobutene under UV light irradiation. Also, the formed ring structure can be opened up by

photolysis reaction [176,177]. Photoisomerization-based SMP is mainly indexed as the polymer containing azobenzene molecules. Under a certain wavelength of irradiation, the molecules undergo reversible transformation between cis-conformation and trans-conformation to drive the macroscopic deformation to the polymer [178–182]. Photoplasticization-actuated SMP refers to the polymer containing spiropyrans. When spiropyrans are excited by UV light, the C-O bonds of the molecular structure are cleaved, thus forming ring-opened structures. These ring-opened structures weaken the interaction force of the polymer molecular chains, which is conducive to the movement of the amorphous region and the soft segment crystallization region for the shape restoration of the polymer. Additionally, the polymer turns purple. Then, through either visible light irradiation or heating, the spiropyran molecules shift from ring-opened structures to ring-closed structures, and the polymer turns orange [183]. Below is a detailed summary of the three types of photochemical-actuated SMPs.

The preparation method for the first photocycloaddition-based SMPs was to graft cinnamic acid (CA) onto acrylate copolymer networks [51]. When irradiated with a wavelength larger than 260 nm, two CA molecules within the thin film experienced poly-cyclization reaction to form cyclobutene. Meanwhile, the temporary shape was fixed. When the wavelength was decreased below 260 nm, the cyclobutene experienced photolysis reaction, with the thin film returning to the original status. The temperature of the polymer was remained unchanged during the photo-controlled deformation, suggesting that the shape morphing behavior was responsive to external light sources.

Photocycloaddition-based smart polymer based on poly(L-lactide)-co-poly(ethylene glycol) (named PLA-PEG) was developed by Xie et al. [184]. The anthracene groups underwent [4 + 4] photodimerization under a 365 nm ultraviolet light irradiation. Then, the formed photodimer cleaved to the original monomers as a result of exposure to 254 nm UV light. The authors conducted test on the photo-actuated shape memory processes of the thin film PLA-PEG (Fig. 13a). The experimental results indicated that sample D retained the temporary shape and recovered its original status under UV irradiation with the wavelength of 365 nm and 254 nm, respectively. The shape fixation ratio (R_f) and the shape recovery ratio (R_r) were calculated as 58.9% and 79.6%, respectively [185].

As a typical intelligent soft material, liquid crystal elastomer (LCE) has both elasticity and liquid crystal anisotropic characteristics and multi-field sensitivity. It has a wide range of application fields such as intelligent structure design and control, new acousto-optic electronic devices, and soft robot development. Yu's group [52] applied photo-responsive isomeric azobenzene as a liquid crystal element to prepare LCE. Under a 366 nm UV light irradiation, azobenzene groups were transformed into cis-structures, thus causing the shift of LCE from nematic structure to isotropic structure. Macroscopically, the LCE thin film exhibited shape bending behavior. When irradiated by a visible light of greater than 540 nm, the LCE was transformed from isotropic phase to nematic phase, and the sample showed shape recovery behaviors macroscopically (Fig. 13b).

Spiropyran compounds not only have photochromic and force-chromic features, but also produce photoplasticization effects [186–188], which make them suitable for preparing photoplasticization-actuated SMP. Zhang et al. [189] developed UV-responsive SMPs by mixing spiropyran compounds with the shape memory EVA matrix. It was found that the pure EVA cannot exhibit shape changing behavior, while 0.5 wt% and 3 wt% spiropyran contents of the thin films produced shape changing performance upon UV light irradiation (Fig. 13c). Fig. 13e shows the photo-actuated deformation and photochromic mechanisms of spiropyran compounds. According to the photoplasticization effect, the authors designed a reflector with a micropattern array as shown in Fig. 13d. The polymers with both color-changing and photo-actuated shape memory capability have a prospect of widespread applications, for example, optical information storage, anti-counterfeiting, bionic camouflage and color-changing

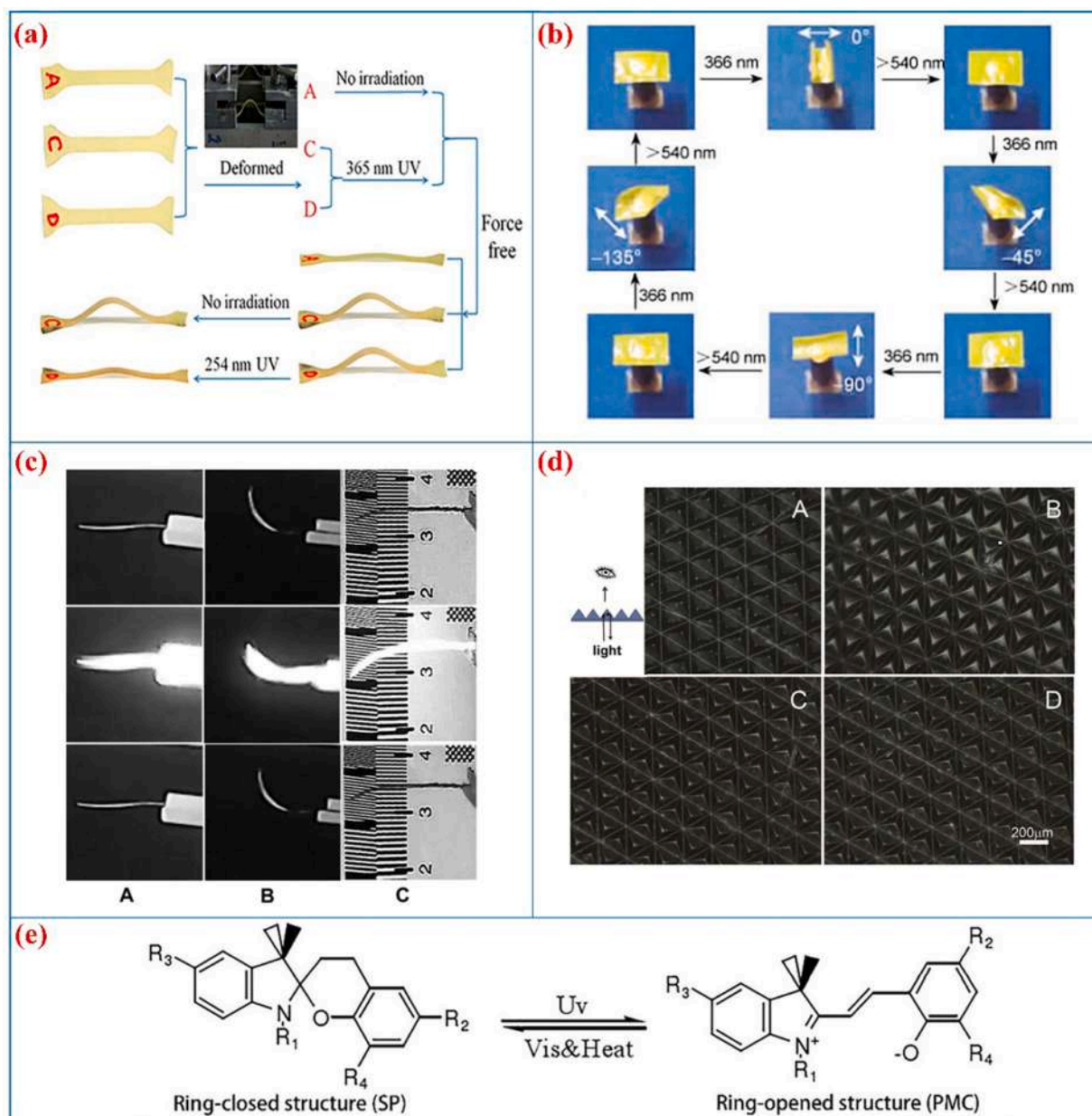


Fig. 13. (a) The photos of qualitative researches of the thin film A, C and D. (b) The 3D motion of the thin film under different wavelength irradiation. (c) The shape changing behavior of EVA films triggered by UV light irradiation. A was pure EVA, B and C were the EVA film containing 0.5 wt% and 3 wt% spiropyran, respectively; (d) the photos of an EVA / 3 wt% spiropyran reflector with a microprism array, among them. A was the original shape, B was temporary shape, C and D were recovered shape under 30 mW/cm² ultraviolet light irradiation for 1 min and 70 °C for 1 min, respectively. (e) The deformation and discoloration mechanism of spiropyran molecules.

(a) [184]. Copyright 2016 American Chemical Society. (b) [52]. Copyright 2010 Royal Society of Chemistry. (c, d) [189]. Copyright 2014 Royal Society of Chemistry. (e) [190]. Copyright 2019 Royal Society of Chemistry.

smart clothing [190].

Among the photochemical-actuated SMPs, as compared to SMPs actuated by cinnamic acid groups and azobenzene groups, the studies on the SMPs actuated by spiropyran are quite limited due to the smaller deformation ratio associated with the photoplasticization effect. However, the spiropyran-based SMPs possess photochromic and forcechromic property, thus widening the scope of their applications.

3.4.2. Photothermal-actuated SMPs

One common strategy for fabricating photothermal-actuated SMPs is doping photothermal nanoparticles into thermal-responsive SMP matrix. When they are irradiated with a certain of light, the photothermal nanoparticles can directly convert light energy into heat energy, then,

the SMP matrix is slowly heated over the T_{trans} to drive shape recovery [191]. There are a wide variety of photothermal fillers used for the fabrication of photothermal-actuated SMPs, including carbon black, carbon nanotubes, graphene, graphene oxide, gold nanoparticles, gold nanorods, silver nanowires, rare earth organic complexes and so on. [192–199].

The first photothermal-actuated SMP composite was prepared by mixing carbon nanotubes (CNTs) and SMPU [200]. The authors conducted study on the near-infrared light-actuated shape memory properties of the samples containing carbon black (CB) and CNTs, respectively, which led to the finding that the shape recovery ratio of the CB / SMPU composite ranged from 25% to 30%. In contrast, the CNTs / SMPU composite recovered the original shape within as fast as 5 s, and

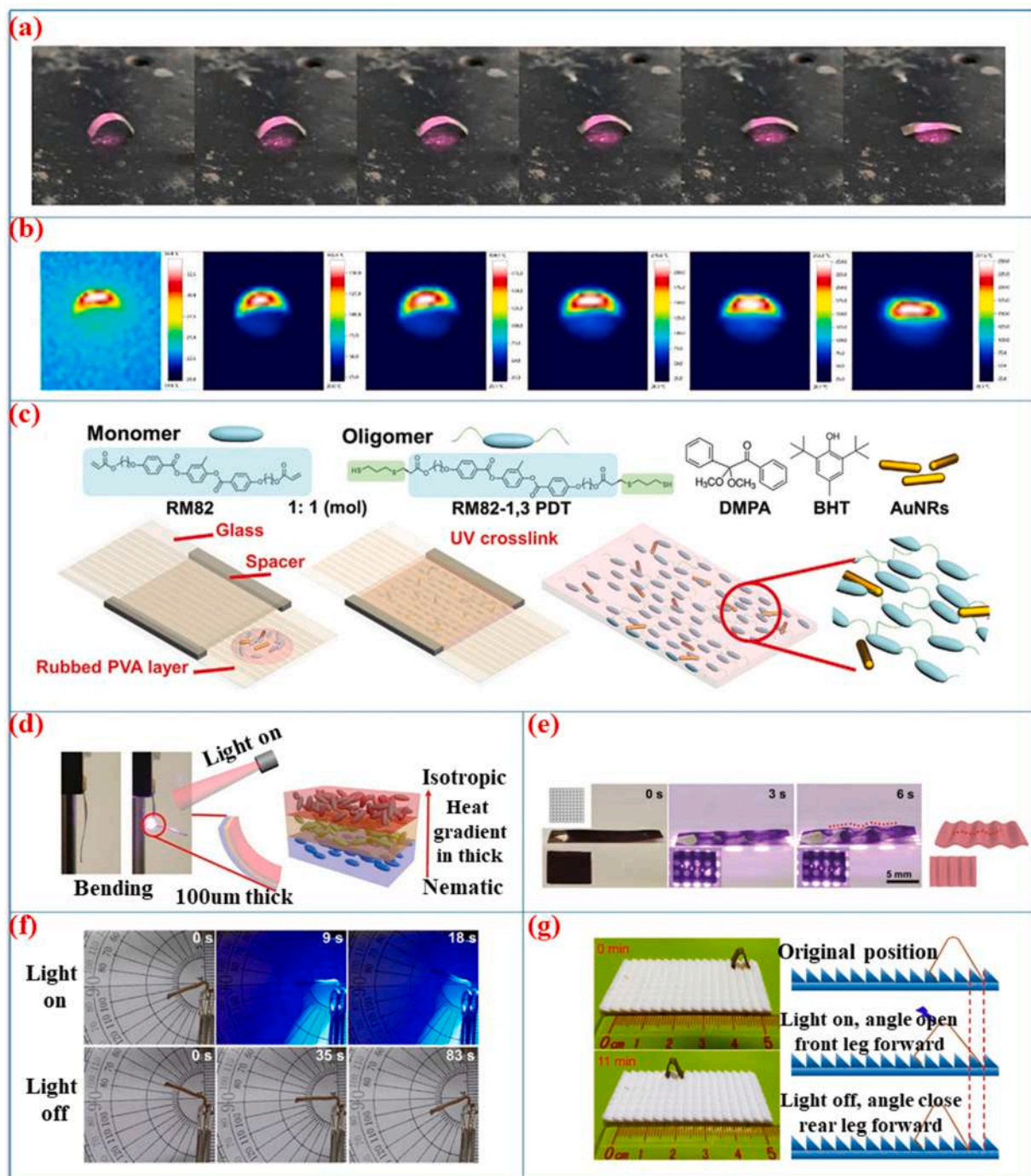


Fig. 14. (a) Shape recovery process of the AgNWs / SMPI thin film actuated by near-infrared light irradiation; (b) the temperature distribution of the thin film on the thermal infrared image. (c) The fabrication process of AuNRs/LCE films; (d) the diagram of the shape bending mechanism; (e) the film is exposed to a photomask, forming a wave pattern structure. (f) The images of the sample when the light was turned on and off; (g) the images and diagram of the microrobot self-locomotion. (a,b) [201]. Copyright 2018 Jilin University. (c-e) [202]. Copyright 2020 Wiley-VCH. (f,g) [230]. Copyright 2018 American Chemical Society.

the shape recovery ratio was nearly 100%. The synergy between the anisotropy of CNTs and the crystalline segments of polyurethane is responsible for this phenomenon. Yao et al. [201] studied NIR light-actuated shape memory polyimide (SMPI) films by coating the surface of SMPI with a layer of silver nanowires (AgNWs) with photothermal effect and conductive property (Fig. 14a and Fig. 14b). As one of the most promising engineering plastics in the 21st century, polyimide is referred to as a “problem solver”, especially in the field of microelectronics technology. Thus, the SMPI and composite are expected to be applied as remote sensing circuit or protection circuit, which is of great

significance to guiding practical applications.

It is well known that thermotropic liquid crystals could form a certain degree of orientation and orderly arrangement at low temperature, which cause the appearance of nematic phase in the molecular structure. With the temperature increasing, the mobility of liquid crystal molecules could be enhanced, which makes the molecular structure exhibit an isotropic state. Macroscopically, the thermotropic liquid crystals perform shape change upon thermal stimulus. However, Zhang et al. combined LCE and gold nanorods (AuNRs) to obtain the composite possess light-controlled shape morphing property (Fig. 14c), so that the

Table 4
The development of photo-actuated SMPs in recent years.

Photo-actuated SMP	Group	Type	Wavelength
SMPU[200]	CNTs	Photothermal type	808 nm
Acrylate copolymer[51]	Cinnamic acid	Photochemical type	$\lambda_1 > 260$ nm; $\lambda_2 < 260$ nm
LCE[52]	Azobenzene	Photochemical type	$\lambda_1 = 330\text{--}380$ nm; $\lambda_2 > 420$ nm
LCE[202]	Gold nanorod	Photothermal type	785 nm
EVA[189]	Spiropyrans	Photochemical type	365 nm
PCL-co-PEG[184]	Anthracene	Photochemical type	$\lambda_1 > 260$ nm; $\lambda_2 < 260$ nm
PCL[232]	TiN	Photothermal type	800 nm
SMPU, EVA matrix[233]	Azobenzene, AuNPs, Nd(TTA) ₃ Phen, Yb(TTA) ₃ Phen, Sm(TTA) ₃ Phen	Photochemical type and photothermal type	UV light; 520 nm; 808 nm; 980 nm; 1064 nm
PCL[230]	Polydopamine nanospheres	Photothermal type	365 nm
SMPI[201]	Silver nanowire	Photothermal type	808 nm
PVA[207]	PAN fibers	Photothermal type	808 nm
EVA[225]	p-aminodiphenylimide	Photothermal type	365 nm
SMPU[234]	Azobenzene, NaYF ₄ : Yb 25 mol%, Er 2 mol%@NaYF ₄ : Nd 30 mol % Core-Shell	Photochemical type and photothermal type	UV light; 808 nm
Poly (vinyl butyral)[210]	GO	Photothermal type	808 nm
Poly(methyl methacrylate-co-itaconic acid)[212]	Sm(TTA)Phen(NO ₃) ₃	Photothermal type	1064 nm

LCE was not limited by thermal-actuated deformation [202]. Under the near-infrared light irradiation with a wavelength of 800 nm, AuNRs could absorb and convert light energy into heat energy, and transfer the heat energy to the LCE matrix. When near-infrared light switches on and off, the LCE transforms between nematic phase and isotropic state, so, the LCE film shows shape deformation and recovery macroscopically (Fig. 14d). After that, the author demonstrated the wave pattern deformation and recovery of the LCE film in Fig. 14e. This work opens the door toward creating reprogrammable and remote actuated soft robots by combining LCE and photothermal nanoparticles.

Conventional photothermal-actuated SMP has the drawbacks of one-way shape response deformation, which limits their utilization fields. In this case, multifunctional, and biodegradable SMPs have received intensive attention and represent the most popular research direction [203–209]. For example, researchers applied graphene oxide (GO), xylene diisocyanate, and poly (vinyl butyral) (PVB) to construct NIR light-actuated shape memory crosslinked polymer composites [210, 211]. When the composite was exposed to 1.4 W/cm² near-infrared light irradiation for 5 min, the permanent shape was re-deformed, thus enabling the potential applications in soft robots and self-deploying structures. Besides, the rare earth filler with a fluorescent function is also an important photothermal absorber. Photothermal responsive multi-functional SMP composites based on rare earth organic complexes Sm(TTA)Phen(NO₃)₃ [212] and poly(methyl methacrylate-co-itaconic acid) were prepared by Wang et al. [213]. The composites emitted fluorescence under UV light and exhibited shape morphing behavior under the near-infrared light irradiation with a wavelength of 1064 nm.

Apart from the one-way SMP, photothermal-actuated two-way shape memory polymers (i.e. 2 W-SMP) were also prepared, which provide a new perspective for smart materials in the area of actuator and soft robot fields [214–221]. Such as photothermal nanoparticles as CNTs, gold nanoparticles, polydopamine nanospheres and so on were doped into the reversible thermal-actuated SMP matrix for absorbing the light of a certain wavelength and converting light energy into heat energy, so as to actuate the two-way shape memory matrix materials like semi-crystalline EVA [222], semi-crystalline polyurethane [223], semi-crystalline PCL [224], and so on. Leng's group [225] fabricated an UV-actuated two-way SMP composite (EVA / p-AP) by introducing photothermal filler p-aminodiphenylimide [226] into shape memory EVA matrix. It implies that the sample switched reversibly upon UV on-off stimulation. Polydopamine (PDA) nanospheres possess high

photothermal conversion properties due to their strong 400–500 nm light absorption [227–229]. Wang et al. prepared photothermal-actuated two-way SMP composites by doping PDA nanospheres into shape memory PCL matrix [230]. As shown in Fig. 14 f, the composite showed reversible angle changes and two-way shape morphing behavior when the light was turned on and off. This is the first report on the light responsive two-way SMP with PDA nanospheres as photothermal fillers. The authors also designed a self-locomotion microrobot as given in Fig. 14 g. The tensile strength reached 1.1 MPa, which was about 3 times higher than that of most mammalian skeletal muscle (0.35 MPa) [231]. Therefore, such reversible photothermal-actuated PDA / PCL SMPs hold the potential of practical applications in artificial muscles and actuators.

The above-mentioned typical examples reflect the research progress made in photo-actuated SMPs, e.g. photochemical-actuated SMPs, photothermal-actuated SMPs, multi-functional photothermal-actuated SMPs, and photothermal-actuated two-way SMPs, etc. In order to fully demonstrate the development of photo-actuated SMPs, the photo-actuated SMPs and actuation wavelength are summarized in Table 4.

4. Multi-stimuli selective control and staged transformation

The multi-stimuli selective control of complex SMPs systems is crucial for promoting their utilization fields [235,236], e.g. selective actuators [237], information storage [238], adjustable sensors [239], and flexible robots [240], etc. Meanwhile, the multiple shape memory polymer systems capable of multistage shape transformation behaviors have become increasingly significant over the past years [241–248].

4.1. Multi-stimuli selective control

Multi-stimuli selective control of SMP has the characteristics of multi-response and controllability. According to different application scenarios, suitable stimulation methods can be selected to drive the shape morphing, which enormously improves the adaptability of intelligent devices. Typically, a multi-wavelength sensitive SMP composite was fabricated by Fang et al. [233]. Among them, azobenzene group was grafted onto SMPU molecular chains, by contrast, Sm(TTA)₃Phen, Yb(TTA)₃Phen, Nd(TTA)₃Phen, and gold nanoparticles (AuNPs) were selectively doped into the thermal-response shape memory EVA matrix [249–251]. When irradiated at 1064 nm, 520 nm, 808 nm, and 980 nm,

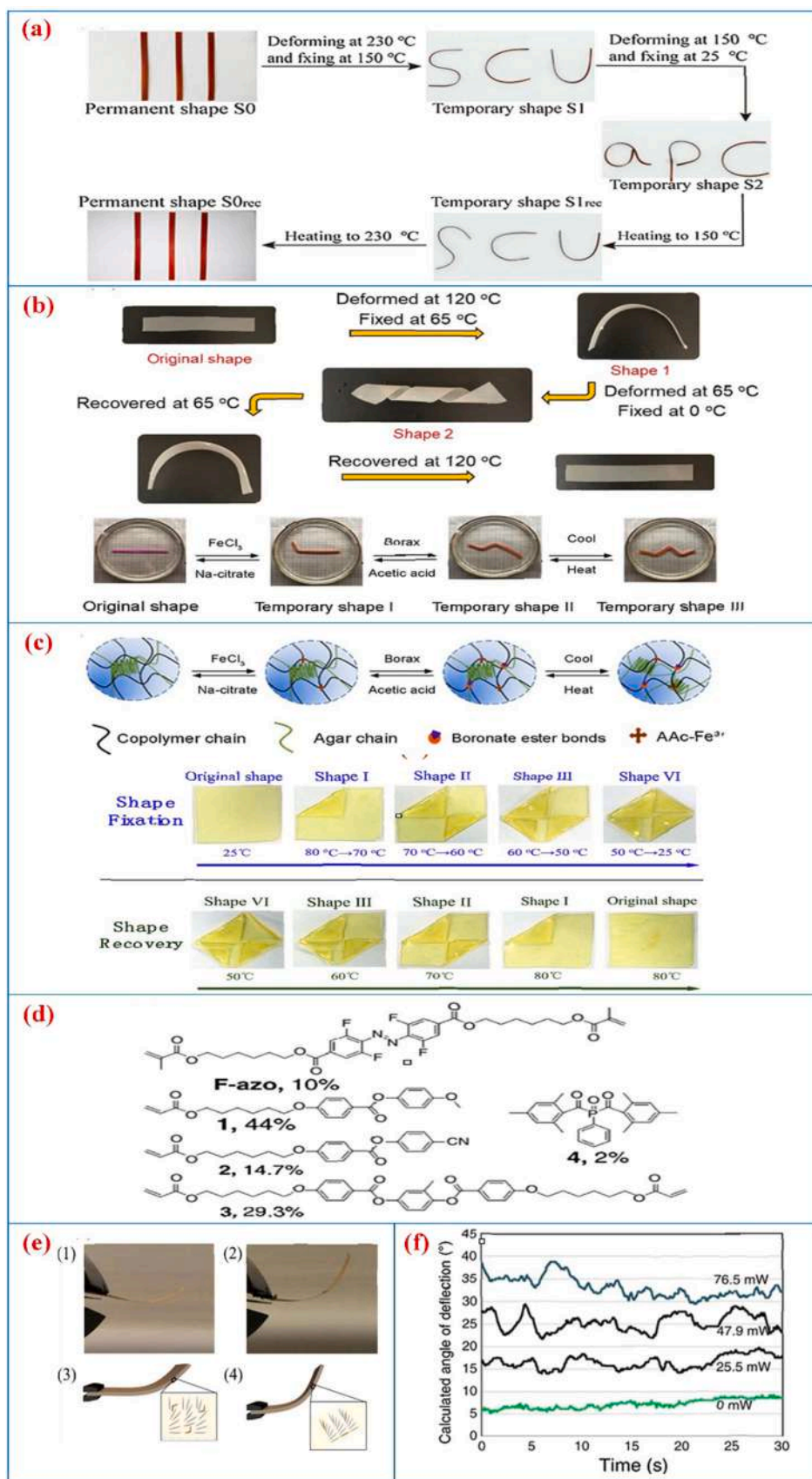


Fig. 16. (a) The photos of triple-shape memory performances of the smart thermosets. (b) The triple-shape memory performances of the poly(ester urethane)s sample. (c) The images of quadruple shape memory performances of the hydrogels. (d) The images of the quintuple-shape memory performances of the zwitterionic poly-urethanes. (e) The molecular components of the LCE; (f) the photos of the sample after irradiation on 530 nm green light and 405 nm blue light; (g) the deflection angle-time curve of LCE films during exposure to green light and blue light. (a) [269]. Copyright 2020 Springer. (b) [270]. Copyright 2020 Wiley. (c) [272]. Copyright 2020 Springer. (d) [273]. Copyright 2018 Elsevier. (e-g) [278]. Copyright 2016 Nature Publishing Group.

as well as UV light, the multi-segments and multi-stimuli of EVA-Sm, EVA-Au, EVA-Nd, EVA-Yb and azo-PU thin films exhibited shape changes sequentially (Fig. 15b). Besides, the sequence of light irradiations with different wavelengths had a significant impact on the shape recovery process, as shown in Fig. 15c and Fig. 15d. The combination of the photochemical-actuated SMP and the photothermal-actuated SMP in the composite system provides a new idea for the preparation of multiwavelength selective responsive SMPs, which is conducive to broadening the scope of applications for the photo-actuated SMPs.

Origami techniques are being investigated and used in space structures and are also applied to biological advancements. Origami creates deployable structure that morphs from 2D to 3D, which is also inseparable from the multi-stimuli selective controlled smart polymers. Li et al. [252] applied Fe^{3+} / poly(acrylic acid) (PAA) / poly(ethylene oxide) (PEO) and PDA / PAA / PEO composite film to design a multi-stimuli actuated origami with selective shape morphing capability. It could be folded into plane shapes, before being transformed into a series of targeted 3D shapes when UV or visible light, and near-infrared light or heating were applied, respectively. This is related to the reduction and oxidation of Fe^{3+} [253–255]. Besides, the group continued to incorporate polydopamine nanoparticles into the PEO / PAA matrix, with the shape recovery of the paper airplane, bionic flower and plastic hasp actuated by NIR irradiation (Fig. 15e). The 3D shape transformations of smart origami structure with complex, flexible and controllable shape morphing behaviors enriched the strategy of selective control on SMP.

Radiofrequency (RF) field is also a flexible remote-controlled strategy for selective control. He and colleagues [256] demonstrated the selective control on shape memory CNTs-SMP, Fe_3O_4 -SMP, and neat SMP through two radiofrequency (RF) fields (13.56 MHz and 296 kHz respectively) and heating fields, in sequence. And the selective control of polymers could be applied in smart switches and actuators with multi-task and multiple capabilities.

Most of the photothermal particles absorb and convert near-infrared light energy, such as graphene, gold nanoparticles, polydopamine particles, etc., but very few particles absorb ultraviolet light energy, which limits the diversified development of light-controlled SMP. Here, the SMP architecture formed by $\text{Zn}(\text{Mebip})_2(\text{NTf}_2)_2$ / epoxy composite and neat epoxy resin showed selective response to UV light and heating (Fig. 15f-h) [257]. Among them, $\text{Zn}(\text{Mebip})_2(\text{NTf}_2)_2$ can directly convert UV light energy into thermal energy [258]. The authors applied smart composite to design the robot hands capable to grab and release the metal spring, as shown in Fig. 15i. This also provides a novel approach for the intelligent soft robot, that is, by selectively driving a certain segment of the multi-stimuli SMP, it can complete the task of remotely grasping the target.

Also, researchers have made plenty of effort on exploiting the selective, responsive SMPs with multifunctionalities, which made them suitable for preparing biomedical equipment, smart actuator and so on. For example, Yang's group [259] developed the selective controllable actuation, fast self-repairing supramolecular networks consisting of 2-ureido-4-pyrimidone supramolecular, poly(ethylene glycol), and poly(ϵ -caprolactone). Huang et al. [260] designed multi-stimuli selective shape changes poly(lactic acid) / epoxidized natural rubber / Fe_3O_4 composites, which not only possessed magnetic and photo responsive shape memory properties upon alternating magnetic field and 808 nm NIR irradiation, but also had superior biocompatibility and exhibited broad prospects in biomedical fields. Also, using an azobenzene-containing LCE and single-walled CNTs / LCE composite, Wang et al. prepared a thermal / UV / NIR triple-stimuli-responsive shape memory LCE, which can be selectively controlled by adjusting the wavelength of light irradiation.

4.2. Staged transformation

Multiple shape memory polymers [261–268] can be programmed into diverse temporary shapes and perform multi-stage shape recovery

upon external stimuli, including light, heat, magnetic, electric fields and so on. Ning et al. [269] prepared triple-shape memory thermosets based on the bismaleimide polymer and bisallyl compounds with dynamic ester bonds. Fig. 16a shows that the SMPs exhibit triple-shape memory behaviors under heating stimulation to 150 °C and 230 °C, in sequence. Karasu et al. [270] designed multiple shape memory poly(ester urethane) which consisted of poly(1,4-butylene adipate), poly(butylene succinate) and poly(hexamethylene dodecanoate). The SMPs were fixed into two different temporary shapes at 65 °C and 0 °C, respectively, as shown in Fig. 16b. Also, by reheating to 65 °C and 120 °C, the sample showed sequential shape changes respectively, which made it applicable in temperature-sensitive actuators.

Through reasonable molecular structure design strategies, quadruple and quintuple shape morphing polymers were also been constructed, among them, the quadruple SMP can be programmed to three temporary shapes, while the quintuple SMP can be programmed to four temporary shapes. Zhao et al. [271] developed the quadruple shape memory organic-inorganic copolymers consisting of double-decker silsesquioxane, 2-ureido-4[1 H]-pyrimidinone and polycyclooctadiene. Due to the interaction between quadruple hydrogen bonds, the SMP possessed self-healing properties as well. Wang et al. [272] fabricated the quadruple shape memory hydrogels consisting of acrylic acid, acrylamide, agar and poly(vinyl alcohol). Within the borax solution, the smart hydrogels exhibited self-healing behavior due to plenty of borate bonds present in the SMPs. Fig. 16c shows the quadruple shape memory behaviors of the SMP under heat, acetic acid and Na-citrate stimulation. Besides, Zhuo et al. [273] prepared shape memory zwitterionic polyurethanes, with up to quintuple shape memory behaviors triggered by heating or moisture. Fig. 16d shows the quintuple-shape unfolded behaviors at 50 °C, 60 °C, 70 °C, and 80 °C in succession. Gao et al. [274] designed a programmable and malleable quintuple-shape memory polymer based on a type of poly(vinyl alcohol derivative) with a broad range of glass transition temperature. The unique feature of the multiple SMP is that they can remember multiple temporary shapes while being programmed into complex shapes, thus addressing the problems of single shape and single function and enabling the adaptability to complex environments. They have a high potential to be applied in smart valves, fixation devices, biomedical engineering and aerospace environment, etc.

In addition to the multiple SMPs, multi-stimuli responsive SMPs hybrid composites have also been explored to achieve high shape programmability and stated shape recovery behaviors. Thermal- and water-actuated shape memory rubber composites were fabricated by natural *Eucommia ulmoides* rubber and polyethylene oxide [275]. The composites exhibited both high mechanical properties and double-stimuli shape morphing behaviors. By introducing dynamic imine bonds into styrene-butadiene rubber / graphene composites, a thermal- and NIR-actuated shape memory vitrimer exhibited high mechanical property and malleability [276]. It paved a way for the development of various vitrimers by combining nanoparticles, polymers and dynamic covalent chemistries. Besides, the shape memory nanocomposites consisting of poly(butylene succinate)-co-poly(ϵ -caprolactone) multi-segments copolymer and MWCNTs were designed [277]. The nanocomposites produced multi-stimuli shape memory effects under electric and NIR irradiation, which showed the shape fixed ratio and recovery ratio both over 98%.

Another interesting multi-stage shape deformation intelligent system is the self-oscillating LCE material. Kumar et al. [278] designed a self-oscillating sunlight-actuated LCE actuator capable of continuous chaotic oscillatory motion when exposed to blue and green light (Fig. 16e and Fig. 16 f). After irradiation with the green light of 530 nm for several seconds, the LCE film was made flat, which was because the $n-\pi^*$ transition of the cis isomers led to a slight reduction in the local molecular order. After irradiation with a 405 nm blue light, the LCE film showed a bent shape because of cis-trans photoisomerization in the azobenzene groups. As illustrated by the curves in Fig. 16 g, the

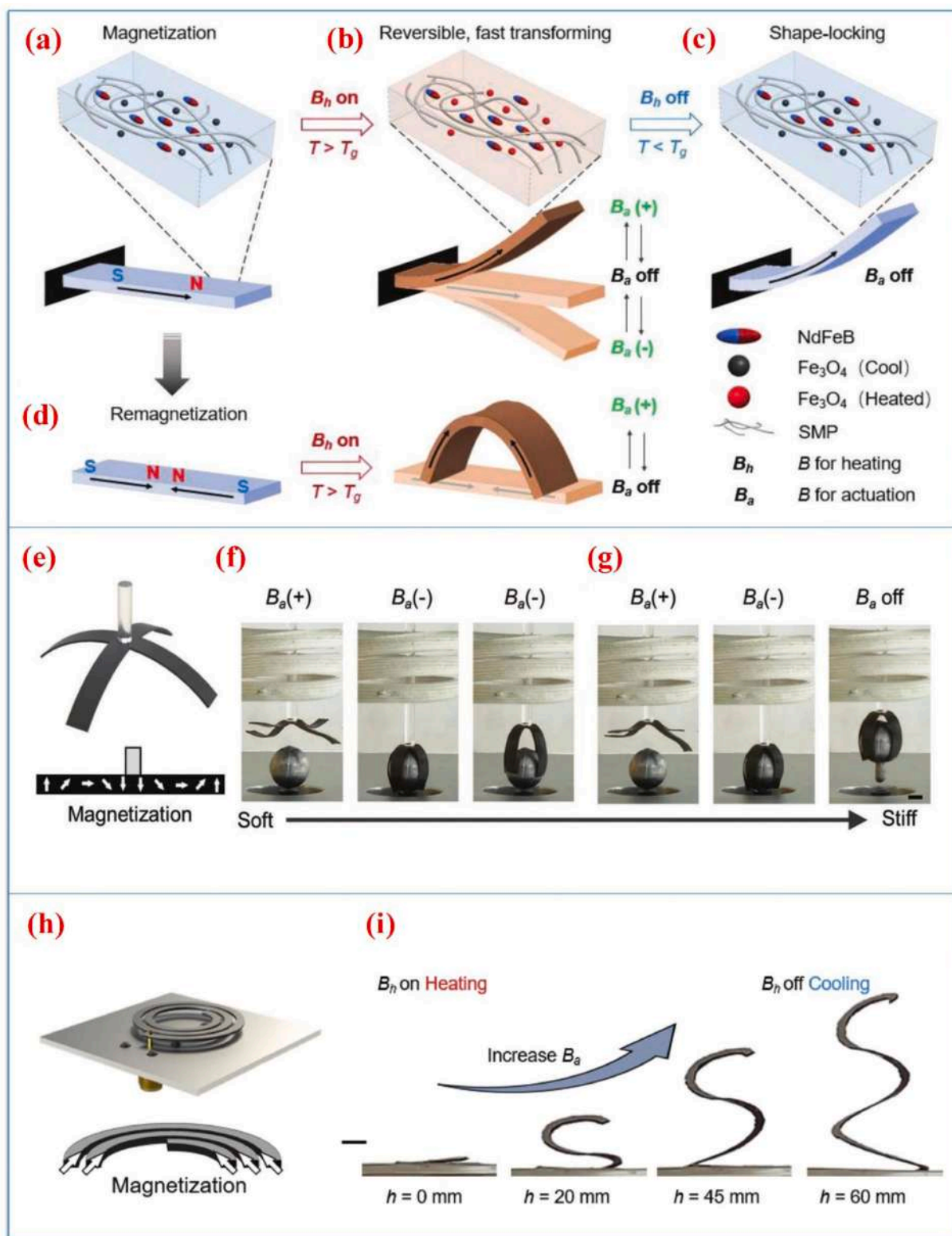


Fig. 17. The shape memory performances of the M-SMP: (a) the M-SMP was hard at low temperature and could not be triggered through a B_a actuation field; (b) the M-SMP became soft and could be triggered through a B_h magnetic field; (c) the M-SMP was cooled and became stiff when B_h was switched off; (d) the M-SMP was reprogrammed according to the magnetization curves; (e) a diagram of four-arm gripper; (f, g) the gripper grabbed the ball; (h) the diagram of an adjustable antenna; (i) the adjustable antenna was actuated by different B_a field.

[284] Copyright 2020 Wiley-VCH.

Table 5
The multi-stage shape transformation and multi-stimuli selective controlled SMPs.

Multi-materials	Multi-stimuli control	Multi-stage shape transformation	Application
SMPU, azobenzene group, Sm(TTA) ₃ Phen, Yb(TTA) ₃ Phen, Nd(TTA) ₃ Phen, AuNPs[233]	UV light, 1064 nm, 980 nm, 808 nm, 520 nm	Multi-segments and quintuple-stimuli shape transformation	Programmable actuators, anti-counterfeiting materials, soft robots
Fe ³⁺ / (PAA) / PEO and PDA / PAA / PEO composite [252]	UV, visible light, near-infrared light, heating	Multi-segments and quadruple-stimuli shape transformation	Origami structure
CNTs-SMP, Fe ₃ O ₄ -SMP, and neat SMP[256]	13.56 MHz and 296 kHz radiofrequency fields, heating fields	Multi-segments and triple-stimuli shape transformation	Smart switches and actuators
Zn(Mebip) ₂ (NTf ₂) ₂ / epoxy composite and neat epoxy resin[257]	UV light, heating fields	Multi-segments and double-stimuli shape transformation	Robot hands
Bismaleimide polymer and bisallyl compounds with dynamic ester bonds[269]	150 °C, 230 °C	Single-segment and triple-shape transformation	Temperature-sensitive actuators
Acrylic acid, acrylamide, agar and poly(vinyl alcohol) hydrogels[272]	Heating, acetic acid and Na-citrate stimulation	Single-segment and quadruple-shape transformation	Biomedical device
Shape memory zwitterionic polyurethanes[273]	Heating or moisture	Single-segment and quintuple-shape transformation	Smart valves, fixation devices
Styrene-butadiene rubber / graphene composites [276]	Heating, NIR irradiation	Single-segment and double-stimuli shape transformation	Smart control devices
MWCNTs / Poly(butylene succinate)-co-poly(ε-caprolactone) copolymer composite[277]	Electric field, NIR irradiation	Single-segment and double-stimuli shape transformation	Smart control devices
LCE[278]	Blue and green light	Single-segment and double-stimuli shape transformation	Self-oscillating actuator
Fe ₃ O ₄ and NdFeB / acrylate based amorphous polymer composites[284]	Different frequency B _a fields	Multi-segments and multi-stimuli shape transformation	Gripper, flexible morphing antenna
SMP-Fe ₃ O ₄ , SMP- <i>p</i> -aminodiphenylimide, SMP-MWNTs and neat SMP[287]	Alternating magnetic field, UV light, radiofrequency field, and heating field	Multi-segments and quadruple-stimuli shape transformation	Information storage carriers

oscillatory motion was driven by molecular isomerization reactions. Its uniqueness is reflected in the fact that it can convert solar energy into mechanical motion as self-morphing soft actuator. This intelligent material can simulate living systems, including heartbeat, cell cycling and biorhythms, etc., which will be a major advancement in human science and technology.

Several reports have demonstrated that multi-stage shape programming SMP systems can perform diverse motions upon multi-stimuli, which provide a new perspective for the autonomously operating soft robots. Zhang et al. [234] mixed 4-cyano-4'-pentyloxyazobenzene (5CAZ) and up-conversion luminescent nanoparticles (UCNPs) (diameter 20 nm) into SMPU matrix for preparing UV-vis-NIR responsive SMP composites and programmable light-controlled bionic finger [279, 280]. The 5CAZ acted as a "photo-switch", which allowed the trans-cis isomerization under UV light and visible light irradiation. While UCNPs can transform near-infrared light into green fluorescence [281–283]. The authors also used the photo-actuated SMP film to prepare the bionic finger, thus exhibiting the upward bending and downward bending sequentially as a result of the exposure to NIR and UV light irradiation.

Furthermore, a smart gripper based on multi-stimuli SMP was fabricated by Ze et al. using two types of magnetic particles (Fe₃O₄ and NdFeB) and acrylate based amorphous polymer (named M-SMP), which had shown reprogrammable, reversible shape transformation and locking capacities (Fig. 17a and Fig. 17b) [284]. The researchers demonstrated the shape locking and shape reprogrammable properties (Fig. 17c and Fig. 17d), respectively, based on which a smart four-arm gripper was designed that can grip the 23 g lead ball (Fig. 17e-g). Furthermore, by utilizing the advantages of M-SMP in shape locking and shape transformation properties, the author designed an adjustable morphing antenna (Fig. 17h-i). This shape transformation soft SMP material can address the challenge of multi-functional shape manipulations, and could be applied in intelligent soft robots as well as reconfigurable and flexible morphing antenna, etc.

Besides, due to their multi-stage programmability and shape transformation, the multi-segments multi-stimuli responsive SMPs are widely also utilized to store information. It is known that morse code is a basic coding program in which the information gets converted into dots ("•") and dashes ("-") [285,286], and multi-stage intelligent SMPs can program the morse code and achieve information encryption. Leng et al. [287] designed the programmable shape-memorizing language code

patterns comprised of SMP-Fe₃O₄, SMP-*p*-aminodiphenylimide, SMP-MWNTs and neat SMP, and were triggered by alternating magnetic field, UV light, radiofrequency field, and heating field according to a preset stimulation process. The authors demonstrated the fabrication process of the Morse code on the surface of the multi-segments SMP composites, thus providing a new solution to the concealing and recovery of the Morse code. The information on "HARBIN INSTITUTE OF TECHNOLOGY" could be obtained through the decryption of Morse codes on SMP sample, proving the feasibility of application in smart information storage carriers.

A list of multi-stage shape transformation and multi-stimuli selective controlled SMPs are shown in Table 5. From the above, it can be understood that the multi-stage programming and multi-stimuli control of single- and multi-shape memory polymers have enabled flexible design for extensive applications. A wide variety of smart architectures including bionic stents, drug delivery and release, soft robots and actuators, etc. have been constructed according to the requirements of projects [288–293]. Although there have been progresses in the multi-stimuli SMPs, complex preparation strategies are still a challenge, which will be a popular topic of future research.

5. 4D printing

3D printing is an advanced manufacturing technology intended for the rapid fabrication of complex 3D structure according to computer-aided 3D models. 4D printing was first proposed in 2014 by the Tibbits group from Massachusetts Institute of Technology [294]. 4D printing is developed on the foundation of 3D printing with the addition of a time dimension, and the structure, property, and function of the 4D printed objects change over time under specific environment or stimulus [295–300]. As a further development of 3D printing, 4D printing technology is dynamic and intelligent. It shows some distinct advantages as follows. On the one hand, the printed structure can show change in shape when actuated by proper stimulation. On the other hand, 4D printing technology can be applied to manufacture the complex three-dimensional structures with personalization, intelligence and integrated functionalities in a faster and less costly way. So far, a variety of smart materials have been developed for 4D printing, including shape memory hydrogels [301,302], shape memory polymers [303,304], liquid crystal elastomers [305,306], shape memory alloys [307,308], shape memory ceramics [309,310] and their composites, etc.

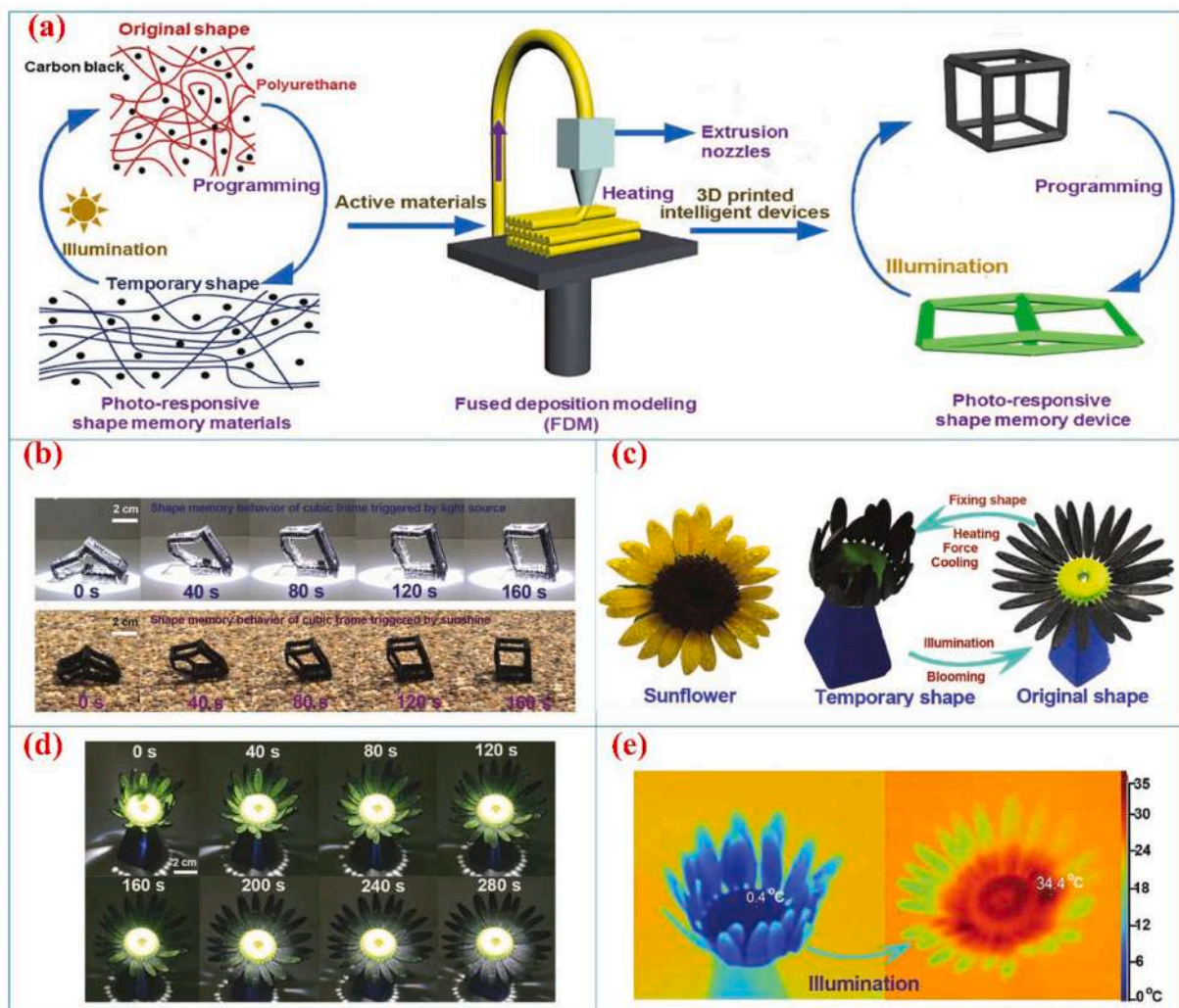


Fig. 18. (a) FDM 4D printing of SMP and shape changes behavior; (b) the shape-shifting process of cubic frame in light source and natural sunlight irradiation, respectively; (c) the “blooming” processes of 4D printing of bionic sunflower; (d) the photos of “blooming” process of bionic sunflower triggered by light source; (e) the thermal infrared images of sunflower from temporary shape to original shape. [325]. Copyright 2017 Wiley-VCH.

[311–314]. This section introduces the state-of-the-art advancement in the 4D printing technology, and the matching printable SMPs.

5.1. 4D printable SMPs

The approaches to 4D printing for SMPs include stereolithography (SLA) [315], digital light processing (DLP) [316], fused deposition modeling (FDM) [317], and direct ink writing (DIW) [318], etc. From the above, it can be understood that SLA and DLP utilize the photochemical process to print products. During the printing process, polymeric monomers or oligomers experience chemical crosslinking reaction under UV light radiation to develop a stable three-dimensional structure. Therefore, SLA and DLP are applicable to the printing of photo curable resins [319]. FDM is a bottom-up extrusion technique involving a nozzle extruder, of which the materials are thermoplastic solid SMPs and SMPs wires [320]. DIW is quite similar to FDM printing technology, with the rheological property of the ink as a critical parameter. There are many materials suitable for DIW, e.g. polymers [321], ceramics [322], metal particles [323] and multi-materials [324].

According to the manufacturing properties, SMPs can be divided into two categories: thermoplastic and thermosetting. The printing technologies of thermoplastic SMPs mainly include FDM and DIW. Among them, FDM printing utilizes thermoplastic solid wires, such as shape

memory thermoplastic polyurethane wire, shape memory thermoplastic polylactic acid wire, and shape memory thermoplastic polycaprolactone wire, etc. While DIW printing uses viscous liquid inks, such as UV crosslinking poly(lactic acid)-based inks, shape memory poly(D,L-lactide-co-trimethylene carbonate), and waterborne shape memory polyurethane mixed with polyethylene oxide ink. By contrast, the printing methods of thermosetting SMPs mainly include SLA and DLP, and the photosensitive resins involve shape memory acrylate resin, shape memory epoxy resin, and shape memory polyurethane acrylate, etc. The typical 4D printable SMP materials and the applicable printing technology will be introduced as follows.

Using thermoplastic SMPU and photothermal conversion carbon black nanoparticles, researchers prepared photo-responsive shape memory composites for 4D printing (Fig. 18a) [325]. With the layer-by-layer FDM printing technology, the composite was then manufactured into pre-designed shape memory structures. The authors demonstrated the shape-shifting process of the cubic frame and bionic sunflower structures irradiated by light source and natural sunlight (Fig. 18b, Fig. 18c and Fig. 18d). After 160 s of light source illumination, the bionic sunflower bloomed completely, and the temperature changes occurring during the shape recovery processes were characterized by thermal infrared images (Fig. 18e). This printing approach offers great chances for the design and preparation of personalized remote-actuated

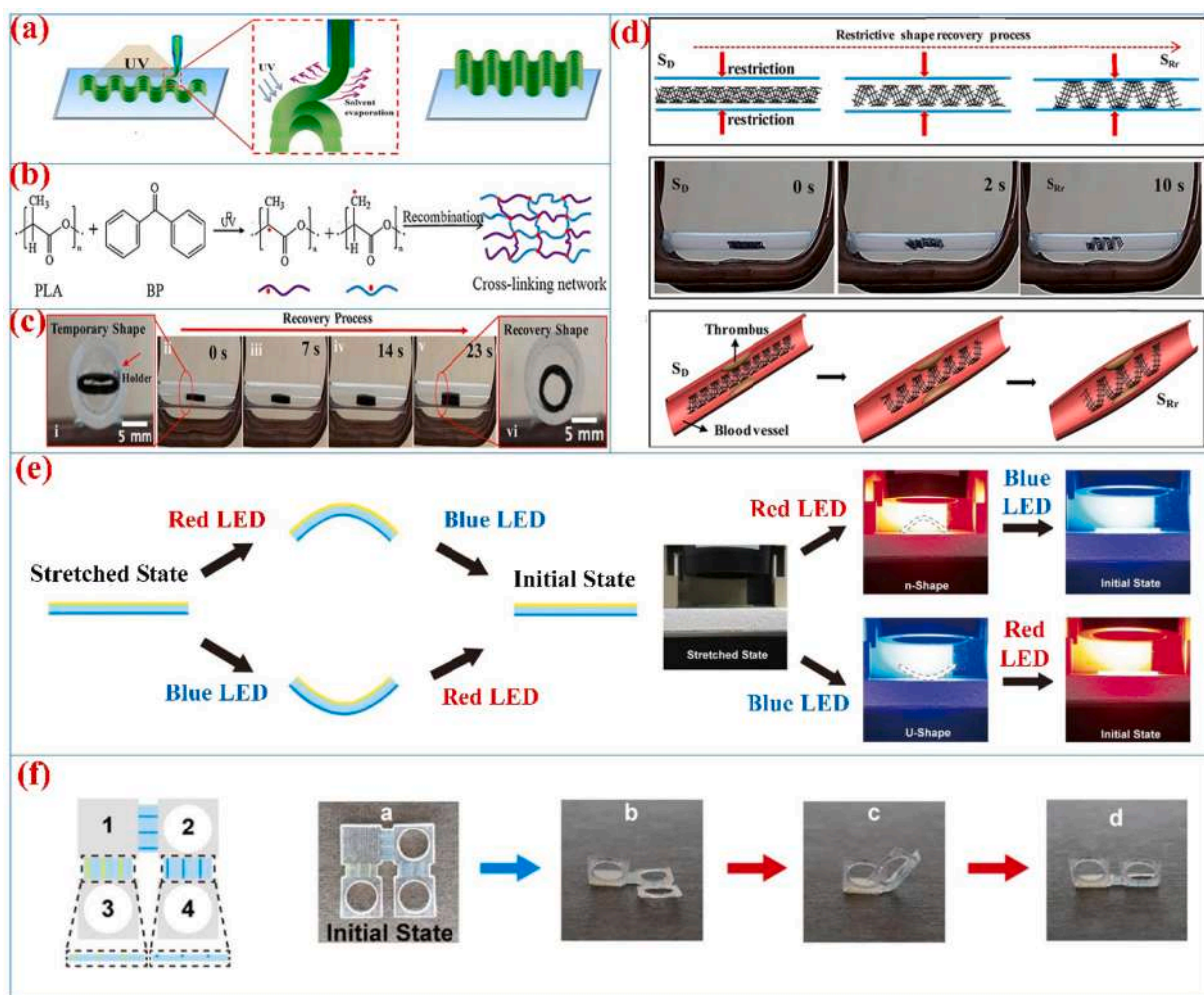


Fig. 19. (a) The schematic diagram of DIW 4D printing technology and shape recovery of the printed products under AMF actuation; (b) the UV crosslinking reaction between PLA and BP; (c) the shape recovery progresses of the sample under 30 kHz AMF; (d) the 4D printing of spiral scaffold and its shape memory process. (e) The dual-step actuation of multicolor composites; (f) the multicolor hinged shape-shifting structure for multistep actuation. (a-d) [318]. Copyright 2017 American Chemical Society. (e,f) [328]. Copyright 2020 Nature Publishing Group.

smart devices.

Using DIW technology and the PLA-based inks (including PLA, benzophenone (BP) and Fe_3O_4), an active shape-morphing SMP biological scaffold was fabricated, which could be triggered by heating or magnetic field [318]. When the inks were pushed out by DIW printer, the fast evaporation of solvent led to the fast liquid-solid transition of the inks, thus forming the personalized 4D printable structure (Fig. 19a). The chemical reaction mechanism was that PLA and BP experienced free radical crosslinking reaction under UV irradiation (Fig. 19b) [326,327]. The authors presented the shape memory process of the 4D printing of biological scaffold in a narrow vessel (Fig. 19c and Fig. 19d). It was demonstrated as effective in solving blood vessel embolism diseases by re-expanding the narrow vessel accumulated with thrombus. In simple terms, the 4D printed self-deployable scaffold can expand in the vessel to make the blood flow as normal. This technology can enable the customization of unique stent structure according to the patient's circumstance. These characteristics of the 4D printable inks have demonstrated unrivalled advantages in respect of bioengineering.

Another similar to the DIW approach is inkjet printing technique. Jeong et al. [328] applied inkjet printing to fabricate the multicolor SMP composites with selective shape-morphing capability under color-dependent light irradiation. The authors designed the multicolor SMP composites based on glassy shape memory polymer fibers in a rubbery matrix and fabricated the multicolor hinged shape-shifting

structure (Fig. 19e and Fig. 19f). Under the irradiation with different light wavelengths, the hinged structure can change into different shapes. Compared with the 4D printing of magnetic-actuated SMPs, the selective photo-actuated SMPs show incomparable advantages. This is because its size, direction and position of various light sources can be adjusted selectively. Thus, the 4D printable photo-actuated SMPs are widely adopted in advanced actuators, soft robots and smart deployable structures.

SLA and DLP techniques are advanced manufacturing technologies in which photosensitive resin is rapidly cured under the irradiation of UV light from a laser. For example, epoxy resin has epoxy groups that undergo ring-opening reaction under UV light. Also, acrylate resin contains $\text{C}=\text{C}$ bonds which have free radical reaction under UV light. Shan et al. [329] applied SLA technology and shape memory epoxy acrylate solution to produce a smart electrical valve actuator, which can be utilized in fire alarm and monitor systems. The innovation achieved by the research is that the shape memory property of the 4D printable SMP structure was combined with the conductive properties of silver paste to enable an electric control function. When the SMP structure was in temporary shape state, the electrical circuit was closed with the LED bulb on. While the SMP structure returned to the original shape state, and the electrical circuit was opened with the LED bulb off.

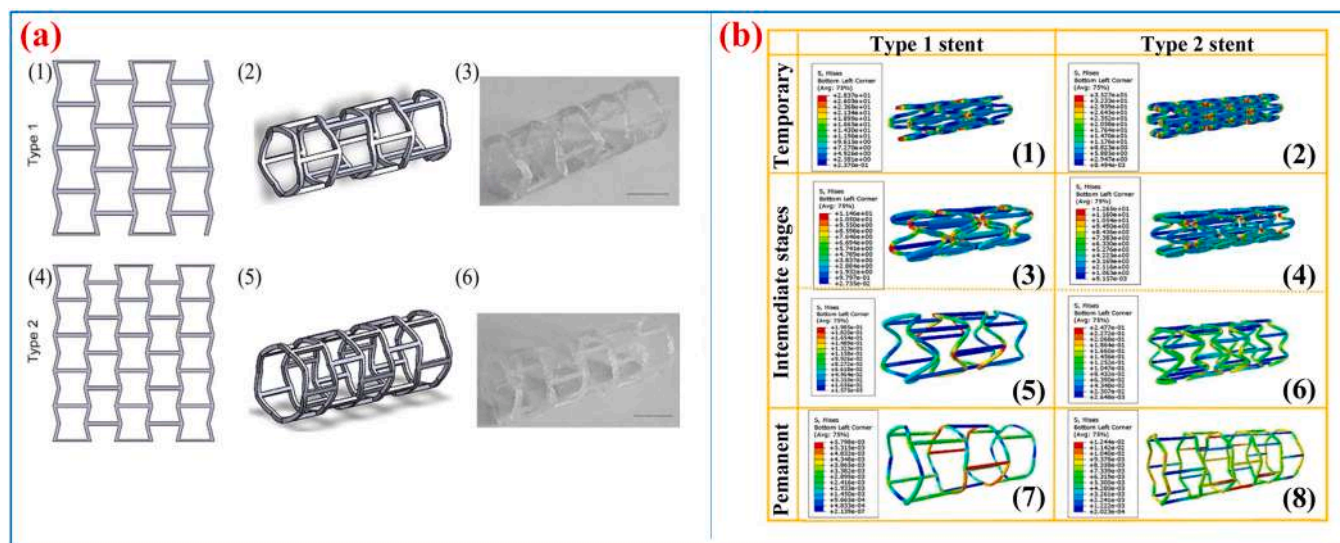


Fig. 20. (a) The two types of 4D printing of NPR stents structure; (b) the simulation images of shape recovery process. (1) and (2) were the temporary shape of printed stents named Type 1 and Type 2, respectively. (3)–(6) were the images of shape recovery processes, (7) and (8) were the permanent shape of the two stents. [339]. Copyright 2020 Springer.

5.2. Personalized printed structures

The 4D printing technology can achieve the efficient fabrication of shape morphing devices with complex shapes and delicate structures. And the personalized SMP structures can be easily constructed, which are integrated with computer-aided molding to fabricate geometrically complex structure, external-stimulus controlling deformation, and multi-functional integration, such as glass sponge-like bionic scaffolds, origami structures, the anisotropic structures with programmable Poisson's ratio, auxetic three-dimensional meta-structures, bioinspired tracheal scaffolds, chiral metamaterials-based scaffolds, smart textiles and self-deployable honeycomb sandwich structures, etc. [330–336].

Conventionally, polymers have a positive Poisson's ratio, which means that the material shrinks in the tensile direction when stretched. Such property hinders the application of SMP structures in some fields. In the past few years, some researchers have paid close attention to the design and 4D printing of polymer structures with negative Poisson's ratio (NPR) effect which expands in the tensile direction within the elastic range when stretched [333]. Due to the peculiar advantages of lightweight and high specific stiffness [337,338], the printed SMP structures with NPR provide higher tensile strength at lower surface coverage as shape-shifting property. For example, Leng's group developed the 4D printing of customized shape-shifting vascular stents with negative Poisson's ratio, so as to enlarge the narrow blood vessel quickly [339]. According to the genetic algorithm [340,341] and the Gibson theory [342], the authors designed two solutions to the 4D printing of NPR topology structure stents (Fig. 20a). They also applied ABAQUS software to simulate the shape changing performance of the vascular stents (Fig. 20b), demonstrating that the stents had outstanding capability of shape memory. This kind of shape-shifting stent also exhibited biodegradable property, which allowed it to replace the metal stents and address the challenges of thrombosis, restenosis and other complications.

The 4D printable biological scaffolds with good biocompatibility have received intensive attention and have been developed rapidly during the last few years. For instance, cell-laden saddle-like scaffold with remote NIR-actuated shape deformation property was designed through 4D bio-printing of alginate / PDA inks (Fig. 21a) [343]. The authors fabricated bilayered alginate scaffold and bilayered alginate / PDA scaffold which exhibited shape morphing in response to heating stimulation and 808 nm near infrared light irradiation (Fig. 21b and

Fig. 21c). As confirmed by the test of the biocompatibility and cell viability, cells outlived well in the bilayered scaffolds before and after NIR light irradiation, with 80% viability preserved over 14 days. Thus, the cell-laden 4D bio-printing of shape-morphing composites is fit for encapsulating living cells and has immense prospects in artificial tissues and organs.

In addition to the photo-actuated 4D printable stent, magnetic-controlled bio-designed and biodegradable tracheal scaffolds are also constructed. Zhao et al. [334] designed a 4D printable magnetic-actuated bio-tracheal scaffold that imitated the microstructure of glass sponge (Figs. 21d–21g), which exhibited enhanced strength, stability and biodegradability, thus solving problems such as scaffold migration and scaffold fracture. The 4D printing of porous structure bone tissue scaffolds (Fig. 21h and Fig. 21i) using non-toxic, environmentally friendly and biocompatible SMP was reported by Leng's group [344]. Also, they did 4D printing of bone repair structures (Fig. 21j) made up of biocompatible PLA / Fe₃O₄ composite filaments [345]. Significantly, the 4D printed bone structure is the first to be fixed into a very small size and injected into the implant place (Fig. 21k). Consequently, the printed stent structure which integrates with multi-functions holds a great potential of application in the biomedical field and has a prospective replacement for the traditional stent structures.

Another interesting intelligent structure is responsive actuator or soft robot. A 4D printed gripper based on shape memory PLA and silver nanowires could grab a small steel ball weighing 2.5 g under 4.5 V electric field [346]. Besides, Yang et al. [347] demonstrated an UV-assisted 4D printing technology that could be applied to print Chinese characteristics, e.g. Terracotta Warriors, Kungfu Panda, and "Bird's Nest" stadium and either elbow protector, and elbow protector models through the shape memory PLA-co-PCL copolyester networks. These reports elaborate that the 4D printing technology was a flexible and well-adapted strategy to manufacture diverse intelligent structures with sophisticated shapes. A list of printable SMP-based materials and structures was presented in Table 6.

Since the concept of 4D printing was put forward, it has received intensive attention from researchers in many areas [348]. The personalized 4D printable structures have presented significant potential of applications in electronics, biomimetics, robotics, and biomedical engineering, e.g. drug-loaded biological stents, minimally invasive surgery, and biological catheters, etc. However, as a new type of

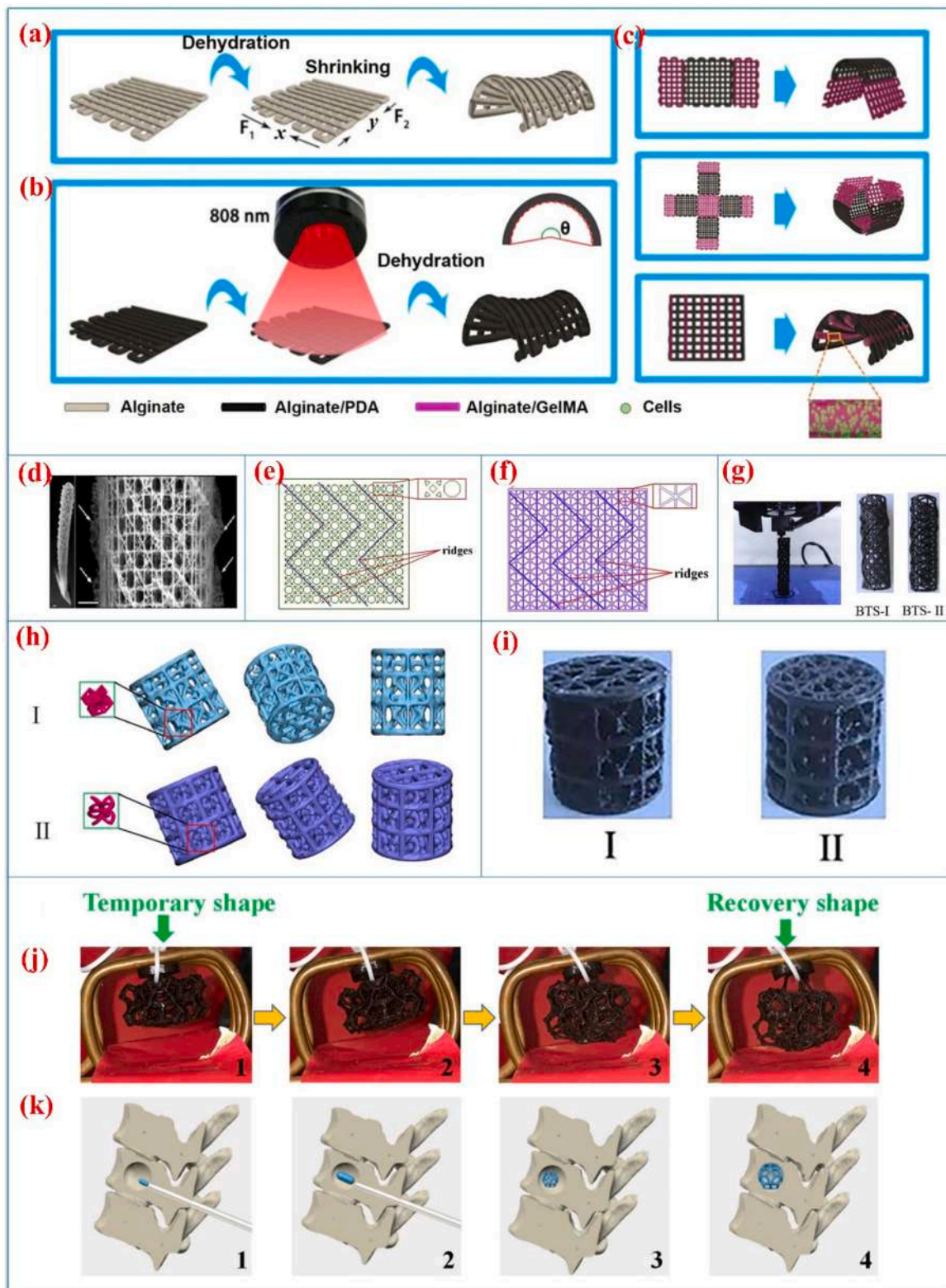


Fig. 21. (a) The shape of the 4D printing of bilayered scaffold was changed from a plane shape to a saddle-like shape; (b) NIR-actuated shape change behavior of the bilayered alginate / PDA scaffold; (c) two-segments scaffolds consisted of alginate / PDA composite and cell-laden alginate / GelMA composite. (d) Photos of a glass sponge structure and cage structure; (e) and (f) the plane images of the deployable structure of two tracheal scaffolds, respectively; (g) the images of the 4D printed bio-tracheal scaffolds (named BTS-I and BTS- II, respectively). (h) Design models of porous bone tissue scaffolds; (i) the bone tissue scaffolds fabricated by 4D printing technology. (j) The shape recovery behavior of 4D printing of PLA / Fe₃O₄ composite structure triggered by magnetic field; (k) the shape memory mechanism of the bone repair tool.

(a-c) [343]. Copyright 2019 IOP Publishing Ltd. (d-g) [334]. Copyright 2019 Elsevier Ltd. (h,i) [344]. Copyright 2020 SPIE. (j,k) [345]. Copyright 2019 Elsevier Ltd.

Table 6
4D printing of SMPs and composites and their applications.

4D Printable materials	Printing technology	Actuation methods	Application
Thermoplastic SMPU/ carbon black nanoparticles filament[325]	FDM	808 nm NIR light	Bionic sunflower, remote actuator
PLA/Fe ₃ O ₄ inks[318]	DIW	30 kHz magnetic field	Biological scaffold in a narrow vessel
Glassy SMP fibers[328]	Inkjet printing	Blue LED, red LED	Light-induced structural changes and remote actuation
Shape memory epoxy acrylate solution, silver paste[329]	SLA	Electrical field	Fire alarm and monitor systems
Thermoplastic SMP / CNTs or SMP / silver paste filament[330]	FDM	Electrical field	Smart textiles
PLA inks[339]	DIW	Thermal field	Vascular stents with negative Poisson's ratio structure
Alginate/ polydopamine (PDA) inks[343]	DIW	808 nm NIR light	Biological scaffolds in artificial tissues and organs
Thermoplastic PLA/ Fe ₃ O ₄ filament[334]	FDM	30 kHz alternating magnetic field	Bio-tracheal scaffold with glass sponge microstructure
Thermoplastic PLA/ Fe ₃ O ₄ filament[344]	FDM	30 kHz alternating magnetic field	Porous structure bone tissue scaffold
Thermoplastic PLA/ silver nanowires filament[346]	FDM	Electrical field	Gripper, actuators
PLA and PCL copolyester polymer [347]	UV-assisted FDM	Thermal field	Medical protective devices

in satisfying the personalized needs of huge market and patients.

6. Prospective applications

After intensive efforts, researchers have developed a wide variety of intelligent SMP structures for profound usage in actuators, bionic soft robots, aerospace engineering, biomedical engineering, and information storage [353–355]. For example, biocompatible SMPs are widely applied in personalized biological scaffolds, biological extension catheters and atrial septal defect occluder. Photo-actuated SMPs are commonly utilized in reconfigurable / rewritable nano-optical devices, optical information storage, and anti-counterfeiting, etc. Programmable multi-stimuli-actuated SMPs and remote stimuli-actuated SMPs play an important role in bionic soft robots, artificial muscles and dynamically tunable microfluidic devices. The current applications of SMPs are summarized in Fig. 22. And several examples will be briefly introduced for the typical and promising application of SMPs in the following parts.

6.1. Smart actuators

Smart actuator represents a significant direction of application for SMPs. This is because shape memory polymers have the following advantages, such as flexibility, high functionality, large deformation, and light weight, etc. compared with shape memory alloys and shape memory ceramics. For example, a bionic flower with self-healing ability was fabricated using the poly(acrylic acid)-grafted graphene oxide (PAA-GO) mixed into shape memory PVA matrix [356]. When the PAA-GO content reached 3.0 wt%, the self-healing ratio of PVA / PAA-GO composite in the first shape memory cycle was 99.2% and then gradually decreased to 90.6% after 15 shape memory cycles. Under 47 mW/cm² NIR light irradiation, the bud bloomed to its permanent flower shape within 1 min (Fig. 23a). The tensile strength of the SMP composite film was 70.4 MPa and the Young's modulus was 2.8 GPa, thus addressing the low mechanical properties of PVA-based smart actuator.

Further, multi-wavelength light-controlled wireless actuators has boomed during the last decade, which can adapt to more complex environments and achieve more precise controllability of the action. A smart "athlete" was prepared by mixing gold nanorods into azobenzene-based LCE networks (AuNR-ALCN) [357]. Under 365 nm ultraviolet light and 550 nm visible light irradiation, respectively, the azobenzene group produced cis-trans photoisomerization effect to induce the shape memory process of the AuNR-ALCN. When irradiated by a 785 nm near-infrared-light, the gold nanorods absorbed the NIR energy and generated thermal energy to drive shape morphing behavior. Therefore, the smart "athlete" could perform different sporting actions, like push-ups and sit-ups action, which endows it with the potential of applications in artificial muscle (Fig. 23b). In addition, the light control of a tubular liquid crystal microactuator was applied for driving the movement of fluid slugs (Fig. 23c) [358]. Diverse microactuator shapes, including straight, serpentine, 'Y'-shaped and helical shape, were constructed and utilized to achieve the photocontrol on a wide variety of liquids moving along the specific directions. Such photo responsive microactuators would be useful in micro-reactors and micro-optomechanical systems.

It is known that LCE is a very promising material for smart actuators, but in the case of the shielding of opaque barriers, photo actuation of LCE cannot generally be performed since the lights can hardly penetrate the opaque objects. However, microwave actuation is not affected, which can penetrate the LCE and drive the smart object to achieve the pre-designed action. In 2020, a microwave-actuated two-way shape morphing actuator was prepared by polysiloxane-based nematic LCE (Fig. 23d) [359]. The energy conversion of the polysiloxane from microwave radiant energy to thermal energy enabled wireless control on the macroscopic shape change of LCE. Significantly, the LCE exhibited rapid contraction under microwave radiation, and recovered its original

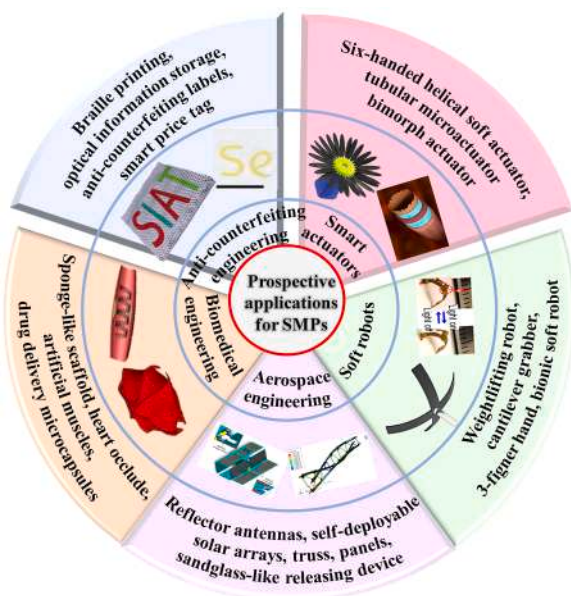


Fig. 22. Diverse applications for intelligent polymers.

technology, 4D printing still faces various challenges, such as lower printing efficiency, smaller volume of printed structures, and shortage of comprehensive theoretical foundations. Researching on SMPs with high biocompatibility, multi-functionality, long term stability and good mechanical properties for 4D printing is a main research direction [349–352]. After continuous development and verification, the utilization and large-scale production of 4D printed objects will perform better

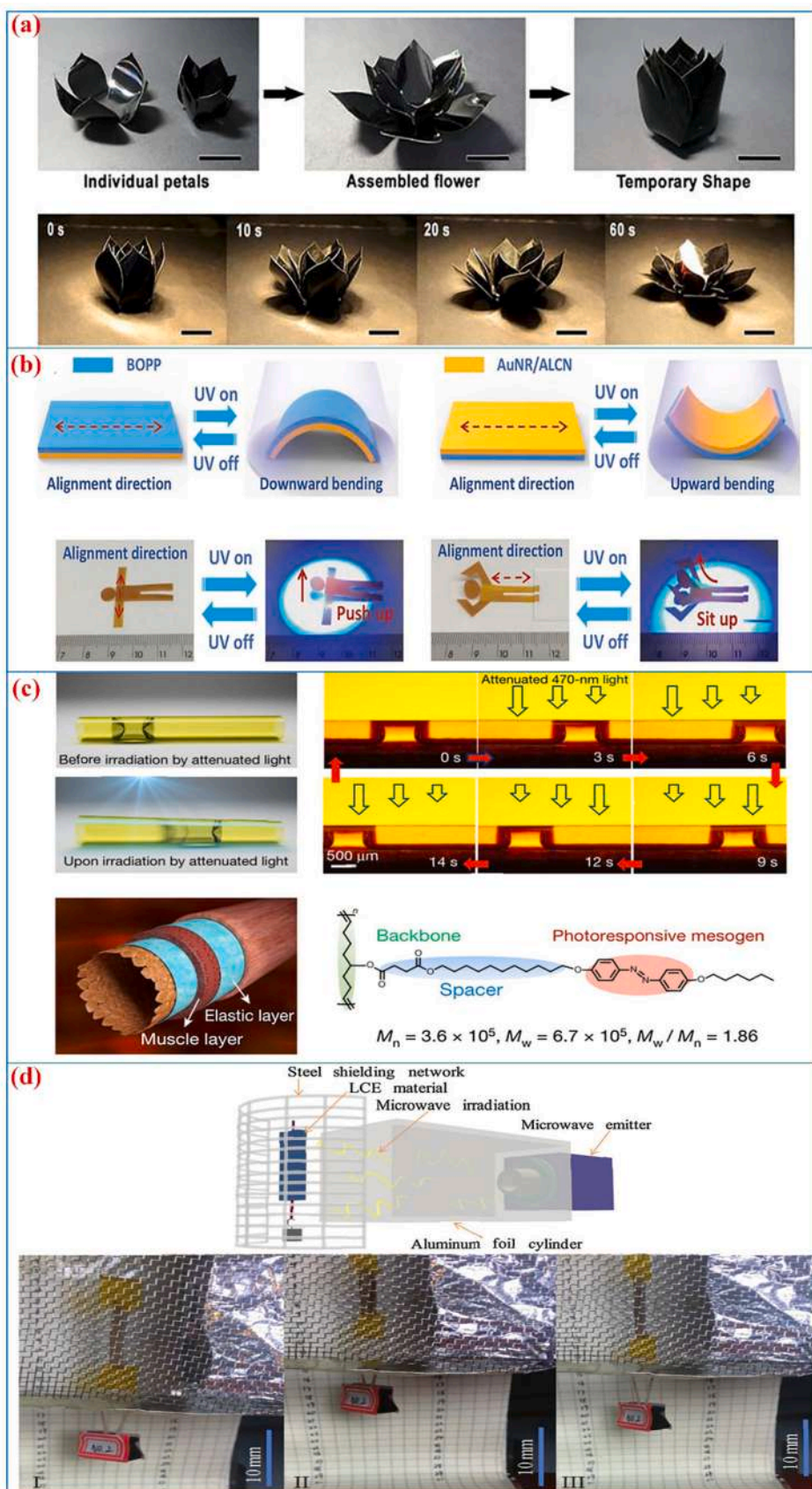


Fig. 23. (a) The shape memory processes of PVA / PAA-GO3% composite film irradiated at 808 nm, 47 mW / cm² NIR light. (b) Two different reversible motion behaviors of the bilayer film by turning on and off UV light. (c) The tubular microactuator actuated by photodeformation. (d) The photos of the microwave actuation behavior of an LCE sample. (a) [356]. Copyright 2019 American Chemical Society. (b) [357]. Copyright 2018 Wiley-VCH. (c) [358]. Copyright 2016 Springer. (d) [359]. Copyright 2020 Royal Society of Chemistry.

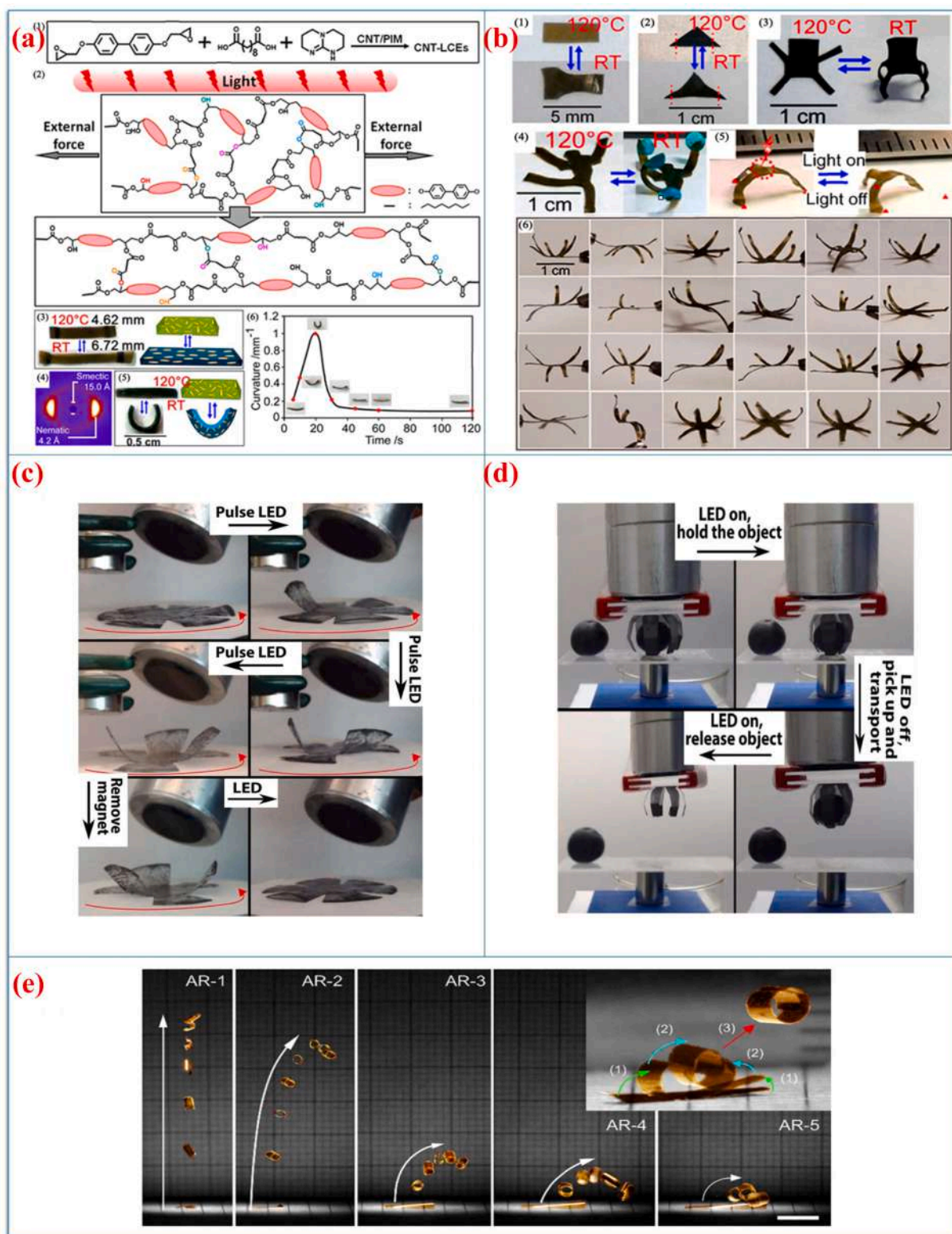


Fig. 24. (a) The synthesis route of CNTs-LCEs and the mechanism of shape change triggered by light irradiation; (b) the reversible shape changes of CNTs-LCE film, triangle, chair, "Hercules", tripod, and six-petal "flower" structures. (c) The photos of rotation of a shape memory flower irradiated with LED; (d) the photos of the grabber grabbing objects. (e) Angle-controlled photomechanical jumping of the azo-LCN soft robots. (a,b) [369]. Copyright 2016 American Chemical Society. (c,d) [370]. Copyright 2019 American Association for the Advancement of Science. (e) [367]. Copyright 2021 Elsevier Ltd.

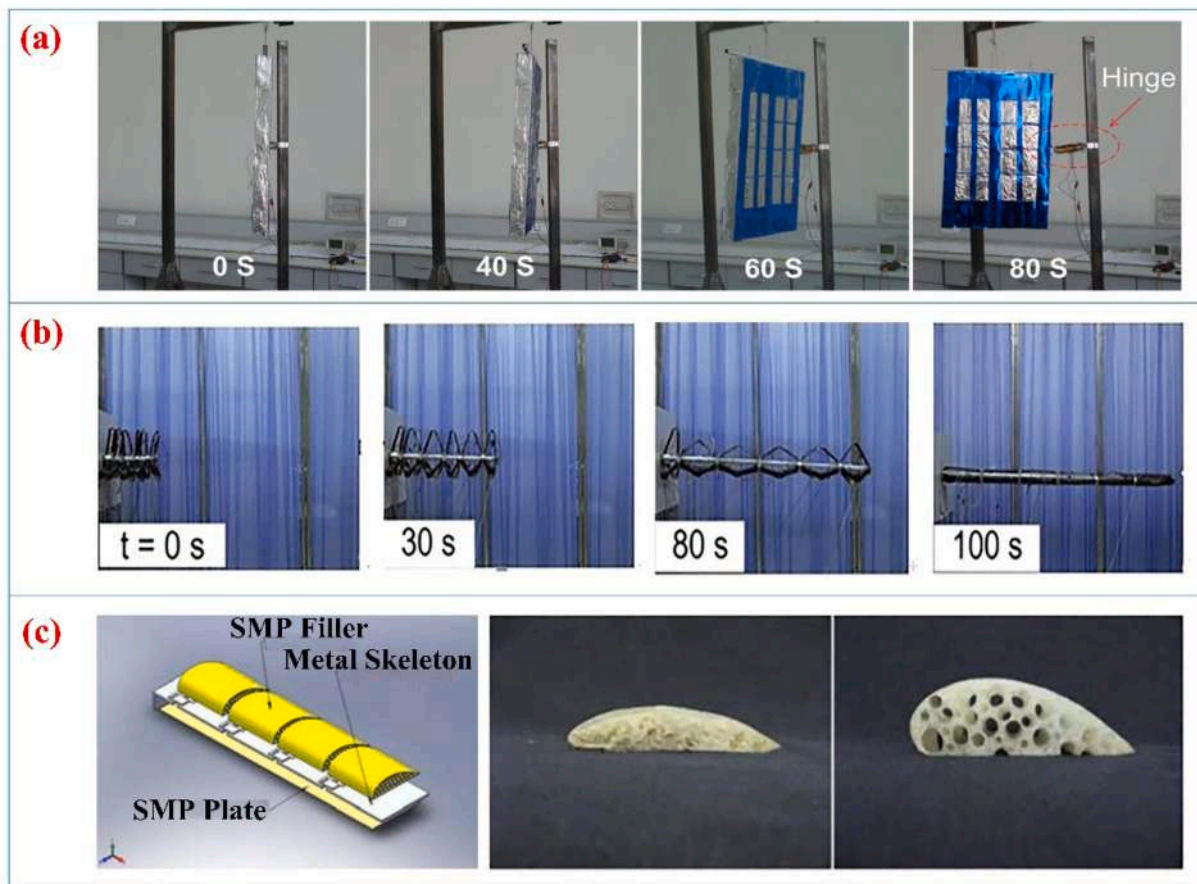


Fig. 25. (a) The deployable behaviors of a solar array actuated by a SMPC hinge. (b) The unfold process of the deployable truss. (c) The illustration of the deployable morphing structure.

(a) [376]. Copyright 2009 IOP Publishing Ltd. (b) [377]. Copyright 2014 Elsevier. (c) [378]. Copyright 2015 Emerald Group Publishing Ltd.

shape when the microwave radiation was switched off. The microwave-actuated LCE showed the advantages of fast start-stop response and energy-saving. Thus, it can be applied as wireless actuator to monitor the intensity of microwave radiation while ensuring convenient manipulation and good sensitivity.

Besides, other stimulus-responsive actuators with multi-functionality are prepared, which significantly diversify the categories of smart actuators. For example, Pringpromsuk et al. [360] designed a multifunctional SMP actuator based on dibutyl adipate and shape memory polyurethane, which was actuated by thermal and electric stimuli and possessed reversible shape deformation property over six cycles. Wang et al. [361] developed a six-handed helical soft actuator which could be triggered by thermal stimulus to catch a live fish in water. Chu et al. [362] fabricated a near-infrared light-actuated SMP with a long-time fluorescence, which could produce multiplexed biomedical fluorescence image during the shape recovery process. Andrew et al. [363] prepared a thermal bimorph actuator on the basis of carbonyl iron particles / EP / silane, which exhibited shape changing capability under the context of alternating magnetic field actuation. In addition, Duarah et al. [364] fabricated microwave-actuated flexible electronic actuators based on the Fe_3O_4 @ MoS_2 / MWCNTs / dopamine / SMPU composites with self-healing and electromagnetic interference shielding capability. Li et al. [365] applied hydrophobic TiO_2 nanoparticles and elastomer film to prepare superhydrophobic elastomer surface, which can perform jumping and fixing, grabbing and release under control by an electric field. Leng et al. [366] fabricated an electroactive SMP composite film based on metal mesh embedding layer and colorless shape memory polyimide layer, which had a high shape memory transition temperature (230°C) and could extend the scope of application for the

electric-actuated SMP actuators in harsh environments. Consequently, an increasing number of smart actuators have been constructed by researchers over the last decade. But there is still a long way to go before realizing the practical application in daily life, due to the inability to industrialize production, long production cycles, and high costs, etc.

6.2. Soft robots

Everything in nature is magical and fascinating. Over the last decade, the bionic soft robots imitating the biological dynamics motion of elephant trunks, mammalian tongues, octopus paws and so on have attracted increasing attention for research and investigation. Bionic robots can displace human beings to accomplish work under harsh conditions such as outer space, arctic regions, high altitude and so on [367,368]. For instance, a photo-actuated CNTs-LCEs soft robot was prepared by using diglycidyl ether of 4,4'-dihydroxybiphenol, sebacic acid, CNTs and a dispersant (PIM) (Fig. 24a) [369]. The sample showed reversible change in length as light irradiation triggered the transition between liquid crystalline phase (25°C) and the isotropic phase (120°C). The authors designed a series of smart structures with shape changing capability (Fig. 24b). Among them, the "flower" structure displayed more than 20 different shape changes under selective NIR light irradiation.

Furthermore, multi-responsive wireless-controlled soft robots have also been designed to replace humans to do more work. Photothermal and magnetic responsive soft robotics (cantilevers, flowers, scrolls, and grabbers) were designed by using the SMP composite consisting of Fe particles and shape memory thermoplastic polyurethane matrix [370]. The multi-stimuli responsive "flower" soft robotics and "grabber" show

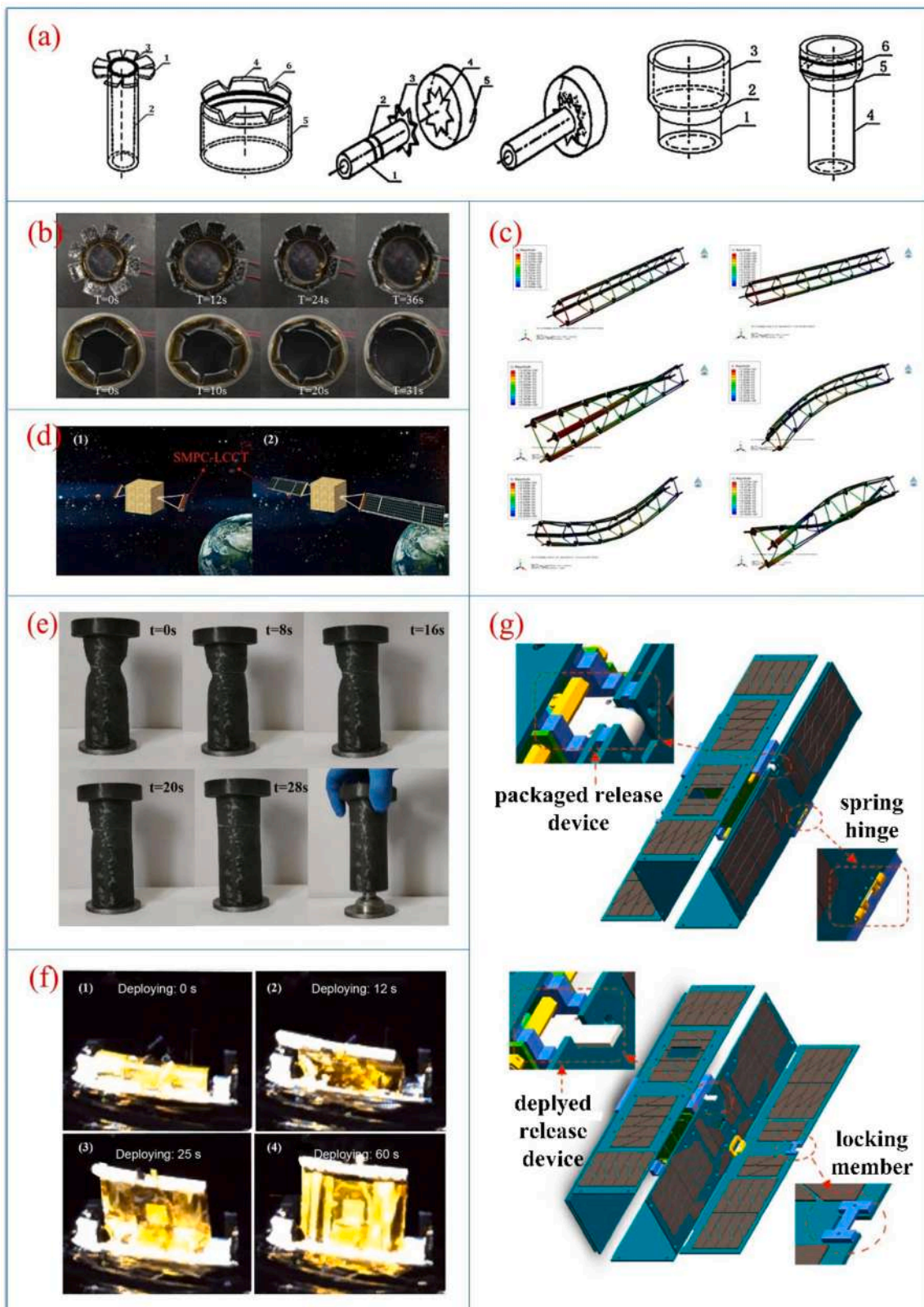


Fig. 26. (a) The release devices of the "lotus", "eight paws", and "bamboo", respectively; (b) the bending deformation recovery behavior of the inner and outer cylinder of the "lotus" device. (c) Finite element was used to simulate the first six vibration modes of three-longitudinal beam truss. (d) The conceptual flexible solar array self-deployment in space environment. (e) The shape recovery process of the sandglass-like releasing device. (f) The on-orbit releasing process of the flexible solar array system. (g) The packaging and deployment process of the ultra-light release device. (a,b) [381]. Copyright 2015 Elsevier Ltd. (c) [382]. Copyright 2016 World Scientific Publishing Europe Ltd. (d) [383]. Copyright 2019 Elsevier Ltd. (e) [384]. Copyright 2019 Elsevier Ltd. (f) [387]. Copyright 2020 Springer. (g) [388]. Copyright 2020 Elsevier Ltd.

high flexibility in re-configuration and posture fixation (Fig. 24c and Fig. 24d). In addition, Jeon et al. [367] designed continuous programmable photomechanical jumping for untethered miniaturized soft robots, which was fabricated by azo and liquid crystal polymer networks (named azo-LCN). Under light irradiation, the programmable soft robots can achieve continuous jumping to overcome obstacles within 5 s, and the jumping height and angle are controllable (Fig. 24e). The soft robots can move instantaneously like jumping athletes such as frogs and fleas, and achieve fast jumps at low energy costs, thereby they have significant application prospects in complex terrain, obstacles and other environments.

Another type of bionic soft robot was a photo-thermal self-folding 3-finger hand, which was prepared by 4D printing of shape memory composites (consisted of carbon black, polystyrene and chitosan) [371]. The 3-finger hand exhibited bend motion under 808 nm near-infrared-light irradiation. The self-folding bionic hand fabricated by 4D printing technology laid foundation for the further manufacture of more complex and flexible soft robots. Additionally, Kim et al. [372] reported the 4D printable soft electronics robots with negative Poisson's ratios, which consisted of ferromagnetic microparticles and elastomer. They exhibited a series of shape changes under light, heat, solvent, electric or magnetic stimuli. The authors also demonstrated other SMP soft robots with complex shape-morphing capabilities, e.g. a mechanical bionic soft robot that can jump, and a micro-robot that can crawl, roll and catch objects. Hence, based on the remote-actuated SMPs, multi-responsive SMPs, and multi-functional SMPs, researchers can fabricate wireless-controlled, programmable, reprogrammable or reconfigurable soft robots to adapt to different application scenarios and environments.

6.3. Aerospace engineering

The space environment is much harsher than that of atmosphere. Many polymers are subject to severe erosion by atomic oxygen and UV light irradiation in space, thus causing the loss of mass, deteriorating performances, and even the complete loss of function [373]. Epoxy resin-based, polyimide-based and cyanate ester-based SMPs are demonstrated to have excellent tolerance capability in outer-space environment [374]. Besides, according to the review conducted by Liu and her colleagues, SMPC can be designed into a variety of space deployable structures, such as reflector antennas, deployable panels, self-deployable solar arrays and morphing structures, etc. [375].

Considering the carrying capacity of the rocket and the needs of large-scale space structures, deployable structures came into being. Most deployable structures rely on electromechanical systems or mechanical arms for deployment. The SMP can be used as the driving component of a new spatially expandable structure, which can be driven by the shape memory characteristics of the polymer without complicated mechanical equipment. Lan et al. [376] prepared a styrene-based SMP composite (SMPC) strengthened by carbon fibers, and then demonstrated the practicability of a deployable SMPC hinge structure. By testing the deployment behavior of a solar array (Fig. 25a), the authors verified that the SMPC hinge could recover the original angle within approximately 80 s and that the solar array could be deployed upon a voltage of 20 V. The author also tested the shape recovery ratio which exceeded 90%. Leng's group [377] designed a space deployable truss structure using the multilayer carbon fiber strengthened by the epoxy SMP composites. When the voltage and electric current reached 38 V and 0.2 A, respectively, the self-deployable truss unfolded within 100 s (Fig. 25b). Due to these characteristics of the truss structure, it could be used for both solar panel and deployable antenna.

There are a large number of researches on the materials, structure, deformation, and radiation performance of SMPs in aerospace field which have provided a firm basis for the practical utilization. For example, a deployable morphing structures based on SMP filler, mechanical skeleton and SMP plate was exhibited in Fig. 25c [378]. When

the SMP filler was restored from the temporary shape to the original shape, the standard airfoil developed. After being heated by 80 W resistance heating film, the deployable morphing structure exhibited shape deployment property within 98 s. Also, a cubic deployable SMPC structure was designed by four dependent spatial cages, with each spatial cage having 12 three-longeron SMPC truss booms and end connections [379]. As revealed by the experimental results of ground simulation, the smart structure possessed self-deployment capability under 465 s electric field actuation. Besides, the deployable structures were verified by on-orbit experiments on satellite. Researchers tested the mechanical properties of epoxy-based SMPs at a time when the SMPs were exposed to 1×10^5 Gy and 1×10^6 Gy radiation dosage environments for up to 140 days [380]. After irradiated by 1×10^6 Gy radiation, the tensile strength reached 26 MPa and elastic modulus reached 1.36 GPa, respectively. Compared with the original materials, the shape recovery ratio of the irradiated SMP exceeded 95%, showing only slight degradation. Thus, the epoxy-based SMPs had bright prospects in aerospace environment due to the properties of resistance to space radiation, light weight and high strength.

Furthermore, various bionic space-deployable structures have been constructed one after another, which is also inseparable from the support of smart materials. "Lotus", "eight paws", and "bamboo" shaped locking-release devices were fabricated by styrene-based SMPCs (Fig. 26a) [381]. After heating, the inner cylinder of the "lotus" device could bend 90° outwards within 36 s, and the outer cylinder could bend 90° inwards within 31 s, thus releasing the locked objects (Fig. 26b). Li et al. [382] prepared shape memory, highly reliable, light weight and self-deployable truss structures, and established three-longeron truss finite element models with the assistance of ABAQUS software. The result of experiment test on the first six order vibration modes of the truss was consistent with that of the finite element simulation (Fig. 26c). Liu et al. [383] designed a lenticular tube based on SMP composites to control the unfolding of the flexible solar array in space environment (Fig. 26d). The self-deployable solar cell sheets were crimped and gathered in a small volume during the launching process. When the deployment mission was initiated, the lenticular tube was heated and the solar array exhibited the self-deployment behavior.

In addition, epoxy-based SMP and SMPC was used to design a sandglass-like releasing device, which exhibited shape recovery behavior within 28 s (Fig. 26e) [384]. The maximum locking force of the intelligent device was 4000 N, so that the intelligent device can lock and release big load in aerospace field. Besides the epoxy resin, cyanate composite also becomes a candidate material for aerospace due to its high glass transition temperature and radiation resistance. A tip-loaded deployable truss was based on shape memory cyanate composite, which had a high shape memory transition temperature of 195°C and could be used in space components, e.g. space probe, antenna, the tip mass of the gravity gradient boom and so on [385]. Lan et al. [386] conducted study on the deformation behavior and thermomechanical properties of carbon fiber strengthened SMP composite laminate, which had a reversible strain of 9.6% and allowed a wide prospect of applications in aerospace for foldable structures.

Several reports have been demonstrated that many self-deployable structures were practically utilized in aerospace engineering. This further validates the feasibility of the SMP-based space-deployable structure and their replacement of metals and ceramics in future spacecraft. Leng's group [387] reported the world's first spaceflight on-orbit verification of a self-deployable solar array device. According to the photos sent back to the ground from the SJ20 Geostationary Satellite, the solar array device had approximately 100% shape recovery performance within 60 s (Fig. 26f). The releasing mechanisms were actuated by the cyanate-based SMPC laminates, which showed such advantages as low impact and repeatable testability over traditional electro-explosive devices. Zhang et al. [388] designed an ultraviolet light responsive release device integrated with screen-printed heaters to latch and release the solar array of CubeSat. Fig. 26g shows the

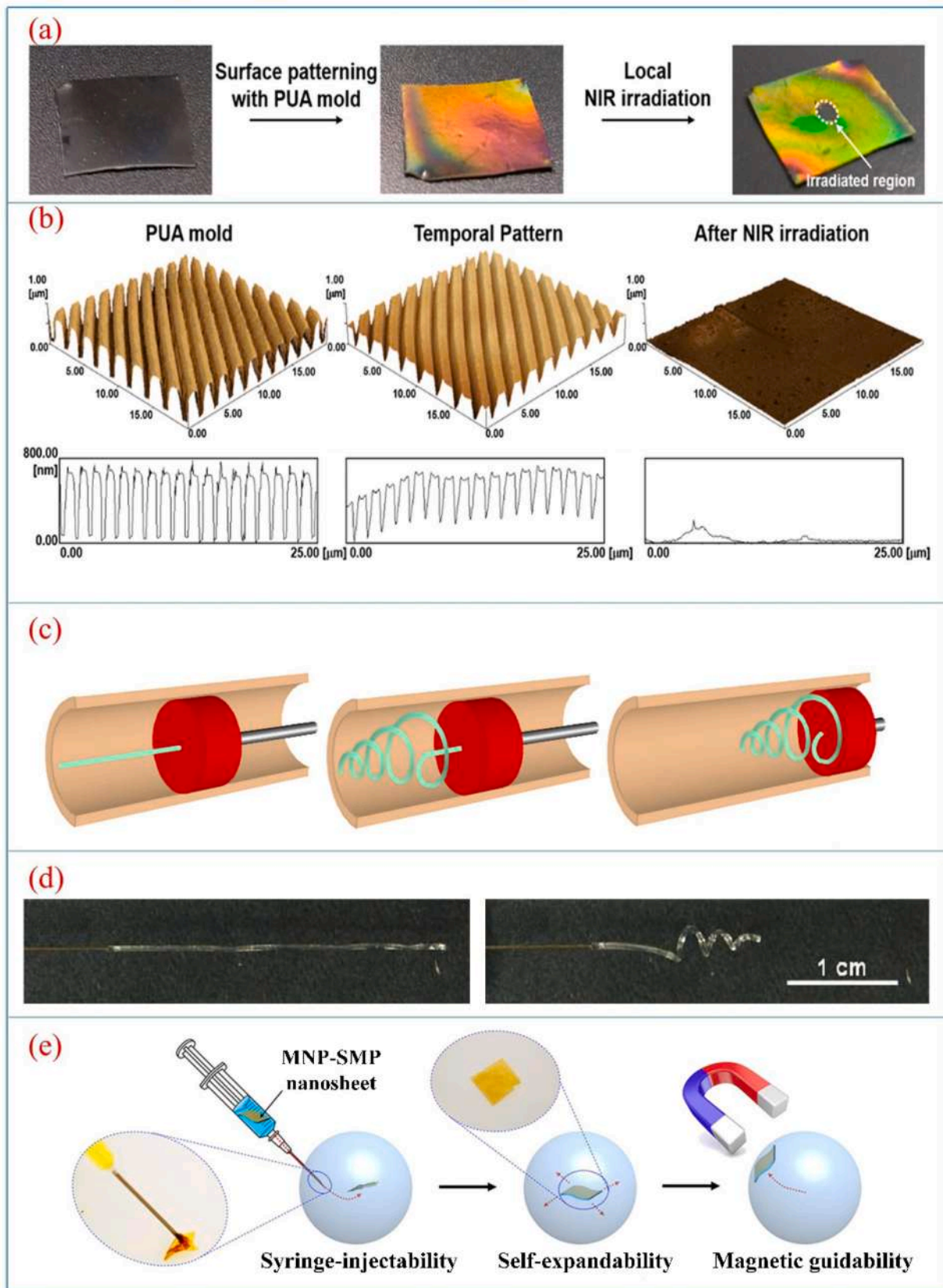


Fig. 27. (a) The images of the TiN-PCL composites, before programming, after programming and after the near-infrared light irradiation; (b) the 3D AFM surface and topographic pictures of PU mold with dimension 800 nm 1:1. (c) The diagram of endovascular thrombectomy using NIR-actuated SMP micro-actuator; (d) the shape memory behavior of SMP microactuator triggered by NIR irradiation. (e) The schematic illustration of the ultrathin film: MNP-SMP nanosheet. (a,b) [232]. Copyright 2016 American Chemical Society. (c,d) [399]. Copyright 2005 Optical Society. (e) [404]. Copyright 2019 American Chemical Society.

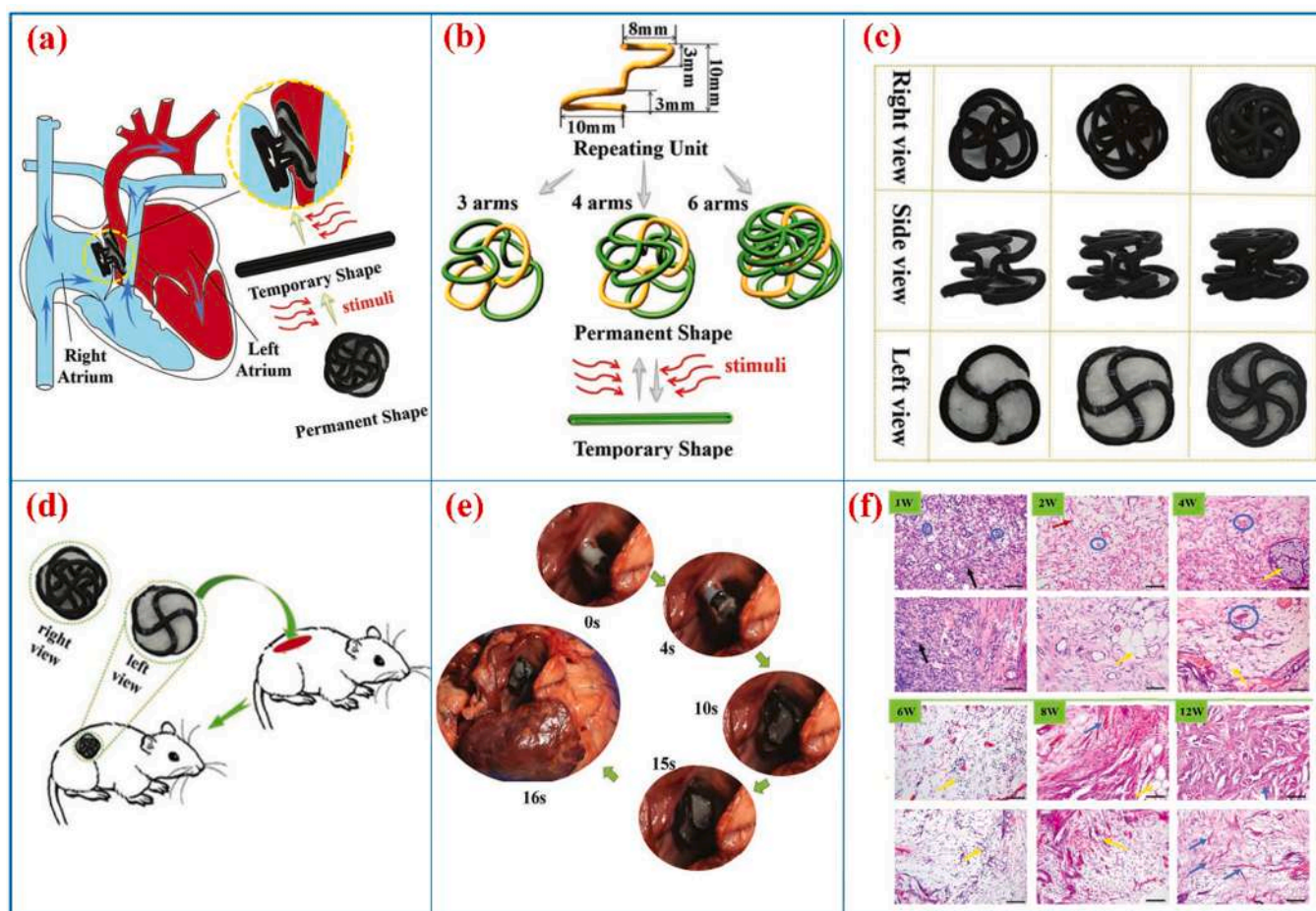


Fig. 28. (a) The diagram of the ASD prototype before and after treatment with an occluder; (b) the structural design of 3 / 4 / 6 arms occluders; (c) the photos of the 4D printing of occluders; (d) the diagram of the implantation process of the occluder in a rat; (e) the shape recovery process of the four-arm occluder triggered by magnetic field; (f) the observation of the tissues adjacent of the occluder in the rat at different time points, scale bar: 400 μm. [406]. Copyright 2019 Wiley-VCH.

packaging and deployment process of the ultra-light release device. The locking forces obtained through experiment and simulation showed excellent consistency. Liu et al. [389] prepared a 3-layer deployable hinge, which had a great deployed stiffness property and surface morphology. The authors used the smart hinge to assemble the solar array prototype and passed the ground deployment verification test. Therefore, such smart deployable structure had broad prospect of engineering applications in space, e.g. hinge, truss, antenna and so on. Moreover, these SMP composites and structures can be used in other astronomical programs, such as Mars exploration. This goal is very ambitious and challenging, but can be achievable it in the near future.

6.4. Biomedical engineering

SMPs can be widely applied in diverse biomedical settings, including drug release, clinical surgery, medical equipment, and degradable structures, etc. [390]. For example, the surgical SMP sutures with self-shrinking function are capable of automatic contraction from the pre-deformed status actuated by human body temperature [391]. Satoshi et al. [232] doped a photothermal absorber titanium nitride into shape memory polychinolactone to fabricate a near-infrared light-actuated shape memory TiN-PCL composite, which was then manufactured into a groove structure for the potential application in biomedical settings, such as cell manipulations, drug delivery and release (Fig. 27a and Fig. 27b).

Along with photo-actuated SMPs, magnetic-actuated SMPs also have

promising prospect of application in biomedical settings. A porous 3D structural sponge-like SMP (PCL matrix and gold nanoparticles) scaffold actuated by NIR irradiation or magnetic field was designed by Mohadeseh et al. [392]. The sponges showed super-high absorption capacity because of a high average porosity of $93 \pm 1.8\%$. The combination of porous structure and shape memory function endowed the scaffold with several distinctive properties for biological tissue engineering, e.g. high permeability and high porosity degree [393,394]. As mentioned in previous reports, electrospinning technique was one of popular technique to prepare porous scaffold [395–397]. The porous SMP scaffold can be utilized to provide structural support for the growth of organism tissue. Gold nanoparticles were added to absorb magnetic energy or a 532 nm light energy and generate the heat energy required to drive the deformation of the porous scaffold under magnetic or light stimulus [398].

Except for the shape-shifting biological scaffold, other medical equipments have been designed. Ward et al. [399] developed an intra-vascular therapeutic device using NIR-actuated SMP composites (epoxy / optical fiber) to mechanically remove the thrombus and restore the blood flow in brain (Fig. 27c and Fig. 27d). The deployment of the smart micro-actuator in an in vitro thrombotic vascular occlusion model proved that this clinical treatment device was promising in treating ischemic stroke. Ware et al. [400] reported a three-dimensional neural probe interface structure by combining shape memory biomedical materials with flexible electronic devices.

Another important biomedical engineering application are drug

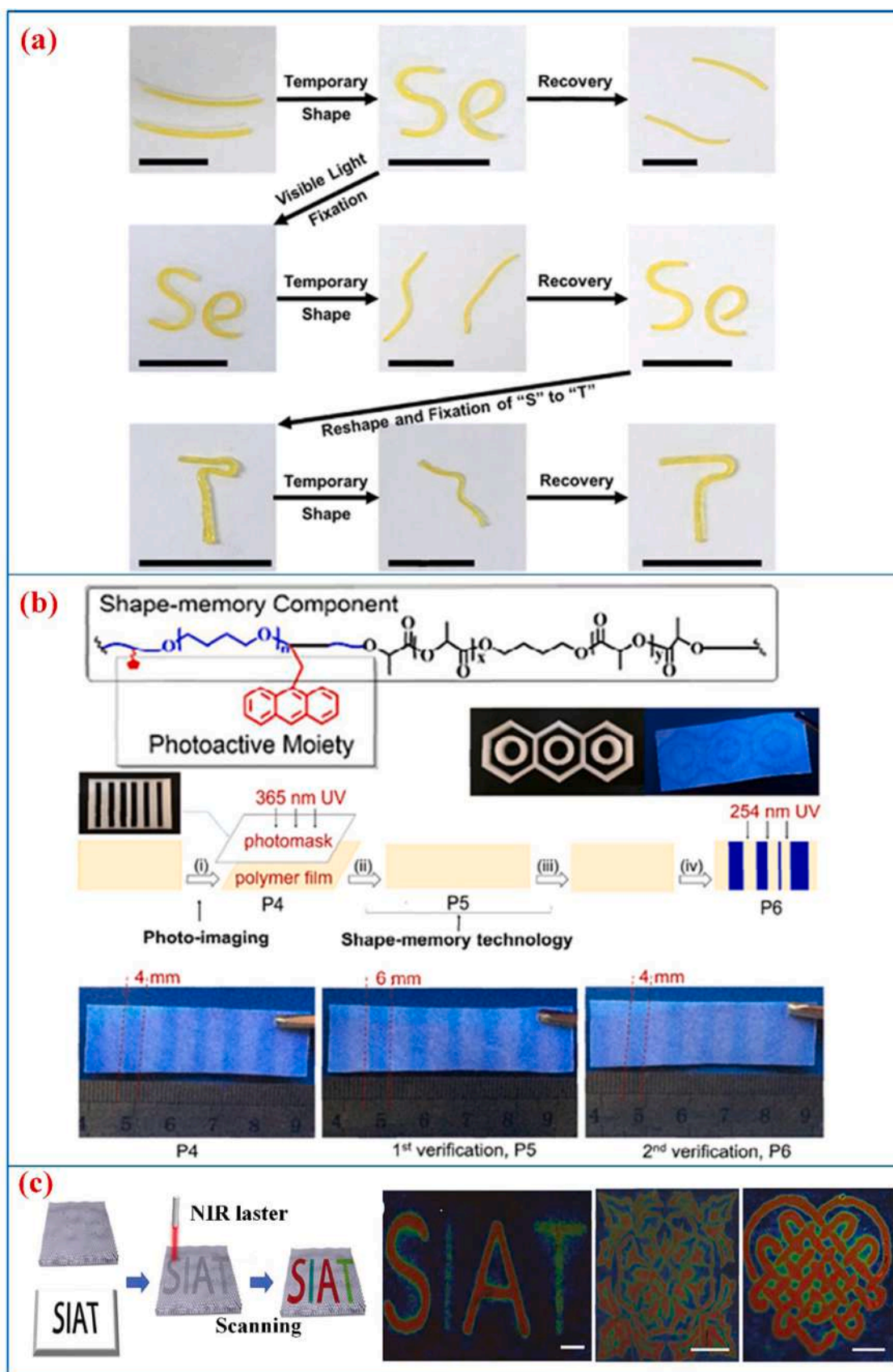


Fig. 29. (a) The permanent deformation and shape memory behavior of the samples under visible light irradiation and heating stimulus, respectively. (b) Double anti-counterfeiting film molecular structure and anti-counterfeiting process. (c) NIR-programmable multi-color copying of the SMP-based PC papers. (a) [412]. Copyright 2017 American Chemical Society. (b) [413]. Copyright 2018 Royal Society of Chemistry. (c) [414]. Copyright 2020 Royal Society of Chemistry.

delivery and release, for instance, the drugs delivery microcapsules with active deformation were fabricated by Leng et al. [401]. The SMP capsules possessed hollow structure for storing a large internal volume of drugs, and the speed of drug release was controlled by the active deformation to the SMP structure. Gai et al. [402] designed the polylactic acid nano and microchamber arrays which released drugs under ultrasound field actuation. The photo-actuated SMP as prepared by azobenzene and β -cyclodextrin with host-guest interactions was used to control protein release [403]. Furthermore, an ultrathin film (710 nm thick) consisting of shape memory polyurethane and magnetic nanoparticles (MNPs), namely, MNPs-SMP nanosheets, which can be injected using medical needle, and had self-expanded behavior under body temperature. Afterwards, they reached the predetermined location under the guidance of an external magnetic field (Fig. 27e) [404]. The smart nanosheets would be applied to develop injectable and self-expandable medical devices that can transfer drugs, cells, and special biological tissues using minimally invasive therapy.

From the above reports, it was known that researchers have made many biomedical devices using remote-actuated SMPs, but few clinical trials have verified and elaborated on them, which caused the disparity between theoretical research and practical application [405]. Leng et al. [406] conducted in-depth exploration into the 4D printing of magnetic-actuated heart occluder and demonstrated its histocompatibility, biodegradability and shape deformability through animal medicine experiments (Figs. 28a-28f). Three types of occluder frames with 3 / 4 / 6 arms (Fig. 28b) were printed using shape memory PLA / Fe₃O₄ magnetic nanocomposites. According to the medicine test, the smart heart occluder had excellent biocompatibility and degradability. The application of SMP in medical engineering is promising as the biocompatible materials, intelligent structure designs, and personalized surgical plans. With the help of scientific optimization, numerous smart materials and 4D printing techniques, personalized medical plan will usher in a golden age in the field of biomedicine.

6.5. Anti-counterfeiting engineering

Anti-counterfeiting engineering is of great significance to information security and luxury protection. Anti-counterfeiting products have the characteristics of unique identity, security, easy verification, and long storage period. Among them, multifunctional, wireless-controlled and programmable SMPs can be used as information carriers for advanced anti-counterfeiting [407–411]. Ji et al. [412] combined diselenide bonds with polyurethane to prepare a thermosetting SMP. Due to the dynamic reversibility of the diselenide bonds, the SMP can be reprogrammed to permanent shape under visible light irradiation. When the temperature rose to 80 °C, the sample would change from the temporary "Se" shape to the original straight shape (Fig. 29a). Moreover, the temporary shape "Se" can be reconfigured into the permanent shape after 6 h of visible light irradiation. The innovation is that it combines the visible light plasticity and shape memory effects to obtain a reconfigurable smart polymer, which endows it with the potential of application for braille printing, rewritable printing, and anti-counterfeiting purposes.

Another typical case is double anti-counterfeiting systems, which is designed by integrating 4D printing, photo-imaging and shape change properties [413]. Fig. 29b shows the molecular structure of SMP and the schematic diagram of anti-counterfeiting process. The addition of the image information on anthracene-containing SMP thin film with a photomask relied on localized photocycloaddition under a 365 nm light irradiation. Then, the SMP thin film was stretched and fixed into a temporary shape. The stored information, including shape change information and image information, was verified through heating and a 254 nm light irradiation, respectively. Therefore, the SMP thin film could be used for optical information storage and luxury anti-counterfeiting. Also, Wang et al. [414] reported a SMP-based photonic crystals paper which has rewritable, programmable excellent

colorful copying capability, and can transform information from a paper with pre-printed black letters or complex images via scanning with NIR light (Fig. 29c), so, it holds great promise in the fields of smart tags, and anti-counterfeiting labels.

7. Conclusions and outlooks

Shape memory polymers are prominent stimuli-responsive smart materials with intriguing potentials of application in such fields as aerospace, flexible electronic devices, robotics, biomedical devices and sensors, etc. In this review, we have summarized the progress made in the advanced shape memory polymers over the past decades. The advantages of remote-actuation, multistage shape transformation, multi-stimulus selective control and personalized 4D printing have enabled diverse and effective utilization of SMPs in various intelligent structures and systems. In spite of this, there remain some problems restricting the further development and application of SMPs. For instance, magnetic-actuated SMPs undergo insufficient clinical experiments before being used in living organisms. Photothermal-actuated SMPs and magnetic-thermal-actuated SMPs are slow in recovering their original shape (>10 s). The process of preparing microwave-actuated SMPs and ultrasound-actuated SMPs is complex. Also, the industry has placed demanding requirements on the performance of SMP materials, such as fast response and large recovery force.

The directions of future development for advanced SMPs mainly focus on the following aspects.

(a) The molecular structure design of SMPs for special use in harsh environments are highly required. For example, SMP materials need to be grafted with rigid groups (e.g. aromatic groups, aromatic heterocyclic groups or $C\equiv C$ bonds, etc.) before use in extreme harsh aerospace conditions. In the field of medical biology, SMPs are required to have high biocompatibility and good biodegradability through appropriate design of molecular structure. For the application of SMP drug release carriers, the kinetics of drug release in different SMP molecules must be calculated. (b) It is important to realize the high-precision programming and actuation of the shape memory behaviors of SMPs and SMPs. With the aid of computer design, the 4D printing of highly programmable SMP structures to personalized and integrated requirements is particularly meaningful. (c) Appropriate models are needed to quantitatively assess and predict the contribution of different factors that affect the mechanical performance and reliability of SMP-based actuator, soft robot and sensor. (d) Artificial intelligence is one of the most researched fields in the 21st century, and the combination between artificial intelligence and SMP-based smart actuators is certainly one interesting direction for the future research on intelligent systems. (e) It is significant to apply the lessons from nature to get intelligent SMP materials with better biocompatibility and environmental adaptability to meet the requirements of modern industries, e.g. robust artificial muscles, self-healing morphing stents, and disguised color-changing intelligent soft robots, etc.

Although the reviewed progresses in SMP research are very exciting and promising, the promotion of practical applications is relative backward and there is still a long way to go for achieving complete industrialization. It is firmly believed that the massive demand will drive a significant breakthrough in the theory and technology of SMPs. The shape memory polymers will stand out in the field of smart materials and present its practical value in many kinds of fields.

Declaration of Competing Interest

The authors declare that they have no known competing financial interests or personal relationships that could have appeared to influence the work reported in this paper.

Acknowledgements

This work is supported by the Heilongjiang Touyan Innovation Team Program.

References

- [1] S.K. Melly, L.W. Liu, Y.J. Liu, J.S. Leng, *J. Mater. Sci.* 55 (2020) 10975–11051, <https://doi.org/10.1007/s10853-020-04761-w>.
- [2] S.T. Li, R. Zhang, G.H. Zhang, L.Y.Z. Shuai, W. Chang, X.Y. Hu, M. Zou, X. Zhou, B.G. An, D. Qian, Z.F. Liu, *Nat. Commun.* 13 (2022) 1331, <https://doi.org/10.1038/s41467-022-29088-9>.
- [3] R. Wang, Y.N. Shen, D. Qian, J.K. Sun, X. Zhou, W.C. Wang, Z.F. Liu, *Mater. Horiz.* 7 (2020) 3305–3315, <https://doi.org/10.1039/d0mh01003k>.
- [4] Z.S. Liu, R. Zhang, Y.C. Xiao, J.T. Li, W. Chang, D. Qian, Z.F. Liu, *Mater. Horiz.* 8 (2021) 1783–1794.
- [5] M. Zou, S.T. Li, X.Y. Hu, X.Q. Leng, R. Wang, X. Zhou, Z.F. Liu, *Adv. Funct. Mater.* 31 (2021) 2007437, <https://doi.org/10.1002/adfm.202007437>.
- [6] X.F. Lv, L.W. Liu, Y.J. Liu, J.S. Leng, *Smart Mater. Struct.* 27 (2018), 105036, <https://doi.org/10.1088/1361-665X/aab9db>.
- [7] H.C. Quan, D. Kisailus, M.A. Meyers, *Nat. Rev. Mater.* 6 (2021) 264–283, <https://doi.org/10.1038/s41578-020-00251-2>.
- [8] A. Subash, B. Kandasubramanian, *Eur. Polym. J.* 134 (2020), 109771, <https://doi.org/10.1016/j.eurpolymj.2020.109771>.
- [9] R. Yu, X. Yang, Y. Zhang, X.J. Zhao, X. Wu, T.T. Zhao, Y.L. Zhao, W. Huang, *ACS Appl. Mater. Inter.* 9 (2017) 1820–1829, <https://doi.org/10.1021/acsmi.6b13531>.
- [10] J. Odent, J.M. Raquez, C. Samuel, S. Barrau, A. Enotiadis, P. Dubois, E. P. Giannelis, *Macromolecules* 50 (2017) 2896–2905, <https://doi.org/10.1021/acs.macromol.7b00195>.
- [11] M.L. de Espinosa, W. Meesorn, D. Moatsou, C. Weder, *Chem. Rev.* 117 (2017) 12851–12892, <https://doi.org/10.1021/acs.chemrev.7b00168>.
- [12] Z. Li, Y. Yang, Z.H. Wang, X.Y. Zhang, Q.M. Chen, X.J. Qian, N. Liu, Y. Wei, Y. Ji, *J. Mater. Chem. A* 5 (2017) 6740–6746, <https://doi.org/10.1039/c7ta00458c>.
- [13] M. Zarek, M. Layani, I. Cooperstein, E. Sachyani, D. Cohn, S. Magdassi, *Adv. Mater.* 28 (2016) 4449–4454, <https://doi.org/10.1002/adma.201503132>.
- [14] X. Wan, F.H. Zhang, Y.J. Liu, J.S. Leng, *Carbon* 115 (2019) 77–87, <https://doi.org/10.1016/j.carbon.2019.08.047>.
- [15] C. Meiorin, D.G. Actis, F.E. Montoro, O.M. Londono, M.I. Aranguren, D. Muraca, P.M. Zelis, M. Knobel, M.A. Mosiewicki, *Phys. Status Solid A* 215 (2018) 1800311, <https://doi.org/10.1002/pssa.201800311>.
- [16] Z.C. Jiang, Y.Y. Xiao, Y. Kang, M. Pan, B.J. Li, S. Zhang, *ACS Appl. Mater. Inter.* 9 (2017) 20276–20293, <https://doi.org/10.1021/acsmi.7b03624>.
- [17] J.M. Korde, B. Kandasubramanian, *Chem. Eng. J.* 379 (2020), 122430, <https://doi.org/10.1016/j.cej.2019.122430>.
- [18] T. Tian, J. Wang, S.S. Wu, Z.J. Shao, T. Xiang, S.B. Zhou, *Polym. Chem.* 10 (2019) 3488–3496, <https://doi.org/10.1039/c9py00502a>.
- [19] L. Peponi, V. Sessini, M.P. Arrieta, I. Navarro-Baena, A. Sonseca, F. Dominici, E. Gimenez, L. Torre, A. Terçjak, D. Lopez, *Polym. Degrad. Stabil.* 151 (2018) 36–51, <https://doi.org/10.1016/j.polymdegradstab.2018.02.019>.
- [20] J.J. Yang, W.D. Zhao, Z. Yang, W.L. He, J.X. Wang, T. Ikeda, L. Jiang, *ACS Appl. Mater. Inter.* 11 (2019) 46124–46131, <https://doi.org/10.1021/acsmi.9b14202>.
- [21] Y. Osada, A. Matsuda, *Nature* 376 (1995) 219, <https://doi.org/10.1038/376219a0>.
- [22] T.T. Zhao, R. Yu, X.P. Li, B. Chen, Y. Zhang, X. Yang, X.J. Zhao, Y.L. Zhao, W. Huang, *Eur. Polym. J.* 101 (2018) 120–126, <https://doi.org/10.1016/j.eurpolymj.2018.02.021>.
- [23] H. Gao L.N. Huang X. Lan L.W. Liu Y.J. Liu J.S. Leng Behavior and Mechanics of Multifunctional Materials and Composites 10165 UNSP 101651B 2017 doi: 10.1117/12.2259938.
- [24] Q.Y. Peng, J.Z. Cheng, S.R. Lu, Y.Q. Li, *Polym. Adv. Technol.* 31 (2020) 15–24, <https://doi.org/10.1002/pat.4743>.
- [25] M. Ansari, M. Golzar, M. Baghani, M. Soleimani, *Polym. Test.* 68 (2018) 424–432, <https://doi.org/10.1016/j.polymtest.2018.04.032>.
- [26] K. Sakurai, Y. Shirakawa, T. Kashiwagi, T. Takahashi, *Polymer* 35 (1994) 4238–4239, [https://doi.org/10.1016/0032-3861\(94\)90602-5](https://doi.org/10.1016/0032-3861(94)90602-5).
- [27] A. Revathi, V. Shalini, S. Joshi, *Adv. Sci.* 9 (2017) 384–390, <https://doi.org/10.1166/asem.2017.1996>.
- [28] Q.Y. Peng, H.Q. Wei, Y.Y. Qin, Z.S. Lin, X. Zhao, F. Xu, J.S. Leng, X.D. He, A. Y. Cao, Y.B. Li, *Nanoscale* 8 (2016) 18042–18049, <https://doi.org/10.1039/c6nr06515e>.
- [29] B.J. Jin, H.J. Song, R.Q. Jiang, J.Z. Song, Q. Zhao, *Sci. Adv.* 4 (2018) eaao3865, <https://doi.org/10.1126/sciadv.aao3865>.
- [30] Y.Q. Fu, W.M. Huang, J.K. Luo, H.B. Lu, *Shape Mem. Polym. Biomed. Appl.* (2015) 167–195, <https://doi.org/10.1016/B978-0-85709-698-2.00009-X>.
- [31] D. Bergman, B. Yang, *Int. J. Struct. Stab. Dy* 16 (2016) 109–112, <https://doi.org/10.1142/S021945541450093X>.
- [32] A.J. Boyle, M.A. Wierzbicki, S. Herting, A.C. Weems, A. Nathan, W. Hwang, D. J. Maitland, *Med. Eng. Phys.* 49 (2017) 56–62, <https://doi.org/10.1016/j.medengphy.2017.07.009>.
- [33] W. Xu, M.C. Wong, Q.Y. Guo, T.Z. Jia, J.H. Hao, *J. Mater. Chem. A* 7 (2019) 16267–16276, <https://doi.org/10.1039/c9ta03382c>.
- [34] Z. Xu, C. Ding, D.W. Wei, R.Y. Bao, K. Ke, Z.Y. Liu, M.B. Yang, W. Yang, *ACS Appl. Mater. Inter.* 11 (2019) 30332–30340, <https://doi.org/10.1021/acsmi.9b10386>.
- [35] W.X. Wang, Y.J. Liu, J.S. Leng, *Coord. Chem. Rev.* 320 (2016) 38–52, <https://doi.org/10.1016/j.ccr.2016.03.007>.
- [36] S.J. Chen, J.L. Hu, H.T. Zhuo, C.W.M. Yuen, L.K. Chan, *Polymer* 51 (2010) 240–248, <https://doi.org/10.1016/j.polymer.2009.11.034>.
- [37] Y.L. Yu, T. Ikeda, *Macromol. Chem. Phys.* 206 (2005) 1705–1708, <https://doi.org/10.1002/macp.200500318>.
- [38] M.H. Yousuf, W. Abuzaid, M. Alkhalid, *Addit. Manuf.* 35 (2020), 101364, <https://doi.org/10.1016/j.addma.2020.101364>.
- [39] B. Yang, W.M. Huang, C. Li, L. Li, *Polymer* 47 (2006) 1348–1356, <https://doi.org/10.1016/j.polymer.2005.12.051>.
- [40] B.S. Lee, B.C. Chun, Y.C. Chung, K.I. Sul, J.W. Cho, *Macromolecules* 34 (2001) 6431–6437, <https://doi.org/10.1021/ma001842i>.
- [41] S.M. Lai, Y.C. Lan, J. Polym. Res. 20 (2013) 140, <https://doi.org/10.1007/s10965-013-0140-6>.
- [42] K.S.S. Kumar, R. Biju, C.P.R. Nair, *React. Funct. Polym.* 73 (2013) 421–430, <https://doi.org/10.1016/j.reactfunctpolym.2012.06.009>.
- [43] Y. Zheng, J.X. Qin, J.B. Shen, S.Y. Guo, *J. Mater. Chem.* 8 (2020) 9593–9601, <https://doi.org/10.1039/d0tc01854f>.
- [44] E.L. Wang, Y.L. Wu, M.Z. Islam, Y.B. Dong, Y.F. Zhu, F.Y. Liu, Y.Q. Fu, Z.H. Xu, N. Hu, *Mater. Lett.* 238 (2019) 54–57, <https://doi.org/10.1016/j.matlet.2018.11.138>.
- [45] X.G. Guo, L.W. Liu, Y.J. Liu, B. Zhao, J.S. Leng, *Smart Mater. Struct.* 23 (2014), 105019, <https://doi.org/10.1088/0964-1726/23/10/105019>.
- [46] J.P. Gu, H. Zeng, Z.B. Cai, H.Y. Sun, *Smart Mater. Struct.* 29 (2020), 095005, <https://doi.org/10.1088/1361-665X/ab9e08>.
- [47] H. Cui, W.C. Tian, Y. Kang, Y.K. Wang, *Mater. Res. Express* 7 (2020), 015706, <https://doi.org/10.1088/2053-1591/ab6b5f>.
- [48] Z.D. Wang, W. Song, L. Ke, Y. Wang, *Mater. Lett.* 89 (2012) 216–218, <https://doi.org/10.1016/j.matlet.2012.08.112>.
- [49] Q. Zhao, H.J. Qi, T. Xie, *Prog. Polym. Sci.* 49–50 (2015) 79–120, <https://doi.org/10.1016/j.progpolymsci.2015.04.001>.
- [50] P.F. Zhang, M. Behl, M. Balk, X.Z. Peng, A. Lendlein, *Macromol. Rapid Comm.* 41 (2020) 1900658, <https://doi.org/10.1002/marc.201900658>.
- [51] A. Lendlein, H.Y. Jiang, O. Junger, R. Langer, *Nature* 434 (2005) 879–882, <https://doi.org/10.1038/nature03496>.
- [52] F.T. Cheng, R.Y. Yin, Y.Y. Zhang, C.C. Yen, Y.L. Yu, *Soft Matter* 6 (2010) 3447–3449, <https://doi.org/10.1039/c0sm00012d>.
- [53] K.K. Westbrook, P.T. Mather, V. Parakh, M.L. Dunn, Q. Ge, B.M. Qi, *Smart Mater. Struct.* 20 (2011), 065010, <https://doi.org/10.1088/0964-1726/20/6/065010>.
- [54] Y. Wu, J.L. Hu, J. Han, Y. Zhu, H. Huang, J. Li, B. Tang, *J. Mater. Chem. A* 2 (2014) 18816–18822, <https://doi.org/10.1039/c4ta03640a>.
- [55] L.F. Fan, M.Z. Rong, M.Q. Zhang, X.D. Chen, *Macromol. Rapid Comm.* 38 (2017) 1700124, <https://doi.org/10.1002/marc.201700124>.
- [56] C. Qian, Y.B. Dong, Y.F. Zhu, Y.Q. Fu, *Smart Mater. Struct.* 25 (2016), 085023, <https://doi.org/10.1088/0964-1726/25/8/085023>.
- [57] S.J. Chen, J.L. Hu, H.T. Zhuo, Y. Zhu, *Mater. Lett.* 62 (2008) 4088–4090, <https://doi.org/10.1016/j.matlet.2008.05.073>.
- [58] T. Chung, A. Romo-Uribe, P.T. Mather, *Macromolecules* 41 (2008) 184–192, <https://doi.org/10.1021/ma071517z>.
- [59] M. Behl, K. Kratz, J. Zotemann, U. Nickel, A. Lendlein, *Adv. Mater.* 25 (2013) 4466–4469, <https://doi.org/10.1002/adma.201300880>.
- [60] T. Defize, R. Riva, J.M. Thomassin, C. Jerome, M. Alexandre, A. Lendlein, D. W. Grijpma, *Adv. Polym. Med.* (2011) 154–161, <https://doi.org/10.1002/masy.201100036>.
- [61] H. Tobushi, T. Hashimoto, S. Hayashi, E. Yamada, *J. Intel. Mat. Syst. Str.* 8 (1997) 711–718, <https://doi.org/10.1177/1045389X9700800808>.
- [62] T. Long, Nguyen, H.J. Qi, F. Castro, K.N. Long, *J. Mech. Phys. Solids* 56 (2008) 2792–2814, <https://doi.org/10.1016/j.jmps.2008.04.007>.
- [63] B. Zhou, Y.J. Liu, J.S. Leng, *Acta Polym. Sin.* 6 (2009) 525–529, <https://doi.org/10.3724/sp.j.1105.2009.00525>.
- [64] J.M. Guo, Harbin Engineering University, Harbin, 2016.
- [65] H. Zeng, J.S. Leng, J.P. Gu, H.Y. Sun, *Int. J. Mech. Sci.* 166 (2020), 105212, <https://doi.org/10.1016/j.ijmecsci.2019.105212>.
- [66] Y.P. Liu, K. Gall, M.L. Dunn, A.R. Greenberg, J. Diani, *Int. J. Plast.* 22 (2006) 279–313, <https://doi.org/10.1016/j.ijplas.2005.03.004>.
- [67] Z.F. Li, Beijing Jiaotong University, Beijing, 2011.
- [68] K.K. Westbrook, V. Parakh, T. Chung, P.T. Mather, L.C. Wan, M.L. Dunn, H.J. Qi, *J. Eng. Mater. Trans. ASME* 132 (2010), 041010, <https://doi.org/10.1115/1.4001964>.
- [69] P. Gilormini, J. Diani, *Cr. Mec.* 340 (2012) 338–348, <https://doi.org/10.1016/j.crme.2012.02.016>.
- [70] W. Zhao, L.Y. Liu, J.S. Leng, Y.J. Liu, *Mech. Mater.* 143 (2020), 103263, <https://doi.org/10.1016/j.mechmat.2019.103263>.
- [71] K. Yu, A.J.W. McClung, G.P. Tandon, J.W. Baur, H.J. Qi, *Mech. Time-Depend. Mat.* 18 (2014) 453–474, <https://doi.org/10.1007/s11043-014-9237-5>.
- [72] Q.F. Zhang, W.W. Lin, Q. Zhang, Y.F. Liu, P.Y. Zhang, *J. Zhejiang Univ. Tech.* 43 (2015) 43–46, <https://doi.org/10.3969/j.issn.1006-4303.2015.01.008>.
- [73] H. Tobushi, N. Ito, K. Takata, S. Hayashi, *Mater. Sci. Forum* 3 (2000) 343–346, <https://doi.org/10.4028/www.scientific.net/MSF.327-328.343>.
- [74] J.H. Kim, T.J. Kang, W.R. Yu, *Int. J. Plast.* 26 (2010) 204–218, <https://doi.org/10.1016/j.ijplas.2009.06.006>.
- [75] X.G. Guo, L.W. Liu, B. Zhou, Y.J. Liu, J.S. Leng, *J. Intel. Mat. Syst. Str.* 27 (2016) 314–323, <https://doi.org/10.1177/1045389X15571380>.
- [76] K. Yu, K.K. Westbrook, P.H. Kao, J.S. Leng, H.J. Qi, *J. Compos. Mater.* 47 (2013) 51–63, <https://doi.org/10.1177/0021998312447647>.

- [77] T. Calvo-Correas, A. Shirole, A. Alonso-Varona, T. Palomares, C. Weder, M. A. Corcuera, A. Eceiza, *Biomacromolecules* 21 (2020) 2032–2042, <https://doi.org/10.1021/acs.biomac.9b01764>.
- [78] X.H. Meng, T. Zhang, J. Zhang, G. Qu, L.J. Wu, H.P. Liu, H. Zhao, B. Zhong, L. Xia, X.X. Huang, G.W. Wen, *Nanotechnology* 31 (2020), 255710, <https://doi.org/10.1088/1361-6528/ab758c>.
- [79] R. Ul Hassan, S. Jo, J. Seok, *J. Appl. Polym. Sci.* 135 (2018) 45997, <https://doi.org/10.1002/app.45997>.
- [80] M.Y. Razaq, M. Behl, U. Noecheh, A. Lendlein, *Polymer* 55 (2014) 5953–5960, <https://doi.org/10.1016/j.polymer.2014.07.025>.
- [81] M. Urban, M. Strankowski, *Materials* 10 (2017) 1083, <https://doi.org/10.3390/ma10091083>.
- [82] R.P. McEvoy, M. McMenamin, G. Ha, J.H. Lang, P. Cantillon-Murphy, *IEEE T. Magn.* 49 (2013) 496–505, <https://doi.org/10.1109/TMAG.2012.2205935>.
- [83] P.R. Buckley, G.H. McKinley, T.S. Wilson, W. Small, W.J. Benett, J.P. Bearinger, M.W. McElfresh, D.J. Maitland, *IEEE T. Bio Med. Eng.* 53 (2006) 2075–2083, <https://doi.org/10.1109/TBME.2006.877113>.
- [84] J.R. Huang, J.F. Fan, S.H. Yin, Y.K. Chen, *Compos. Sci. Tech.* 182 (2019), 107732, <https://doi.org/10.1016/j.compscitech.2019.107732>.
- [85] S. Xu, B.J. Zhao, M. Adeel, H.G. Mei, L. Li, S.X. Zheng, *Polymer* 172 (2019) 404–414, <https://doi.org/10.1016/j.polymer.2019.04.020>.
- [86] C. Liu, J.R. Huang, D.S. Yuan, Y.K. Chen, *Ind. Eng. Chem. Res.* 57 (2018) 14527–14534, <https://doi.org/10.1021/acs.iecr.8b03377>.
- [87] G.D. Soto, C. Meiorin, D. Actis, P.M. Zelis, M.A. Mosiewicki, N.E. Marcovich, *Polym. Test.* 65 (2018) 360–368, <https://doi.org/10.1016/j.polymertesting.2017.12.012>.
- [88] U.N. Kumar, K. Kratz, M. Heuchel, M. Behl, A. Lendlein, *Adv. Mater.* 23 (2011) 4157–4162, <https://doi.org/10.1002/adma.201102251>.
- [89] R. Mohr, K. Kratz, T. Weigel, M. Lucka-Gabor, M. Moneke, A. Lendlein, *Proc. Natl. Acad. Sci. USA* 103 (2006) 3540–3545, <https://doi.org/10.1073/pnas.0600079103>.
- [90] M.Y. Razaq, M. Anhalt, L. Frommann, B. Weidenfeller, *Mat. Sci. Eng. A-Struct.* 444 (2007) 227–235, <https://doi.org/10.1016/j.msea.2006.08.083>.
- [91] X.M. Wang, F.Z. Sun, G.C. Yin, Y.T. Wang, B. Liu, M.D. Dong, *Sensors* 18 (2018) 330, <https://doi.org/10.3390/s18020330>.
- [92] W.C. Xu, X.Z. Hu, S.D. Zhuang, Y.X. Wang, X.Q. Li, L. Zhou, S.N. Zhu, J. Zhu, *Adv. Energy Mater.* 8 (2018) 1702884, <https://doi.org/10.1002/aenm.201702884>.
- [93] Y.M. Liu, C.L. Hou, T.F. Jiao, J.W. Song, X. Zhang, R.R. Xing, J.X. Zhou, L. X. Zhang, Q.M. Peng, *Nanomaterials* 8 (2018) 35, <https://doi.org/10.3390/nano8010035>.
- [94] A. Balogh, A. Domokos, B. Farkas, A. Farkas, Z. Rapi, D. Kiss, Z. Nyiri, Z. Eke, G. Szarka, R. Orkenyi, *Chem. Eng. J.* 350 (2018) 290–299, <https://doi.org/10.1016/j.cej.2018.05.188>.
- [95] C. Zhang, Y. Li, P. Wang, H. Zhang, *Compr. Rev. Food Sci. F.* 119 (2020) 479–502, <https://doi.org/10.1111/1541-4337.12536>.
- [96] A.A. Puchkov, T.K. Tenchurin, V.G. Mamagulashvili, A.D. Shepelev, S. N. Chvalun, *J. Phys. Conf. Ser.* 1347 (2019), 012098, <https://doi.org/10.1088/1742-6596/1347/1/012098>.
- [97] X.Y. Li, Y.N. Xia, *Adv. Mater.* 16 (2004) 1151–1170, <https://doi.org/10.1002/adma.200400719>.
- [98] T. Gong, W.B. Li, H.M. Chen, L. Wang, S.J. Shao, S.B. Zhou, *Acta Biomater.* 8 (2012) 1248–1259, <https://doi.org/10.1016/j.actbio.2011.12.006>.
- [99] A.M. Schmidt, *Macromol. Rapid Comm.* 27 (2010) 1168–1172, <https://doi.org/10.1002/marc.200600225>.
- [100] A. Golbang, M. Kokabi, *Eur. Polym. J.* 47 (2011) 1709–1719, <https://doi.org/10.1016/j.eurpolymj.2011.06.008>.
- [101] U.N. Kumar, K. Kratz, W. Wagermaier, M. Behl, A. Lendlein, *J. Mater. Chem.* 20 (2010) 3404–3415, <https://doi.org/10.1039/b923000a>.
- [102] F.H. Zhang, Z.C. Zhang, C.J. Luo, I.T. Lin, Y.J. Liu, J.S. Leng, S.K. Smoukov, *J. Mater. Chem. C* 3 (2015) 11290–11293, <https://doi.org/10.1039/c5tc02464a>.
- [103] M.Y. Razaq, M. Behl, K. Kratz, A. Lendlein, *Adv. Mater.* 25 (2013) 5730–5733, <https://doi.org/10.1002/adma.201302485>.
- [104] L.A. Wood, F.L. Roth, *J. Appl. Phys.* 15 (1944) 781–789, <https://doi.org/10.1063/1.1707388>.
- [105] N. Prem, D. Sindersberger, B. Striegl, V. Bohm, G.J. Monkman, *Macromol. Chem. Phys.* 221 (2020) 2000149, <https://doi.org/10.1002/macp.202000149>.
- [106] X. Gong, K. Tan, Q. Deng, S.P. Shen, *ACS Appl. Mater. Inter.* 12 (2020) 16930–16936, <https://doi.org/10.1021/acsami.0c01453>.
- [107] H. Meng, G.Q. Li, *Polymer* 54 (2013) 2199–2221, <https://doi.org/10.1016/j.polymer.2013.02.023>.
- [108] S.B. Hong, Y.S. Ahn, J.H. Jang, J.G. Kim, N.S. Goo, W.R. Yu, *Behav. Mech. Multifunct. Mater. Compos.* 9800 (2016) 980005, <https://doi.org/10.1117/1.2218404>.
- [109] X.L. Zang, Y.L. He, Z.Z. Fang, X.S. Wang, J.H. Ji, Y.P. Wang, M.Q. Xue, *Macromol. Mater. Eng.* 305 (2020) 1900581, <https://doi.org/10.1002/adma.201900581>.
- [110] C.M. Wells, M. Harris, L. Choi, V.P. Murali, F.D. Guerra, J.A. Jennings, *J. Func. Biomater.* 10 (2019) 34, <https://doi.org/10.3390/jfb10030034>.
- [111] H. Gao, J.R. Li, F.H. Zhang, Y.J. Liu, J.S. Leng, *Mater. Horiz.* 6 (2019) 931–944, <https://doi.org/10.1039/c8mh01070f>.
- [112] L.Y. Qiao, C. Liu, C.D. Liu, F.Y. Hu, X.Y. Li, C.H. Wang, X.G. Jian, *Eur. Polym. J.* 134 (2020), 109835, <https://doi.org/10.1016/j.eurpolymj.2020.109835>.
- [113] T. Calvo-Correas, A. Shirole, F. Crippa, A. Fink, C. Weder, M.A. Corcuera, A. Eceiza, *Mat. Sci. Eng. C-Mater.* 97 (2019) 658–668, <https://doi.org/10.1016/j.msec.2018.12.074>.
- [114] Y.F. Zhao, J. Chen, *Prog. Nucl. Energ.* 50 (2008) 1–6, <https://doi.org/10.1016/j.pnucene.2007.08.009>.
- [115] S.I. Kim, T. Aida, H. Niiyama, *Sep. Purif. Technol.* 45 (2005) 174–182, <https://doi.org/10.1016/j.seppur.2005.03.006>.
- [116] M. Kent, R. Knocheh, F. Daschner, U.K. Berger, *Food Control* 12 (2001) 467–482, [https://doi.org/10.1016/S0956-7135\(01\)00021-4](https://doi.org/10.1016/S0956-7135(01)00021-4).
- [117] D.A. Jones, T.P. Lelyveld, S.D. Mavrofidis, S.W. Kingman, N.J. Miles, *Resour. Conserv. Recycl.* 34 (2002) 75–90, [https://doi.org/10.1016/S0921-3449\(01\)00088-X](https://doi.org/10.1016/S0921-3449(01)00088-X).
- [118] H. Kalita, N. Karak, *J. Mater. Res.* 28 (2013) 2132–2141, <https://doi.org/10.1557/jmr.2013.213>.
- [119] R.K. Gupta, S.A.R. Hashmi, S. Verma, A. Naik, P. Nair, *J. Mater. Eng. Perform.* 29 (2020) 205–214, <https://doi.org/10.1007/s11665-020-04568-5>.
- [120] A.V. Menon, G. Madras, S. Bose, *Chem. Eng. J.* 352 (2018) 590–600, <https://doi.org/10.1016/j.cej.2018.07.048>.
- [121] C.K. Chou, A.W. Guy, L.L. Kunz, R.B. Johnson, J.J. Crowley, J.H. Krupp, *Bioelectromagnetics* 13 (1992) 469–496, <https://doi.org/10.1002/bem.2250130605>.
- [122] T.V. Pham, T.T. Nguyen, D.T. Nguyen, T.V. Thuan, P.Q.T. Bui, V.N.D. Viet, L. G. Bach, *J. Nanosci. Nanotechnol.* 19 (2019) 1122–1125, <https://doi.org/10.1166/jnn.2019.15926>.
- [123] A.K. Sonker, V. Verma, *J. Appl. Polym. Sci.* 135 (2018) 46125, <https://doi.org/10.1002/app.46125>.
- [124] P. Keangin, U. Narumitbowonkul, P. Rattanadecho, Iop Publishing Ltd, Dirac House, Temple Back, Bristol BS1 6BE, England 2018. <https://doi.org/10.1088/1757-899X/297/1/012037>.
- [125] Z. Tong, X.H. Pei, Z.J. Shen, S.B. Wei, Y. Gao, P. Huang, B.R. Shi, F.C. Sun, T. Fu, *Petrol. Explor. Dev.* 43 (2016) 1097–1106, [https://doi.org/10.1016/S1876-3804\(16\)30128-8](https://doi.org/10.1016/S1876-3804(16)30128-8).
- [126] T. Ghosh, N. Karak, *J. Colloid Interf. Sci.* 540 (2019) 247–257, <https://doi.org/10.1016/j.jcis.2019.01.006>.
- [127] L. Chen, Y.J. Liu, J.S. Leng, *J. Appl. Polym. Sci.* 135 (2018) 45676, <https://doi.org/10.1002/app.45676>.
- [128] A. Francis, *Mater. Res. Express* 5 (2018), 062003, <https://doi.org/10.1088/2053-1591/aacd28>.
- [129] L. Chen, W. Li, X.P. Liu, C. Zhang, H. Zhou, S.W. Song, *J. Appl. Polym. Sci.* 136 (2019) 47563, <https://doi.org/10.1002/app.47563>.
- [130] R.K. Gupta, S.A.R. Hashmi, S. Verma, A. Naik, P. Nair, *J. Mater. Eng. Perform.* 29 (2020) 205–214, <https://doi.org/10.1007/s11665-020-04568-5>.
- [131] H.Y. Du, Z. Song, J.J. Wang, Z.H. Liang, Y.H. Shen, F. You, *Sens. Actuators A Phys.* 228 (2015) 1–8, <https://doi.org/10.1016/j.sna.2015.01.012>.
- [132] H.Y. Du, Y.L. Yu, G.M. Jiang, J.H. Zhang, J.J. Bao, *Macromol. Chem. Phys.* 212 (2011) 1460–1468, <https://doi.org/10.1002/macp.201100149>.
- [133] T. Palav, K. Seetharaman, *Carbohydr. Polym.* 67 (2007) 596–604, <https://doi.org/10.1016/j.carbpol.2006.07.006>.
- [134] K. Yu, Y.J. Liu, J.S. Leng, *RSC Adv.* 4 (2014) 2961–2968, <https://doi.org/10.1039/c3ra43258k>.
- [135] F.H. Zhang, T.Y. Zhou, Y.J. Liu, J.S. Leng, *Sci. Rep.* 5 (2015) 11152, <https://doi.org/10.1038/srep11152>.
- [136] K.K. Patel, R. Purohit, *Sens. Actuators A Phys.* 285 (2019) 17–24, <https://doi.org/10.1016/j.sna.2018.10.049>.
- [137] H.Y. Du, Z. Ren, Y.Y. Xu, *Iran. Polym. J.* 27 (2018) 621–628, <https://doi.org/10.1007/s13726-018-0638-1>.
- [138] M.K. Thakur, V.K. Thakur, R.K. Gupta, A. Pappu, *ACS Sustain. Chem. Eng.* 4 (2016) 1–17, <https://doi.org/10.1021/acsuscemeng.5b01327>.
- [139] Y. Fang, S.Y. Leo, Y.L. Ni, J.Y. Wang, B.C. Wang, L. Yu, Z. Dong, Y.Q. Dai, V. Basile, C. Taylor, P. Jiang, *ACS Appl. Mater. Inter.* 9 (2017) 5457–5467, <https://doi.org/10.1021/acsami.6b13634>.
- [140] T. Ghosh, N. Karak, *RSC Adv.* 8 (2018) 17044–17055, <https://doi.org/10.1039/c8ra01766b>.
- [141] G. Li, G.X. Fei, H.S. Xia, J.J. Han, Y. Zhao, *J. Mater. Chem.* 22 (2012) 7692–7696, <https://doi.org/10.1039/c2jm30848g>.
- [142] A. Boudjellal, D. Trache, K. Khimeche, S.L. Hafsaoui, A. Bougamra, A. Tcharkhtchi, J.F. Durastanti, 0892705720930775, *J. Thermoplast. Compos (2020)*, <https://doi.org/10.1177/0892705720930775>.
- [143] H.C. Liu, J.B. Li, X.X. Gao, B. Deng, G.S. Huang, *J. Polym. Res.* 25 (2017) 24, <https://doi.org/10.1007/s10965-017-1427-9>.
- [144] J. Delaey, P. Dubruel, S. Van Vlierbergh, *Adv. Funct. Mater.* (2020) 1909047, <https://doi.org/10.1002/adfm.201909047>.
- [145] A. Bhargava, K.Y. Peng, J. Stieg, R. Mirzaeifar, S. Shahab, *RSC Adv.* 7 (2017) 45452–45469, <https://doi.org/10.1039/c7ra07396h>.
- [146] A. Bhargava, S. Shahab, *Smart Mater. Struct.* 28 (2019), 055002, <https://doi.org/10.1088/1361-665X/ab0b71>.
- [147] M. Lei, Z. Chen, H.B. Lu, K. Yu, *Nanotechnol. Rev.* 8 (2019) 327–351, <https://doi.org/10.1515/nrtrev-2019-0031>.
- [148] H. Ramaraju, R.E. Akman, D.L. Safranski, S.J. Hollister, *Adv. Funct. Mater.* (2020) 2002014, <https://doi.org/10.1002/adfm.202002014>.
- [149] A. Bhargava, K. Peng, S. Shahab, *Proceedings of SPIE Bellingham USA 2019*. <https://doi.org/10.1117/12.2514362>.
- [150] L. Guo, Y.P. Wang, S.W. Wang, *J. Polym. Sci. Part B: Polym. Phys.* 56 (2018) 1700483, <https://doi.org/10.1002/polb.201700483>.
- [151] V. Srivastava, S.A. Chester, L. Anand, *J. Mech. Phys. Solids* 58 (2010) 1100–1124, <https://doi.org/10.1016/j.jmps.2010.04.004>.
- [152] J. Kost, K. Leong, R. Langer, *Proc. Natl. Acad. Sci. USA* 86 (1989) 7663–7666, <https://doi.org/10.1073/pnas.86.20.7663>.
- [153] B.G. De Geest, A.G. Skirtach, A.A. Mamedov, A.A. Antipov, N.A. Kotov, S.C. De Smedt, G.B. Sukhorukov, *Small* 3 (2010) 804–808, <https://doi.org/10.1002/sml.200600441>.

- [154] X.L. Lu, G.X. Fei, H.S. Xia, Y. Zhao, J. Mater. Chem. A 2 (2014) 16051–16060, <https://doi.org/10.1039/c4ta02726d>.
- [155] G. Li, Q. Yan, H.S. Xia, Y. Zhao, ACS Appl. Mater. Inter. 7 (2015) 12067–12073, <https://doi.org/10.1021/acsami.5b02234>.
- [156] J.J. Han, G.X. Fei, G. Li, H.S. Xia, Macromol. Chem. Phys. 214 (2013) 1195–1203, <https://doi.org/10.1002/macp.201200576>.
- [157] M. Bao, Q.H. Zhou, W. Dong, X.X. Lou, Y.Z. Zhang, Biomacromolecules 14 (2013) 1971–1979, <https://doi.org/10.1021/bm4003464>.
- [158] A. Bhargava, K.Y. Peng, R. Mirzaeifar, S. Shahab, Proceedings of SPIE Bellingham USA 2018. <https://doi.org/10.1117/12.2296739>.
- [159] P.F. Zhang, M. Behl, X.Z. Peng, M.Y. Razzaq, A. Lendlein, Macromol. Rapid Comm. 37 (2016) 1897–1903, <https://doi.org/10.1002/marc.201600439>.
- [160] T. Gilbert, N.M.B. Smeets, T. Hoare, ACS Macro Lett. 4 (2015) 1104–1109, <https://doi.org/10.1021/acsmacrolett.5b00362>.
- [161] J.M.J. Paulusse, D.J.M. van Beek, R.P. Sijbesma, J. Am. Chem. Soc. 129 (2007) 2392–2397, <https://doi.org/10.1021/ja067523c>.
- [162] T.S. Hebner, M. Podgorski, S. Mavila, T.J. White, C.N. Bowman, Angew. Chem. Int. Ed. 61 (2022), e202116522, <https://doi.org/10.1002/anie.202116522>.
- [163] K.J. Chen, X. Kuang, V. Li, G.Z. Kang, H.J. Qi, Soft Matter 14 (2018) 1879–1886, <https://doi.org/10.1039/c7sm02362f>.
- [164] F. Pilate, A. Toncheva, P. Dubois, J.M. Raquez, Eur. Polym. J. 80 (2016) 268–294, <https://doi.org/10.1016/j.eurpolymj.2016.05.004>.
- [165] T.Y. Fang, L.L. Cao, S.P. Chen, J.J. Fang, J. Zhou, L. Fang, C.H. Lu, Z.Z. Xu, Mater. Des. 144 (2018) 129–139, <https://doi.org/10.1016/j.matdes.2018.02.029>.
- [166] L. Fang, S.P. Chen, T.Y. Fang, J.J. Fang, C.H. Lu, Z.Z. Xu, Compos. Sci. Technol. 138 (2017) 106–116, <https://doi.org/10.1016/j.compscitech.2016.11.018>.
- [167] H.J. Zhang, Y. Zhao, ACS Appl. Mater. Inter. 5 (2013) 13069–13075, <https://doi.org/10.1021/am404087q>.
- [168] W. Wagermaier, K. Kratz, M. Heuchel, A. Lendlein, Adv. Polym. Sci. Berl. Ger. (2010), https://doi.org/10.1007/12_2009_25.
- [169] R. Tang, Z.Y. Liu, D.D. Xu, J. Liu, L. Yu, H.F. Yu, ACS Appl. Mater. Inter. 7 (2015) 8393–8397, <https://doi.org/10.1021/acsami.5b01732>.
- [170] Y. Hu, Z. Li, T. Lan, W. Chen, Adv. Mater. 28 (2016) 10548–10556, <https://doi.org/10.1002/adma.201602685>.
- [171] Y.Y. Fei, C. Liu, G. Chen, C.Y. Hong, Polym. Chem. 10 (2019) 3895–3901, <https://doi.org/10.1039/c9py00472f>.
- [172] C.H. Zhu, Y. Lu, J. Peng, J.F. Chen, S.H. Yu, Adv. Funct. Mater. 22 (2012) 4017–4022, <https://doi.org/10.1002/adfm.201201020>.
- [173] F.J. Ge, X.L. Lu, J. Xiang, X. Tong, Y. Zhao, Angew. Chem. Int. Ed. 56 (2017) 6126–6130, <https://doi.org/10.1002/ange.201612164>.
- [174] H.B. Zhang, W.B. Li, H. Liu, S.B. Shang, Z.Q. Song, Mater. Today Commun. 28 (2021), 102490, <https://doi.org/10.1016/j.mtcomm.2021.102490>.
- [175] X.L. Pang, J.A. Lv, C.Y. Zhu, L. Qi, Y.L. Yu, Adv. Mater. 31 (2019) 1904224, <https://doi.org/10.1002/adma.201904224>.
- [176] K.K. Julich-Gruner, C. Lowenberg, A.T. Neffe, M. Behl, A. Lendlein, Macromol. Chem. Phys. 214 (2013) 527–536, <https://doi.org/10.1002/macp.201200607>.
- [177] C. Carlo, L. Angiolini, D. Caretti, E. Corelli, Polym. Adv. Technol. 7 (1996) 379–384, [https://doi.org/10.1002/\(SICI\)1099-1581\(199605\)7:5<33.C0>2.3.CO;2-3](https://doi.org/10.1002/(SICI)1099-1581(199605)7:5<33.C0>2.3.CO;2-3).
- [178] M. Camacho-Lopez, H. Finkelmann, P. Palffy-Muhoray, M. Shelley, Nat. Mater. 3 (2004) 307–310, <https://doi.org/10.1038/nmat1118>.
- [179] R. Ennis, L.C. Malacarne, P. Palffy-Muhoray, M. Shelley, Phys. Rev. E 74 (2006), 061802, <https://doi.org/10.1103/PhysRevE.74.061802>.
- [180] K.M. Lee, T.J. Bunning, T.J. White, Adv. Mater. 24 (2012) 2839–2843, <https://doi.org/10.1002/adma.201200374>.
- [181] Z. Jiang, M. Xu, F.Y. Li, F.Y. Li, Y.L. Yu, J. Am. Chem. Soc. 135 (2013) 16446–16453, <https://doi.org/10.1021/ja406020r>.
- [182] H.F. Lu, M. Wang, X.M. Chen, B.P. Lin, H. Yang, J. Am. Chem. Soc. 141 (2019) 14364–14369, <https://doi.org/10.1021/jacs.9b06757>.
- [183] Y. Zhao, Dongnan University Nanjing China 2017.
- [184] H. Xie, M.J. He, X.Y. Deng, L. Du, C.J. Fan, K.K. Yang, Y.Z. Wang, ACS Appl. Mater. Inter. 8 (2016) 9431–9439, <https://doi.org/10.1021/acsami.6b00704>.
- [185] T. Defize, R. Riva, C. Jerome, M. Alexandre, Macromol. Chem. Phys. 213 (2012) 187–197, <https://doi.org/10.1002/macp.201100408>.
- [186] Z.Y. Tian, A.D.Q. Li, Acc. Chem. Res. 46 (2012) 269–279, <https://doi.org/10.1021/ar300108d>.
- [187] S. Chen, F.J. Jiang, Z.Q. Cao, G.J. Wang, Z.M. Dang, Chem. Commun. 51 (2015) 12633–12636, <https://doi.org/10.1039/c5cc04087f>.
- [188] K.M. Wiggins, J.N. Brantley, C.W. Bielawski, ACS Macro Lett. 1 (2012) 623–626, <https://doi.org/10.1021/mz300167y>.
- [189] X.Z. Zhang, Q.Q. Zhou, H.R. Liu, H.W. Liu, Soft Matter 10 (2014) 3748–3754, <https://doi.org/10.1039/c4sm00218k>.
- [190] H.M. Dou, J.H. Ding, H. Chen, Z. Wang, A.F. Zhang, H.B. Yu, RSC Adv. 9 (2019) 13104–13111, <https://doi.org/10.1039/c9ra01583c>.
- [191] W.Q. Qian, Y.F. Song, D.J. Shi, W.F. Dong, X.R. Wang, H.J. Zhang, Materials 12 (2019) 496, <https://doi.org/10.3390/ma12030496>.
- [192] J. Sun, Q.H. Guan, Y.J. Liu, J.S. Leng, J. Intel. Mat. Syst. Str. 27 (2016) 2289–2312, <https://doi.org/10.1177/1045389X16629569>.
- [193] Q.Y. Guo, C.J. Bishop, R.A. Meyer, D.R. Wilson, L. Olasov, D.E. Schlesinger, P. T. Mather, J.B. Spicer, J.H. Elisseeff, J.J. Green, ACS Appl. Mater. Inter. 10 (2018) 13333–13341, <https://doi.org/10.1021/acsami.8b01582>.
- [194] W.T. Wang, F. Wang, C. Zhang, Z.K. Wang, J.N. Tang, X.R. Zeng, X.J. Wan, ACS Appl. Mater. Inter. 12 (2019) 25233–25242, <https://doi.org/10.1021/acsami.9b13316>.
- [195] Y.Y. Zhang, H.J. Gao, H. Wang, Z.Y. Xu, X.W. Chen, B. Liu, Y. Shi, Y. Lu, L.F. Wen, Y. Li, Z.S. Li, Y.F. Men, X.Q. Feng, W.G. Liu, Adv. Funct. Mater. 28 (2018) 1705962, <https://doi.org/10.1002/adfm.201705962>.
- [196] J.W. Yoo, S. Mitragotri, P. Natl. Acad. Sci. USA 107 (2010) 11205–11210, <https://doi.org/10.1073/pnas.1000346107>.
- [197] S.M. Brosnan, A.M.S. Jackson, Y.P. Wang, V.S. Ashby, Macromol. Rapid Comm. 35 (2014) 1653–1660, <https://doi.org/10.1002/marc.201400199>.
- [198] Y.W. Zheng, J. Li, E. Lee, S. Yang, RSC Adv. 5 (2015) 30495–30499, <https://doi.org/10.1039/c5ra01469g>.
- [199] H.J. Zhang, J.M. Zhang, X. Tong, D.L. Ma, Y. Zhao, Macromol. Rapid Comm. 34 (2013) 1575–1579, <https://doi.org/10.1002/marc.201300629>.
- [200] H. Koerner, G. Price, N.A. Pearce, M. Alexander, R.A. Vaia, Nat. Mater. 3 (2004) 115–120, <https://doi.org/10.1038/nmat1059>.
- [201] J.N. Yao, Jilin University Changchun China 2018.
- [202] Y.C. Wang, A.L. Dang, Z.F. Zhang, R. Yin, Y.C. Gao, L. Feng, S. Yang, Adv. Mater. 32 (2020) 2004270, <https://doi.org/10.1002/adma.202004270>.
- [203] Q. Shen, T. Stalbaum, S. Trabia, T. Hwang, R. Hunt, K. Kim, Proc. SPIE Bellingham USA (2017), <https://doi.org/10.1117/12.2258495>.
- [204] A. Biswas, A.P. Singh, D. Rana, V.K. Aswal, P. Maiti, Nanoscale 10 (2018) 9917–9934, <https://doi.org/10.1039/c8nr01438h>.
- [205] T.A. Kent, M.J. Ford, E.J. Markvicka, C.M. Majidi, Multifunct. Mater. 3 (2020), 025003, <https://doi.org/10.1088/2399-7532/ab835c>.
- [206] J.J. Shang, X.X. Le, J.W. Zhang, T. Chen, P. Theato, Polym. Chem. 10 (2019) 4359–4359, <https://doi.org/10.1039/c9py90111f>.
- [207] Y.K. Bai, J.W. Zhang, X. Chen, ACS Appl. Mater. Inter. 10 (2018) 14017–14025, <https://doi.org/10.1021/acsami.8b01425>.
- [208] J. Zhong, J. Meng, Z.Y. Yang, P. Poulin, N. Koratkar, Nano Energy 17 (2015) 330–338, <https://doi.org/10.1016/j.nanoen.2015.08.024>.
- [209] H.Y. Du, Y.L. Yu, G.M. Jiang, J.H. Zhang, J.J. Bao, Macromol. Chem. Phys. 212 (2011) 1460–1468, <https://doi.org/10.1002/macp.201100149>.
- [210] Y.K. Bai, J.W. Zhang, D.D. Wen, P.W. Gong, X. Chen, Compos. Sci. Technol. 170 (2019) 101–108, <https://doi.org/10.1016/j.compscitech.2018.11.039>.
- [211] B.Q.Y. Chan, S.J.W. Heng, S.S. Liow, K.Y. Zhang, X.J. Loh, Mater. Chem. Front. 1 (2017) 767–779, <https://doi.org/10.1039/c6qm00243a>.
- [212] H. Wang, L. Chen, L. Fang, L.Y. Li, J.J. Fang, C.H. Lu, Z.Z. Xu, Mater. Des. 160 (2018) 194–202, <https://doi.org/10.1016/j.matdes.2018.09.018>.
- [213] H.N. Wang, L. Fang, Z. Zhang, J. Epaarachchi, L.Y. Li, X. Hu, C.H. Lu, Z.Z. Xu, Compos. Part A Appl. S 125 (2019), 105525, <https://doi.org/10.1016/j.compositesa.2019.105525>.
- [214] L.F. Fan, M.Z. Rong, M.Q. Zhang, X.D. Chen, Macromol. Rapid Comm. 39 (2018) 1700714, <https://doi.org/10.1002/marc.201700714>.
- [215] M.D. Monzon, R. Paz, E. Pei, F. Ortega, L. Suarez, Z. Ortega, M.E. Aleman, T. Plucinski, N. Clow, Int. J. Adv. Manuf. Tech. 89 (2017) 1827–1836, <https://doi.org/10.1007/s00170-016-9233-9>.
- [216] J. Fan, G. Li, RSC Adv. 7 (2017) 1127–1136, <https://doi.org/10.1039/c6ra25024f>.
- [217] T. Lv, Z.J. Cheng, E.S. Zhang, H.J. Zhang, Y.Y. Liu, J. Lei, Small 13 (2017) 1503402, <https://doi.org/10.1002/smll.201503402>.
- [218] J.J. Lai, X.J. Li, R.Q. Wu, J.N. Deng, Y. Pan, Z.H. Zheng, X.B. Ding, Soft Matter 14 (2018) 7302–7309, <https://doi.org/10.1039/c8sm01404c>.
- [219] U. Adiyant, T. Larsen, J.J. Zarate, L.G. Villanueva, H. Shea, Nat. Commun. 10 (2019) 4518, <https://doi.org/10.1038/s41467-019-12550-6>.
- [220] G.J.M. Antony, S.T. Aruna, R. Samikkannu, C.S. Jarali, Int. Conf. Front. Mater. Process. (2018).
- [221] K. Kumar, A.P.H.J. Schenning, D.J. Broer, D.Q. Liu, Soft Matter 12 (2016) 3196–3201, <https://doi.org/10.1039/c6sm00114a>.
- [222] X.L. Wu, W.M. Huang, H.X. Tan, J. Polym. Res. 20 (2013) 150, <https://doi.org/10.1007/s10965-013-0150-4>.
- [223] S. Cai, Y.C. Sun, J. Ren, H. Naguib, J. Mater. Chem. B 5 (2017) 8845, <https://doi.org/10.1039/c7tb02068f>.
- [224] D.M. Le, M.A. Tycron, C.J. Fecko, V.S. Ashby, J. Appl. Polym. Sci. 130 (2013) 4551–4557, <https://doi.org/10.1002/app.39604>.
- [225] W.B. Li, Y.J. Liu, J.S. Leng, Compos. Part A Appl. S 110 (2018) 70–75, <https://doi.org/10.1016/j.compositesa.2018.04.019>.
- [226] L. Yu, Q. Wang, J. Sun, C. Li, C. Zou, C. Z.M. He, Z.D. Wang, L. Zhou, L.Y. Zhanga, H. Yang, J. Mater. Chem. A 3 (2015) 13953–13961, <https://doi.org/10.1039/c5ta01894c>.
- [227] Y.L. Liu, K.L. Ai, J.H. Liu, M. Deng, Y.Y. He, L.H. Lu, L. Adv. Mater. 25 (2013) 1353–1359, <https://doi.org/10.1002/adma.201204683>.
- [228] F.O. Obiweulozor, A. GhavamiNejad, B. Maharjan, J. Kim, C.H. Park, C.S. Kim, J. Mater. Chem. B 5 (2017) 5373–5379, <https://doi.org/10.1039/c7tb00539c>.
- [229] L. Yang, Z.H. Wang, G.X. Fei, H.S. Xia, H. Macromol. Rapid Comm. 38 (2017) 1700421, <https://doi.org/10.1002/marc.201700421>.
- [230] K.J. Wang, X.X. Zhu, ACS Biomater. Sci. Eng. 4 (2018) 3099–3106, <https://doi.org/10.1021/acsbomaterials.8b00671>.
- [231] H.M. Tian, Z.J. Wang, Y.L. Chen, J.Y. Shao, T. Gao, S.Q. Cai, ACS Appl. Mater. Inter. 10 (2018) 8307–8316, <https://doi.org/10.1021/acsami.8b00639>.
- [232] S. Ishii, K. Uto, E. Niiyama, M. Ebara, T. Nagao, ACS Appl. Mater. Inter. 8 (2016) 5634–5640, <https://doi.org/10.1021/acsami.5b12658>.
- [233] T.Y. Fang, L.L. Cao, S.P. Chen, J.J. Fang, J. Zhou, L. Fang, C.H. Lu, Z.Z. Xu, Mater. Des. 144 (2018) 129–139, <https://doi.org/10.1016/j.matdes.2018.02.029>.
- [234] P. Zhang, B. Wu, S. Huang, F. Cai, G.J. Wang, H.F. Yu, Polymer 178 (2019), 121644, <https://doi.org/10.1016/j.polymer.2019.121644>.
- [235] Y.J. Zhang, L.L. Wang, W. Gao, T.K. Gu, Z.J. Li, X. Li, R. Li, G.Y. Ye, W.T. Jiang, Y. K. Zhu, H.Z. Liu, Smart Mater. Struct. 28 (2019), 075014, <https://doi.org/10.1088/1361-665X/ab1163>.
- [236] Z.J. Wang, Q.G. He, Y. Wang, S.Q. Cai, Soft Matter 15 (2019) 2811–2816, <https://doi.org/10.1039/c9sm00322c>.

- [237] J.S. Leng, X. Lan, Y.J. Liu, S.Y. Du, *Prog. Mater. Sci.* 56 (2011) 1077–1135, <https://doi.org/10.1016/j.pmatsci.2011.03.001>.
- [238] J.Z. Fan, G.Q. Li, *Nat. Commun.* 9 (2018) 642, <https://doi.org/10.1038/s41467-018-03094-2>.
- [239] H.A. Dinovitzer, A. Laronche, J. Albert, *IEEE Sens. J.* 19 (2019) 5670–5679, <https://doi.org/10.1109/JSEN.2019.2907867>.
- [240] Y.D. Zhang, M.Y. Lu, *Int. J. Med. Robot. Comp.* 16 (2020), e2096, <https://doi.org/10.1002/rcs.2096>.
- [241] M. Baniasadi, E. Yarali, M. Bodaghi, Z. Zolfagharian, M. Baghani, *Int. J. Mech. Sci.* 192 (2021), 106082, <https://doi.org/10.1016/j.jmesci.2020.106082>.
- [242] F. Pilate, R. Mincheva, J. De Winter, P. Gerbaux, L.B. Wu, R. Todd, J.M. Raquez, P. Dubois, *Chem. Mater.* 26 (2014) 5860–5867, <https://doi.org/10.1021/cm5020543>.
- [243] K.K. Julich-Gruner, C. Wenberg, A.T. Neffe, M. Behl, A. Lendlein, *Macromol. Chem. Phys.* 214 (2013) 527–536, <https://doi.org/10.1002/macp.201200607>.
- [244] J. Hatai, C. Hirschhauser, J. Niemeyer, C. Schmuck, *ACS Appl. Mater. Inter.* 12 (2020) 2107–2115, <https://doi.org/10.1021/acsami.9b19279>.
- [245] Y. Dong, J. Wang, X.K. Guo, S.S. Yang, M.O. Ozen, P. Chen, X. Liu, W. Du, F. Xiao, U. Demirci, B.F. Liu, *Nat. Commun.* 10 (2019) 4087, <https://doi.org/10.1038/s41467-019-12044-5>.
- [246] H.S. Luo, X.D. Zhou, Y.C. Xu, H.Q. Wang, Y.T. Yao, G.B. Yi, Z.F. Hao, *Pigm. Resin Technol.* 47 (2018) 1–6, <https://doi.org/10.1108/PRT-03-2017-0032>.
- [247] C.C. Hong, J.C. Chen, *Microfluid. Nanofluids* 11 (2011) 385–393, <https://doi.org/10.1007/s10404-011-0804-7>.
- [248] A. Pal, D. Goswami, R.V. Martinez, *Adv. Funct. Mater.* 30 (2020) 1906603, <https://doi.org/10.1002/adfm.201906603>.
- [249] Y. Liu, B. Shaw, M.D. Dickey, J. Genzer, *Sci. Adv.* 3 (2017), e1602417, <https://doi.org/10.1126/sciadv.1602417>.
- [250] H.H. Xie, J.D. Shao, Y.F. Ma, J.H. Wang, H. Huang, N. Yang, H.Y. Wang, C. S. Ruan, Y.F. Luo, Q.Q. Wang, P.K. Chu, X.F. Yu, *Biomaterials* 164 (2018) 11–21, <https://doi.org/10.1016/j.biomaterials.2018.02.040>.
- [251] W.B. Li, Y.J. Liu, J.S. Leng, *J. Mater. Chem. A* 3 (2015) 24532–24539, <https://doi.org/10.1039/c5ta08513f>.
- [252] G. Li, S.W. Wang, Z.T. Liu, Z.W. Liu, H.S. Xia, C. Zhang, X.L. Lu, J.Q. Jiang, Y. Zhao, *ACS Appl. Mater. Inter.* 10 (2018) 40189–40197, <https://doi.org/10.1021/acsami.8b16094>.
- [253] F. Peng, G.Z. Li, X.X. Liu, S.Z. Wu, Z. Tong, *J. Am. Chem. Soc.* 130 (2008) 16166–16167, <https://doi.org/10.1021/ja807087z>.
- [254] G.E. Giammanco, C.T. Sosnofsky, A.D. Ostrowski, *ACS Appl. Mater. Inter.* 7 (2015) 3068–3076, <https://doi.org/10.1021/am506772x>.
- [255] J. Sima, J. Makannova, *Coord. Chem. Rev.* 160 (1997) 161–189, [https://doi.org/10.1016/S0010-8545\(96\)01321-5](https://doi.org/10.1016/S0010-8545(96)01321-5).
- [256] Z.W. He, N. Satarakar, T. Xie, Y.T. Cheng, J.Z. Hilt, *Adv. Mater.* 23 (2011) 3192–3196, <https://doi.org/10.1002/adma.201100646>.
- [257] Y. Wu, J.L. Hu, C. Zhang, J. Han, Y. Wang, B. Kumar, *J. Mater. Chem. A* 3 (2015) 97–100, <https://doi.org/10.1039/c4ta04881d>.
- [258] M. Burnworth, L.M. Tang, J.R. Kumpfer, A.J. Duncan, F.L. Beyer, G.L. Fiore, S. J. Rowan, C. Weder, *Nature* 472 (2011) 334–U230, <https://doi.org/10.1038/nature09963>.
- [259] J. Yan, M.F. Li, Z.W. Wang, C. Chen, C.Q. Ma, G. Yang, *Chem. Eng. J.* 389 (2020), 123468, <https://doi.org/10.1016/j.cej.2019.123468>.
- [260] J.R. Huang, L.M. Cao, D.S. Yuan, Y.K. Chen, *ACS Sustain. Chem. Eng.* 7 (2019) 2304–2315, <https://doi.org/10.1021/acssuschemeng.8b05025>.
- [261] P. Prathumrat, S. Tiptipakorn, S. Rimdusit, *Smart Mater. Struct.* 26 (2017), 065025, <https://doi.org/10.1088/1361-665X/aa6d47>.
- [262] R. Xiao, C. Zhang, W.M. Huang, *Shape-Mem. Polym. Device Des.* (2017) 113–137, <https://doi.org/10.1016/B978-0-323-37797-3.00004-X>.
- [263] Z.W. Wang, J. Zhao, M. Chen, M.H. Yang, L.Y. Tang, Z.M. Dang, F.H. Chen, M. M. Huang, X. Dong, *ACS Appl. Mater. Inter.* 6 (2014) 20051–20059, <https://doi.org/10.1021/am5056307>.
- [264] J.Y. Xian, J.T. Geng, Y. Wang, L. Xia, *Polym. Adv. Technol.* 29 (2018) 982–988, <https://doi.org/10.1002/pat.4209>.
- [265] F.H. Zhang, Z.C. Zhang, Y.J. Liu, H.B. Lu, J.S. Leng, *Smart Mater. Struct.* 22 (2013), 085020, <https://doi.org/10.1088/0964-1726/22/8/085020>.
- [266] C.W. Lu, Y.P. Liu, X.H. Liu, C.P. Wang, J.F. Wang, F.X. Chu, *ACS Sustain. Chem. Eng.* 6 (2018) 6527–6535, <https://doi.org/10.1021/acssuschemeng.8b00329>.
- [267] A. Lendlein, M. Balk, N.A. Tarazona, O.E.C. Gould, *Biomacromolecules* 20 (2019) 3627–3640, <https://doi.org/10.1021/acs.biomac.9b01074>.
- [268] A. Lendlein, O.E.C. Gould, *Nat. Rev. Mater.* 4 (2019) 116–133, <https://doi.org/10.1038/s41578-018-0078-8>.
- [269] L.J. Ning, L. Yuan, G.Z. Liang, A.J. Gu, *J. Mater. Sci.* 56 (2020) 3623–3637, <https://doi.org/10.1007/s10853-020-05469-7>.
- [270] F. Karasu, C. Weder, *J. Appl. Polym. Sci.* 138 (2020), e49935, <https://doi.org/10.1002/app.49935>.
- [271] B.J. Zhao, H.G. Mei, N. Liu, S.X. Zheng, *Macromolecules* 53 (2020) 7119–7131, <https://doi.org/10.1021/acs.macromol.0c01143>.
- [272] M.Y. Wang, J.P. Zhuge, C.Q. Li, L.B. Jiang, H. Yang, *Iran. Polym. J.* 29 (2020) 569–579, <https://doi.org/10.1007/s13726-020-00821-9>.
- [273] H.T. Zhuo, Z.K. Mei, H. Chen, S.J. Chen, *Polymer* 148 (2018) 119–126, <https://doi.org/10.1016/j.polymer.2018.06.037>.
- [274] S.T. Wang, S.J. Li, L. Gao, *ACS Appl. Mater. Inter.* 11 (2019) 43622–43630, <https://doi.org/10.1021/acsami.9b16205>.
- [275] L. Xia, F.C. Yang, H. Wu, M. Zhang, Z.G. Huang, G.X. Qiu, Z.X. Xin, W.X. Fu, *Polym. Test.* 81 (2019), 106212, <https://doi.org/10.1016/j.polymertesting.2019.106212>.
- [276] Y.J. Liu, Z.H. Tang, Y. Chen, S.W. WU, B.C. Guo, *Compos. Sci. Technol.* 168 (2018) 214–223, <https://doi.org/10.1016/j.compscitech.2018.10.005>.
- [277] M.J. He, W.X. Xiao, H. Xie, C.J. Fan, L. Du, X.Y. Deng, K.K. Yang, Y.Z. Wang, *Mater. Chem. Front.* 1 (2017) 343–353, <https://doi.org/10.1039/c6qm00047a>.
- [278] K. Kumar, C. Knie, D. Bleger, M.A. Peletier, H. Friedrich, S. Hecht, D.J. Broer, M. G. Debije, A.P.H.J. Schenning, *Nat. Commun.* 7 (2016) 11975, <https://doi.org/10.1038/ncomms11975>.
- [279] Z.H. Wang, H.J. Guo, R.J. Gui, H. Jin, J.F. Xia, F.F. Zhang, *Sens. Actuators B Chem.* 255 (2017) 2069–2077, <https://doi.org/10.1016/j.snb.2017.09.010>.
- [280] S. Chen, Y.J. Gao, Z.Q. Cao, B. Wu, L. Wang, H. Wang, Z.M. Dang, G.J. Wang, *Macromolecules* 49 (2016) 7490–7496, <https://doi.org/10.1021/acs.macromol.6b01760>.
- [281] T. Seki, *Macromol. Rapid Commun.* 35 (2014) 271–290, <https://doi.org/10.1002/marc.201300763>.
- [282] H. Yu, J. Mater. Chem. C 2 (2014) 3047–3054, <https://doi.org/10.1039/c3tc31991a>.
- [283] H. Nakano, M. Suzuki, *J. Mater. Chem.* 22 (2012) 3702–3704, <https://doi.org/10.1039/C2JM16517A>.
- [284] Q.J. Ze, X. Kuang, S. Wu, J. Wong, S.M. Montgomery, R.D. Zhang, J.M. Kovitz, F. Y. Yang, H.J. Qi, R.K. Zhao, *Adv. Mater.* 32 (2020) 1906657, <https://doi.org/10.1002/adma.201906657>.
- [285] B. Godt, *IEEE Trans. Inf. Theory* 5 (1959) 17–24, <https://doi.org/10.1109/TTT.1959.1057478>.
- [286] T. Schmidt-Wilcke, K. Rosengarth, R. Luerding, U. Bogdahn, M.W. Greenlee, *Neuroimage* 51 (2010) 1234–1241, <https://doi.org/10.1016/j.neuroimage.2010.03.042>.
- [287] W.B. Li, Y.J. Liu, J.S. Leng, *ACS Appl. Mater. Inter.* 9 (2017) 44792–44798, <https://doi.org/10.1021/acsami.7b13284>.
- [288] Y. Wang, A. Villada, Y. Zhai, Z.N. Zou, Y.Z. Chen, X.B. Yin, J.L. Xiao, *Appl. Phys. Lett.* 114 (2019), 193701, <https://doi.org/10.1063/1.5096767>.
- [289] A. Basit, G. L'Hostis, B. Durand, *Mater. Lett.* 74 (2012) 220–222, <https://doi.org/10.1016/j.matlet.2012.01.113>.
- [290] A. Lendlein, M. Balk, N.A. Tarazona, O.E.C. Gould, *Biomacromolecules* 20 (2019) 3627–3640, <https://doi.org/10.1021/acs.biomac.9b01074>.
- [291] S. Bodkhe, P. Ermanni, *Eur. Polym. J.* 132 (2020), 109738, <https://doi.org/10.1016/j.eurpolymj.2020.109738>.
- [292] Z. Feng, L.G. Xiong, Y.J. Ai, Z. Liang, Q.L. Liang, *Adv. Sci.* 5 (2018) 1800450, <https://doi.org/10.1002/advs.201800450>.
- [293] M. Walter, F. Friess, M. Krus, S.M.H. Zolanvari, G. Grun, H. Krober, T. Pretsch, *Polymers* 12 (2020) 1914, <https://doi.org/10.3390/polym12091914>.
- [294] S. Tibbitts, S. Linor, D. Dikovskiy, S. Hirsch, *Archit. Des.* 84 (2014) 116–121, <https://doi.org/10.1002/ad.1710>.
- [295] F. Momeni, M.M.H.N. Seyed, X. Liu, J. Ni, *Mater. Des.* 122 (2017) 42–79, <https://doi.org/10.1016/j.matdes.2017.02.068>.
- [296] B. Goo, C.H. Hong, K. Park, *Mater. Des.* 188 (2020), 108485, <https://doi.org/10.1016/j.matdes.2020.108485>.
- [297] B.I. Oladapo, E.A. Oshin, A.M. Olawumi, *Nano Struct. Nano Objects* 21 (2020), 100423, <https://doi.org/10.1016/j.nano.2020.100423>.
- [298] B.A. Zhang, W. Zhang, Z.Q. Zhang, Y.F. Zhang, H. Hingorani, Z.J. Liu, J. Liu, Q. Ge, *ACS Appl. Mater. Inter.* 11 (2019) 10328–10336, <https://doi.org/10.1021/acsami.9b00359>.
- [299] J.J. Wu, L.M. Huang, Q. Zhao, T. Xie, *Chin. J. Polym. Sci.* 36 (2018) 563–575, <https://doi.org/10.1007/s10118-018-2089-8>.
- [300] X. Wan, L. Luo, Y.J. Liu, J.S. Leng, *Adv. Sci.* 7 (2020) 2001000, <https://doi.org/10.1002/advs.202001000>.
- [301] M.N.I. Shiblee, K. Ahmed, M. Kawakami, H. Furukawa, *Adv. Mater. Technol.* 4 (2019) 1900071, <https://doi.org/10.1002/admt.201900071>.
- [302] L.X. Lu, T. Tian, S.S. Wu, T. Xiang, S.B. Zhou, *Polym. Chem.* 10 (2019) 1920–1929, <https://doi.org/10.1039/c9py00015a>.
- [303] M. Mazurek-Budzynska, M.Y. Razaq, M. Behl, A. Lendlein, *Funct. Polym.* (2019) 605–663, https://doi.org/10.1007/978-3-319-95987-0_18.
- [304] A.I. Salimov, F.S. Senatov, A. Kalyaev, A.M. Korsunsky, *3D 4D Print. Polym. Nanocompos. Mater.* (2020) 161–189, <https://doi.org/10.1016/B978-0-12-816805-9.00006-5>.
- [305] C.P. Ambulo, J.J. Burroughs, J.M. Boothby, H. Kim, M.R. Shankar, T.H. Ware, *ACS Appl. Mater. Inter.* 9 (2017) 37332–37339, <https://doi.org/10.1021/acsami.7b11851>.
- [306] S.W. Ula, N.A. Traugott, R.H. Volpe, R.R. Patel, K. Yu, C.M. Yakacki, *Liq. Cryst. Rev.* 6 (2018) 78–107, <https://doi.org/10.1080/21680396.2018.1530155>.
- [307] M.P. Caputo, A.E. Berkowitz, A. Armstrong, P. Mullner, C.V. Solomon, *Addit. Manuf.* 21 (2018) 579–588, <https://doi.org/10.1016/j.addma.2018.03.028>.
- [308] H.Z. Lu, C. Yang, X. Luo, H.W. Ma, B. Song, Y.Y. Li, L.C. Zhang, *Mat. Sci. Eng. A-Struct.* 763 (2019), 138166, <https://doi.org/10.1016/j.msea.2019.138166>.
- [309] U. Scheithauer, S. Weingarten, R. John, E. Schwarzer, J. Abel, H.J. Richter, T. Moritz, A. Michaelis, *Materials* 10 (2017) 1368, <https://doi.org/10.3390/ma10121368>.
- [310] K. Liu, T. Wu, D.L. Bourell, Y.L. Tan, J. Wang, M.Q. He, H.J. Sun, Y.S. Shi, J. Q. Chen, *Ceram. Int.* 44 (2018) 21067–21075, <https://doi.org/10.1016/j.ceramint.2018.08.143>.
- [311] S.K. Melly, L.W. Liu, Y.J. Liu, J.S. Leng, *Smart Mater. Struct.* 29 (2020), 083001, <https://doi.org/10.1088/1361-665X/ab9989>.
- [312] M.Y. Shie, Y.F. Shen, S.D. Astuti, A.K.X. Lee, S.H. Lin, N.L.B. Dwijaksara, Y. W. Chen, *Polymers* 11 (2019) 1864, <https://doi.org/10.3390/polym11111864>.
- [313] A.P. Piedad, *J. Funct. Biomater.* 10 (2019) 9, <https://doi.org/10.3390/jfb10010009>.

- [314] Z.C. Shen, Y. Xia, Y.G. Ding, C.Q. Zhao, Y.B. Yang, *J. Mater. Eng.* 47 (2019) 11–18, <https://doi.org/10.11868/j.issn.1001-4381.2018.000610>.
- [315] S.D. Miao, H.T. Cui, M. Nowicki, L. Xia, X. Zhou, S.J. Lee, W. Zhu, K. Sarkar, Z. Y. Zhang, L.J.G. Zhang, *Adv. Biosyst.* 2 (2018) 1800101, <https://doi.org/10.1002/adbi.201800101>.
- [316] Z. Zhao, X. Kuang, J.T. Wu, Q. Zhang, G.H. Paulino, H.J. Qi, D.N. Fang, *Soft Matter* 14 (2018) 8051–8059, <https://doi.org/10.1039/c8sm01341a>.
- [317] V.A. Beloshenko, Y.E. Beygelzimer, Yu.V. Voznyak, B.M. Savchenko, V. Yu Dmitrenko, *J. Appl. Polym. Sci.* (2018) 45727, <https://doi.org/10.1002/APP.45727>.
- [318] H.Q. Wei, Q.W. Zhang, Y.T. Yao, L.W. Liu, Y.J. Liu, J.S. Leng, *ACS Appl. Mater. Inter.* 9 (2017) 876–883, <https://doi.org/10.1021/acsami.6b12824>.
- [319] Y.Y. Pan, C. Zhou, Y. Chen, *J. Manuf. Sci. Eng.* 134 (2012), 051011, <https://doi.org/10.1115/1.4007465>.
- [320] W.J. Hendrikson, J. Rouwkema, F. Clementi, C.A. van Blitterswijk, S. Fare, L. Moroni, *Biofabrication* 9 (2017), 031001, <https://doi.org/10.1088/1758-5090/aa8114>.
- [321] M.A. Skylar-Scott, S. Gunasekaran, J.A. Lewis, *Proc. Natl. Acad. USA* 113 (2016) 6137–6142, <https://doi.org/10.1073/pnas.1525131113>.
- [322] J.T. Muth, P.G. Dixon, L. Woish, L.J. Gibson, J.A. Lewis, *Proc. Natl. Acad. USA* 114 (2017) 1832–1837, <https://doi.org/10.1073/pnas.1616769114>.
- [323] M.A. Skylar-Scott, M. Jochen, C.W. Visser, J.A. Lewis, *Nature* 575 (2019) 330–335, <https://doi.org/10.1038/s41586-019-1736-8>.
- [324] L.L. Lebel, B. Aissa, M.A. El Khakani, D. Theriault, *Adv. Mater.* 22 (2010) 592–596, <https://doi.org/10.1002/adma.200902192>.
- [325] H. Yang, W.R. Leow, T. Wang, J. Wang, J.C. Yu, K. He, D.P. Qi, C.J. Wan, X. D. Chen, *Adv. Mater.* 29 (2017) 1701627, <https://doi.org/10.1002/adma.201701627>.
- [326] G.H. Koo, J. Jang, *J. Appl. Polym. Sci.* 127 (2013) 4515–4523, <https://doi.org/10.1002/app.38056>.
- [327] C. Decker, *Prog. Polym. Sci.* 21 (1996) 593–650, [https://doi.org/10.1016/0079-6700\(95\)00027-5](https://doi.org/10.1016/0079-6700(95)00027-5).
- [328] H.Y. Jeong, B.H. Woo, N. Kim, Y.C. Jun, *Sci. Rep.* 10 (2020) 6258, <https://doi.org/10.1038/s41598-020-63020-9>.
- [329] W.B. Shan, Y.F. Chen, M. Hu, S.G. Qin, P. Liu, *Mater. Res. Express* 7 (2020), 105305, <https://doi.org/10.1088/2053-1591/abbd05>.
- [330] T.T. Nguyen, J. Kim, *Fiber Polym.* 21 (2020) 2364–2372, <https://doi.org/10.1007/s12221-020-9882-z>.
- [331] H. Liu, H. He, B. Huang, *Macromol. Mater. Eng.* 305 (2020) 2000295, <https://doi.org/10.1002/mame.202000295>.
- [332] H.W. Kang, S.J. Lee, L.K. Ko, C. Kengla, J.J. Yoo, A. Atala, *Nat. Biotechnol.* 34 (2016) 312–319, <https://doi.org/10.1038/nbt.3413>.
- [333] T.Z. Liu, L.W. Liu, C.J. Zeng, Y.J. Liu, J.S. Leng, *Compos. Sci. Technol.* 186 (2019), 107935, <https://doi.org/10.1016/j.compscitech.2019.107935>.
- [334] W. Zhao, F.H. Zhang, J.S. Leng, Y.J. Liu, *Compos. Sci. Technol.* 184 (2019), 107866, <https://doi.org/10.1016/j.compscitech.2019.107866>.
- [335] X.Z. Xin, L.W. Liu, Y.J. Liu, J.S. Leng, *Adv. Funct. Mater.* 30 (2020) 2004226, <https://doi.org/10.1002/adfm.202004226>.
- [336] X.Z. Xin, L.W. Liu, Y.J. Liu, *Smart Mater. Struct.* 29 (2020), 065015, <https://doi.org/10.1088/1361-665X/ab85a4>.
- [337] M.H. Fu, F.M. Liu, L.L. Hu, *Compos. Sci. Technol.* 160 (2018) 111–118, <https://doi.org/10.1016/j.compscitech.2018.03.017>.
- [338] J. Huang, Q.H. Zhang, F. Scarpa, Y.J. Liu, J.S. Leng, *Compos. Part B-Eng.* 140 (2018) 35–43, <https://doi.org/10.1016/j.compositesb.2017.12.014>.
- [339] C. Lin, L.J. Zhang, Y.J. Liu, J.S. Leng, *Sci. China Technol. I Sci.* 63 (2020) 578–588, <https://doi.org/10.1007/s11431-019-1468-2>.
- [340] H. Adeli, N.T. Cheng, *J. Aerosp. Eng.* 6 (1993) 315–328, [https://doi.org/10.1061/\(ASCE\)0893-1321\(1993\)6:4\(315\)](https://doi.org/10.1061/(ASCE)0893-1321(1993)6:4(315)).
- [341] M. Kociecki, H. Adeli, *Eng. Appl. Artif. Intel.* 32 (2014) 218–227, <https://doi.org/10.1016/j.engappai.2014.01.010>.
- [342] L.J. Gibson, M.F. Ashby, *Proc. R. Soc. Lond. A* 382 (1982) 43–59, <https://doi.org/10.1098/rspa.1982.0088>.
- [343] Y.X. Luo, X. Lin, B.R. Chen, X.Y. Wei, *Biofabrication* 11 (2019), 045019, <https://doi.org/10.1088/1758-5090/ab39c5>.
- [344] W. Zhao, L.W. Liu, J.S. Leng, et al., *J. Appl. Polym. Sci.* (2019), <https://doi.org/10.1117/12.2514545>.
- [345] F.H. Zhang, L.L. Wang, Z.C. Zheng, Y.J. Liu, J.S. Leng, *Compos. Part A-Appl. S* 125 (2019), 105571, <https://doi.org/10.1016/j.compositesa.2019.105571>.
- [346] L.H. Shao, B.X. Zhao, Q. Zhang, Y.F. Xing, K. Zhang, *Extrem. Mech. Lett.* 39 (2020), 100793, <https://doi.org/10.1016/j.eml.2020.100793>.
- [347] C.Y. Cheng, H. Xie, Z.Y. Xu, L. Li, M.N. Jiang, L. Tang, K.K. Yang, Y.Z. Wang, *Chem. Eng. J.* 396 (2020), 125242, <https://doi.org/10.1016/j.cej.2020.125242>.
- [348] G.L. Ying, N. Jiang, S. Mahar, Y.X. Yin, R.R. Chai, X. Cao, J.Z. Yang, A.K. Miri, S. Hassan, *Y.S. Zhang, Adv. Mater.* 30 (2018) 1805460, <https://doi.org/10.1002/adma.201805460>.
- [349] M. Bodaghi, A.R. Damanpack, W.H. Liao, *Mater. Des.* 135 (2017) 26–36, <https://doi.org/10.1016/j.matdes.2017.08.069>.
- [350] M. Bodaghi, A.R. Damanpack, W.H. Liao, *Smart Mater. Struct.* 25 (2016), 105034, <https://doi.org/10.1088/0964-1726/25/10/105034>.
- [351] A. Zolfagharian, A. Kaynak, M. Bodaghi, A.Z. Kouzani, S. Gharraie, S. Mahavandi, *Appl. Sci.* 10 (2020) 3020, <https://doi.org/10.3390/app10093020>.
- [352] M. Falahati, P. Ahmadvand, S. Safaee, Y.C. Chang, Z.Y. Lyu, R. Chen, L. Li, Y. Lin, *Mater. Today* 40 (2020) 215–245, <https://doi.org/10.1016/j.mattod.2020.06.001>.
- [353] Y.F. Guo, Z.Y. Lv, Y.R. Huo, L.J. Sun, S. Chen, Z.H. Liu, C.L. He, X.P. Bi, X.Q. Fan, Z.W. You, *J. Mater. Chem. B* 7 (2018) 123–132, <https://doi.org/10.1039/c8tb02462f>.
- [354] Y.F. Zhang, N.B. Zhang, H. Hingorani, N.Y. Ding, D. Wang, C. Yuan, B. Zhang, G. Y. Gu, Q. Ge, *Adv. Funct. Mater.* 29 (2019) 1806698, <https://doi.org/10.1002/adfm.201806698>.
- [355] L. Santo, F. Quadrini, A. Accettura, W. Villadei, *Procedia Eng. Amst. Neth.* (2014), <https://doi.org/10.1016/j.proeng.2014.11.124>.
- [356] T. Li, Y. Li, X.H. Wang, X. Li, J.Q. Sun, *ACS Appl. Mater. Inter.* 11 (2019) 9470–9477, <https://doi.org/10.1021/acsami.8b21970>.
- [357] X.L. Lu, H. Zhang, G.X. Fei, B. Yu, *Adv. Mater.* 30 (2018) 1706597, <https://doi.org/10.1002/adma.201706597>.
- [358] J.A. Lv, Y.Y. Liu, J. Wei, E.Q. Chen, L. Qin, Y.L. Yu, *Nature* 537 (2016) 179–184, <https://doi.org/10.1038/nature19344>.
- [359] X.X. Wang, Y.C. Wang, X.X. Wang, H.Y. Niu, B.Y. Ridi, J.C. Shu, X.Y. Fang, C.S. Li, B.S. Wang, Y.C. Gao, L.G. Sun, M.S. Cao, *Soft Matter* 16 (2020) 7332–7341, <https://doi.org/10.1039/d0sm00493f>.
- [360] S. Pringpromsuk, H. Xia, Q.Q. Ni, *Sens. Actuators A-Phys.* 313 (2020), 112207, <https://doi.org/10.1016/j.sna.2020.112207>.
- [361] D. Wang, L. Li, B. Zhang, Y.F. Zhang, M.S. Wu, G.Y. Gu, Q. Ge, *Int. J. Solids Struct.* 199 (2020) 169–180, <https://doi.org/10.1016/j.ijsolstr.2020.04.028>.
- [362] C.Z. Chu, Z. Xiang, J. Wang, H. Xie, T. Xiang, S.B. Zhou, *J. Mater. Chem. B* 8 (2020) 8061–8070, <https://doi.org/10.1039/d0tb01237h>.
- [363] A.D.M. Charles, A.N. Rider, S.A. Brown, C.H. Wang, *Compos. Part B* 196 (2020), 108091, <https://doi.org/10.1016/j.compositesb.2020.108091>.
- [364] R. Duarah, A. Deka, N. Karak, *Express Polym. Lett.* 14 (2020) 542–555, <https://doi.org/10.3144/expresspolymlett.2020.44>.
- [365] Y. Li, J.R. Li, L.W. Liu, Y.F. Yan, Q. Zhang, N. Zhang, L.L. He, Y.J. Liu, X. F. Zhang, D.L. Tian, J.S. Leng, *Adv. Sci.* 7 (2020) 2000772, <https://doi.org/10.1002/advs.202000772>.
- [366] X.Z. Huang, F.H. Zhang, J.S. Leng, *Appl. Mater.* Today 21 (2020), 100797, <https://doi.org/10.1016/j.apmt.2020.100797>.
- [367] J. Jeon, J.C. Choi, H. Lee, W. Cho, K. Lee, J.G. Kim, J.W. Lee, K. Joo, M. Cho, H. R. Kim, J.J. Wie, *Mater. Today* (2021), <https://doi.org/10.1016/j.mattod.2021.04.014>.
- [368] T. Ashuri, A. Armani, R.J. Hamidi, T. Reasnor, S. Ahmadi, K. Iqbal, *Biomed. Eng. Lett.* 10 (2020) 369–385, <https://doi.org/10.1007/s13534-020-00157-6>.
- [369] Y. Yang, Z.Q. Pei, Z. Li, Y. Wei, Y. Ji, *J. Am. Chem. Soc.* 138 (2016) 2118, <https://doi.org/10.1021/jacs.5b12531>.
- [370] J.A.C. Liu, J.H. Gillen, S.R. Mishra, B.A. Evans, J.B. Tracy, *Sci. Adv.* 5 (2019) eaaw2897, <https://doi.org/10.1126/sciadv.aaw2897>.
- [371] A. Zolfagharian, A. Kouzani, B. Nasri-Nasrabadi, S. Adams, *Int. Conf. Des. Technol.* 2 (2017) 15, <https://doi.org/10.18502/keg.v2i2.590>.
- [372] Y. Kim, H. Yuk, R.K. Zhao, S.A. Chester, X.H. Zhao, *Nature* 558 (2018) 274–279, <https://doi.org/10.1038/s41586-018-0185-0>.
- [373] F.F. Li, L.W. Liu, X. Lan, C.T. Pan, Y.J. Liu, J.S. Leng, Q. Xie, *Smart Mater. Struct.* 28 (2019), 075023, <https://doi.org/10.1088/1361-665X/ab18b7>.
- [374] F. Xie, L.W. Liu, X.B. Gong, L.N. Huang, J.S. Leng, Y.J. Liu, *Polym. Degrad. Stab.* 138 (2017) 91–97, <https://doi.org/10.1016/j.polymdegradstab.2017.03.001>.
- [375] Y.J. Liu, H.Y. Du, L.W. Liu, J.S. Leng, *Smart Mater. Struct.* 23 (2014) 23001–23022, <https://doi.org/10.1088/0964-1726/23/2/023001>.
- [376] X. Lan, Y.J. Liu, H.B. Lv, X.H. Wang, J.S. Leng, S.Y. Du, *Smart Mater. Struct.* 18 (2009), 024002, <https://doi.org/10.1088/0964-1726/18/2/024002>.
- [377] R.R. Zhang, X.G. Guo, Y.J. Liu, J.S. Leng, *Compos. Struct.* 112 (2014) 226–230, <https://doi.org/10.1016/j.compstruct.2014.02.018>.
- [378] J.S. Leng, K. Yu, J. Sun, Y.J. Liu, *Aircr. Eng. Aerosp. Tec.* 87 (2015) 218–223, <https://doi.org/10.1108/AEAT-06-2013-0118>.
- [379] F.F. Li, L.W. Liu, X. Lan, X.J. Zhou, W.F. Bian, Y.J. Liu, J.S. Leng, *Int. J. Smart NanoMater.* 7 (2016) 106–118, <https://doi.org/10.1080/19475411.2016.1212948>.
- [380] J.S. Leng, F. Xie, X.L. Wu, Y.J. Liu, *J. Intel. Mat. Syst. Str.* 25 (2014) 1256–1263, <https://doi.org/10.1177/1045389x13504474>.
- [381] H.Q. Wei, L.W. Liu, Z.C. Zhang, H.Y. Du, Y.J. Liu, J.S. Leng, *Compos. Struct.* 133 (2015) 642–651, <https://doi.org/10.1016/j.compstruct.2015.07.107>.
- [382] F.F. Li, L.W. Liu, X. Lan, T. Wang, X.Y. Li, F.L. Chen, W.F. Bian, Y.J. Liu, J.S. Leng, *Int. J. Appl. Mech.* 8 (2016) 1640009, <https://doi.org/10.1142/S1758825116400093>.
- [383] Z.X. Liu, Q.F. Li, W.F. Bian, X. Lan, Y.J. Liu, J.S. Leng, *Compos. Struct.* 223 (2019), 110936, <https://doi.org/10.1016/j.compstruct.2019.110936>.
- [384] H.X. Zhao, X. Lan, L.W. Liu, Y.J. Liu, J.S. Leng, *Compos. Struct.* 223 (2019), 110958, <https://doi.org/10.1016/j.compstruct.2019.110958>.
- [385] F.F. Li, L.W. Liu, L.Z. Du, Y.J. Liu, J.S. Leng, *Compos. Struct.* 242 (2020), 112196, <https://doi.org/10.1016/j.compstruct.2020.112196>.
- [386] X. Lan, L.W. Liu, Y.J. Liu, J.S. Leng, *J. Appl. Polym. Sci.* 137 (2020) 48532, <https://doi.org/10.1002/app.48532>.
- [387] X. Lan, L.W. Liu, J.S.F.H. Zhang, Z.X. Liu, L.L. Wang, Q.F. Li, F. Peng, S.D. Hao, W. X. Dai, X. Wan, Y. Tang, M. Wang, Y.Y. Hao, Y. Yang, C. Yang, Y.J. Liu, J.S. Leng, *Sci. China Tech. Sci.* 63 (2020) 1436–1451, <https://doi.org/10.1007/s11431-020-1681-0>.
- [388] D. Zhang, L.W. Liu, J.S. Leng, Y.J. Liu, *Compos. Struct.* 232 (2019), 111561, <https://doi.org/10.1016/j.compstruct.2019.111561>.
- [389] Z.X. Liu, X. Lan, W.F. Bian, L.W. Liu, Q.F. Li, Y.J. Liu, J.S. Leng, *Compos. Part B Eng.* 193 (2020), 108056, <https://doi.org/10.1016/j.compositesb.2020.108056>.
- [390] S. Singh, P. Tripathi, A. Bhatnagar, C.R.P. Patel, A.P. Singh, S.K. Dhawan, B. K. Gupta, O.N. Srivastava, *RSC Adv.* 5 (2015) 107083–107087, <https://doi.org/10.1039/c5ra19273k>.

- [391] A. Lendlein, R. Langer, *Science* 296 (2002) 1673–1676, <https://doi.org/10.1126/science.1066102>.
- [392] M. Zare, N. Parvin, M.P. Prabhakaran, J.A. Mohandesi, S. Ramakrishna, *Compos. Sci. Technol.* 184 (2019), 107874, <https://doi.org/10.1016/j.compscitech.2019.107874>.
- [393] Q.P. Pham, U. Sharma, A.G. Mikos, *Tissue Eng.* 12 (2006) 1197–1211, <https://doi.org/10.1089/ten.2006.12.1197>.
- [394] M. Bao, X.X. Lou, Q.H. Zhou, W. Dong, H.H. Yuan, Y.Z. Zhang, *ACS Appl. Mater. Inter.* 6 (2014) 2611–2621, <https://doi.org/10.1021/am405101k>.
- [395] S.H. Jiang, G.G. Duan, J. Schobel, S. Agarwal, A. Greiner, *Compos. Sci. Technol.* 88 (2013) 57–61, <https://doi.org/10.1016/j.compscitech.2013.08.031>.
- [396] H.T. Zhuo, J.L. Hu, S.J. Chen, *Mater. Lett.* 62 (2008) 2074–2076, <https://doi.org/10.1016/j.matlet.2007.11.018>.
- [397] A. Baji, Y.W. Mai, S.C. Wong, M. Abtahi, P. Chen, *Compos. Sci. Technol.* 70 (2010) 703–718, <https://doi.org/10.1016/j.compscitech.2010.01.010>.
- [398] B. Sun, Y.Z. Long, F. Yu, M.M. Li, H.D. Zhang, W.J. Li, T.X. Xu, *Nanoscale* 4 (2012) 2134–2137, <https://doi.org/10.1039/c2nr11782g>.
- [399] W. Small, T.S. Wilson, W.J. Benett, J.M. Loge, D.J. Maitland, *Opt. Express* 13 (2005) 8204–8213, <https://doi.org/10.1364/OPEX.13.008204>.
- [400] F.H. Zhang, T.H. Zhao, D. Ruiz-Molina, Y.J. Liu, C. Roscini, J.S. Leng, S. K. Smoukov, *ACS Appl. Mater. Inter.* 12 (2020) 47059–47064, <https://doi.org/10.1021/acsami.0c14882>.
- [401] T. Ware, D. Simon, K. Hearon, C. Liu, S. Shah, J. Reeder, N. Khodaparast, M. P. Kilgard, D.J. Maitland, R.L. Rennaker, W.E. Voit, *Macromol. Mater. Eng.* 297 (2012) 1193–1202, <https://doi.org/10.1002/mame.201200241>.
- [402] M.Y. Gai, J. Frueh, T.Y. Tao, A.V. Petrov, V.V. Petrov, E.V. Shesterikov, S. I. Tverdokhlebov, G.B. Sukhorukov, *Nanoscale* 9 (2017) 7063–7070, <https://doi.org/10.1039/c7nr01841j>.
- [403] D.S. Wang, M. Wagner, H.J. Butt, S. Wu, *Soft Matter* 11 (2015) 7656–7662, <https://doi.org/10.1039/c5sm01888a>.
- [404] K. Yamagishi, A. Nojiri, E. Iwase, M. Hashimoto, *ACS Appl. Mater. Inter.* 11 (2019) 41770–41779, <https://doi.org/10.1021/acsami.9b17567>.
- [405] X. Li, W.K. Liu, Y.M. Li, W.L. Lan, D.G. Zhao, H.C. Wu, Y. Feng, X.L. He, Z. Li, J. H. Li, F. Luo, H. Tan, *J. Mater. Chem. B* 8 (2020) 5117–5130, <https://doi.org/10.1039/d0tb00798f>.
- [406] C. Lin, J.X. Lv, J.S. Leng, F.H. Zhang, J.R. Li, Y.J. Liu, L.W. Liu, J.S. Leng, *Adv. Funct. Mater.* 29 (2019) 1906569, <https://doi.org/10.1002/adfm.201906569>.
- [407] S. Pearson, D. Vitucci, Y.Y. Khine, A. Dag, H.X. Lu, M. Save, L. Billon, M. H. Stenzel, *Eur. Polym. J.* 69 (2015) 616–627, <https://doi.org/10.1016/j.eurpolymj.2015.04.001>.
- [408] X.L. Lu, H. Zhang, G.X. Fei, B. Yu, X. Tong, H.S. Xia, Y. Zhao, *Adv. Mater.* 30 (2018) 1706597, <https://doi.org/10.1002/adma.201706597>.
- [409] Q.S. Xia, Z.C. Zhang, H. Mei, Y.J. Liu, J.S. Leng, *Compos. Commun.* 21 (2020), 100403, <https://doi.org/10.1016/j.coco.2020.100403>.
- [410] Z. Chen, D.H. Zhao, B.H. Liu, G.D. Nian, X.K. Li, J. Yin, S.X. Qu, W. Yang, *Adv. Funct. Mater.* 29 (2019) 1900971, <https://doi.org/10.1002/adfm.201900971>.
- [411] Y. Chen, X. Zhao, C. Luo, Y. Shao, M.B. Yang, B. Yin, *Compos. Part A-Appl. S.* 135 (2020), 105931, <https://doi.org/10.1016/j.compositesa.2020.105931>.
- [412] S.B. Ji, F.Q. Fan, C.X. Sun, Y. Yu, H.P. Xu, *ACS Appl. Mater. Inter.* 9 (2017) 33169–33175, <https://doi.org/10.1021/acsami.7b11188>.
- [413] H. Xie, C.Y. Cheng, L. Li, X.Y. Deng, K.K. Yang, Y.Z. Wang, *J. Mater. Chem. C* 6 (2018) 10422–10427, <https://doi.org/10.1039/C8TC03504K>.
- [414] Y.L. Wang, Q.L. Zhao, X.M. Du, *Mater. Horiz.* 7 (2020) 1341–1347, <https://doi.org/10.1039/d0mh00150c>.



Xiaofei Wang is currently pursuing the doctoral degree under the supervision of Prof. Jinsong Leng, and current research activities focus on synthesis and characterization of photo-actuated shape memory polymer and smart polymers.



Yang He received his Ph.D. in Tribo Engineering Science in 2016 from Southampton University and is currently a postdoc at Harbin Institute of Technology. Yang's research is centered on advanced materials, ranging from shape memory polymers and composites for smart structures to luminescent coatings for damage detection and location.



Yanju Liu is a full professor in the Department of Aerospace Science and Mechanics at the Harbin Institute of Technology (HIT), China. She obtained her Ph.D. degree in material science from HIT, China in 1999. Her research interests are in the field of smart materials and structures, including stimuli-responsive materials, such as ER/MR fluids, electroactive polymers, shape memory polymers, and their composites.



Jinsong Leng is a full Professor at Harbin Institute of Technology. He received his B.S. and Ph.D. in engineering mechanics and composite materials from HIT in 1990 and 1996, respectively. His research interests cover shape memory polymers and composites, 4D printing, sensors and actuators, structural health monitoring, and multifunctional nanocomposites. Prof. Leng is the Vice President of ICCM and the Vice President of CSCM, and was elected as member of Chinese Academy of Sciences, Foreign Member of Academia Europe, World Fellow of ICCM, Fellow of AAAS, SPIE, IOP, RAES and IMMM and Associate Fellow of AIAA.